



ConnectFlow

Technical Summary

Version 13.1 – 4 November 2024

Contact Us

ConnectFlow Support Team
gw.support@global.amentum.com

Table of Contents

1	Introduction	2
1.1	Documentation.....	2
1.2	Continuum Porous Medium (CPM) Capabilities	2
1.3	Discrete Fracture Network (DFN) Capabilities	4
1.4	Combined (CPM/DFN) Capabilities	6
1.5	Quality Assurance	6
1.6	ConnectFlow Users.....	7
1.6.1	The iCONNECT Club.....	7
2	Concepts within the Continuous Porous Medium model.....	8
2.1	Relevant Physical Processes	8
2.2	Groundwater Movement.....	9
2.3	Groundwater Pressure	11
2.4	Groundwater Chemistry	12
2.5	Temperature / Heat	13
2.6	Radionuclide Transport.....	13
2.6.1	Advection.....	13
2.6.2	Molecular Diffusion.....	14
2.6.3	Hydrodynamic Dispersion	14
2.6.4	Rock Matrix Diffusion.....	16
2.6.5	Sorption	16
2.6.6	Anion Exclusion.....	17
2.6.7	Effect of Organic Complexants	17
2.6.8	Radioactive Decay and Ingrowth	17
2.7	Conceptual Models.....	17
2.8	Geometric Framework.....	18
2.9	Spatial Assignment of Parameters	19
2.10	Boundary Conditions.....	19
2.11	Stochastic Modelling.....	19
2.12	Implicit representation of Tabular Features (Fracture Zones) using IFZ.....	20
3	Physical processes that can be modelled in Continuous Porous Medium models.....	23
3.1	Groundwater flow.....	23
3.1.1	Physical Processes.....	23
3.1.2	Parameters Required.....	23
3.1.3	Initial and Boundary Conditions.....	24

3.1.4	2D Areal Groundwater Flow.....	24
3.2	Groundwater Flow and Heat Transport.....	24
3.2.1	Physical Processes.....	24
3.2.2	Parameters Required.....	25
3.2.3	Initial and Boundary Conditions.....	26
3.3	Unsaturated Groundwater Flow.....	26
3.3.1	Physical Processes.....	26
3.3.2	Parameters Required.....	26
3.3.3	Initial and Boundary Conditions.....	27
3.4	Unsaturated Groundwater Flow and Heat Transport.....	28
3.4.1	Physical Processes.....	28
3.4.2	Parameters Required.....	28
3.4.3	Initial and Boundary Conditions.....	29
3.5	Radionuclide Transport.....	29
3.5.1	Physical Processes.....	29
3.5.2	Parameters Required.....	30
3.5.3	Initial and Boundary Conditions.....	30
3.6	Radionuclide Transport in Unsaturated Flow.....	31
3.6.1	Physical Processes.....	31
3.6.2	Parameters Required.....	32
3.6.3	Initial and Boundary Conditions.....	32
3.7	Coupled Groundwater Flow and Solute Transport.....	33
3.7.1	Physical Processes.....	33
3.7.2	Parameters Required.....	33
3.7.3	Initial and Boundary Conditions.....	34
3.8	Coupled Groundwater Flow, Solute Transport and Heat Transport.....	34
3.8.1	Physical Processes.....	34
3.8.2	Parameters Required.....	35
3.8.3	Initial and Boundary Conditions.....	36
4	Numerical methods used for Continuous Porous Medium models.....	37
4.1	Spatial Discretisation.....	37
4.1.1	Approach.....	37
4.1.2	Grid Generation.....	37
4.1.3	Formulation of the Equations.....	39
4.1.4	Use of Constraints.....	40

4.2	Temporal Discretisation	41
4.3	Solution Methods and Treatment of Non-Linearities	42
4.4	Mass-Conserving Particle Tracking	42
4.5	Using the Mass-Conserving Method to Create a Particle Tracking Library	45
4.6	Rock Matrix Diffusion	47
4.6.1	Finite Volume Implementation of Rock Matrix Diffusion	48
4.7	Reactive Transport.....	51
5	Concepts within the Discrete Fracture Network model.....	55
5.1	Model Domain	56
5.2	Fracture Generation.....	57
5.3	Fracture Network Characterisation	58
5.4	Known Fractures	60
5.5	Random Fractures	61
5.5.1	Variable Apertures on Fractures	62
5.5.2	Fracture Subdivision (“Tessellation”).....	62
5.6	Engineered Features.....	63
5.7	Fracture Intersections.....	64
5.8	Boundary Conditions.....	65
6	Numerical Methods used for Discrete Fracture Network Models.....	66
6.1	Geometric Analysis	66
6.2	Percolation Analysis.....	66
6.3	Steady State Constant Density Groundwater Flow.....	66
6.4	Full Permeability Tensor (Upscaling).....	75
6.5	Efficient Implementation	76
6.6	Calculation of Effective Permeabilities for Many Blocks.....	77
6.7	Effective Permeability of an Internal Block.....	77
6.8	Transient Flow Modelling.....	78
6.9	Engineered Features.....	80
6.10	Two-Dimensional Networks	80
6.11	Modelling the Effect of Stress on a Fracture Network	81
6.12	Tracer Transport.....	81
6.12.1	Exact Particle Tracking (Standard Method)	82
6.12.2	Exact Particle Tracking (Mass-Conserving Method)	82
6.12.3	Approximate Particle Tracking	85
6.13	Coupled Groundwater Flow and Salt Transport	87

6.14	Multi-Component Solute Transport	91
6.14.1	Background	91
6.14.2	Mathematical Representation of Multi-Component Solute Transport in DFN	92
6.14.3	Implementation of Multi-Component Solute Transport in DFN	92
6.15	Rock Matrix Diffusion in a DFN Model	94
6.15.1	Background	94
6.15.2	Mathematical Representation of RMD in a DFN	94
6.15.3	Implementation of RMD in a DFN	95
6.16	Reactive Transport in DFN Models.....	96
6.16.1	Introduction	96
6.16.2	Rock Matrix Diffusion.....	96
6.16.3	Mineral Quantities	96
7	Concepts within Combined Models.....	98
7.1	Nesting of Sub-Models.....	98
7.2	Representation of Fractures	100
7.3	Current Physics	102
7.3.1	CPM Physics	102
7.3.2	DFN Physics.....	102
7.3.3	Nested DFN/CPM physics.....	102
7.4	Boundary Conditions.....	103
7.4.1	DFN Equations	103
7.4.2	CPM Equations.....	104
7.5	Interface Conditions.....	104
7.5.1	Approach 1 (“Mass Lumping”).....	104
7.5.2	Approach 2 (“Distributed Flux”).....	105
7.6	Transport	106
8	Simulation Setup and Execution	107
8.1	ConnectFlow Graphical User Interface	107
9	Output.....	110
9.1	CPM Outputs.....	110
9.2	DFN Outputs	112
9.2.1	Standard Output File	112
9.2.2	Graphical Output.....	113
9.2.3	Inspecting the Network.....	113
9.2.4	Examining the Pressure and Flow Solutions	113

	9.2.5 Tracer Transport	113
	9.2.6 3D Visualisation.....	114
10	Nomenclature and Units	116
11	References	119

Executive Summary

ConnectFlow is Amentum's suite of groundwater modelling software that combines a continuum porous medium (CPM) module and a discrete fracture network (DFN) module. ConnectFlow can be used very flexibly to model groundwater flow and transport in both fractured and porous media on a variety of scales.

The following documentation is available for ConnectFlow:

- ConnectFlow Technical Summary Document;
- ConnectFlow Command Reference Manual;
- ConnectFlow Verification Document;

This document, the Technical Summary Document, provides information on the calculation methods used by ConnectFlow, which gives understanding of the mathematical basis for the results obtained.

COPYRIGHT AND OWNERSHIP OF ConnectFlow

The ConnectFlow program makes use of the TGSL subroutine library.

All rights to the TGSL subroutine library are owned by Amentum.

All documents describing the ConnectFlow program and TGSL subroutine library are protected by copyright and should not be reproduced in whole, or in part, without the permission of Amentum.

1 Introduction

ConnectFlow is Amentum's suite of groundwater modelling software that includes the capability to model continuum porous medium (CPM) models and discrete fracture network (DFN) models, as well as nested sub-models into a combined CPM/DFN model. Hence, ConnectFlow is very flexible tool for modelling groundwater flow and transport in both fractured and porous media on a variety of scales.

This document provides a general overview of ConnectFlow, including a description of the equations solved and the numerical methods used. This document describes technical aspects of building and solving separate or nested CPM/DFN models. Additional more detailed information about the capabilities and potential applications of ConnectFlow is available from Jacobs on request.

ConnectFlow is written in standard Fortran 2003 and is therefore portable across a range of computing platforms, from desktop PCs running windows to Linux clusters. The software is available from Amentum by contacting the support team (gw.support@global.amentum.com) or from a download at www.connectflow.com.

ConnectFlow is also available through the international collaboration within the iCONNECT Club (see section 1.6.1).

1.1 Documentation

A comprehensive set of documentation has been produced for ConnectFlow. The following manuals are available:

- **ConnectFlow Technical Summary Document** (this document). This document provides a general technical overview of the software, including a description of the equations solved and the numerical methods used.
- **ConnectFlow Online Help**. Part of the ConnectFlow graphical user interface (GUI), it describes how to use ConnectFlow. It also includes tutorials covering the main functionality of the software.
- **ConnectFlow Verification Document**. This document describes the testing of ConnectFlow's capabilities.
- **ConnectFlow Reference Manual**. A set of HTML pages that describe, in detail, the commands and keywords available in the ConnectFlow input language used to specify the model, the calculations to be carried out, and the post-processing required. The command hierarchy is reproduced by the hyperlinks between the pages.

1.2 Continuum Porous Medium (CPM) Capabilities

The Continuous Porous Medium (CPM) modelling module was the first part of ConnectFlow to be developed. It has been developed over a period of more than 30 years (since 1984) and has been verified extensively in international comparison exercises.

The CPM module can be used to model the following physics and geometries:

- groundwater flow in saturated and unsaturated conditions;
- saline groundwater flow with density dependent on concentration;
- coupled groundwater flow and heat transport with density dependent on temperature;
- saline groundwater flow and heat transport with density dependent on concentration and temperature;
- solute transport with chemical reactions;
- groundwater flow and solute transport in a dual porosity system;
- contaminant transport, including the effects of advection, dispersion, sorption and with solubility limitation;
- radioactive decay chains, including interacting chains linked by solubility limitation of a common radionuclide;

- flow and transport in 3D, 2D vertical sections, 2D areal and 2D radial geometries;
- steady-state and time-dependent behaviour;
- deterministic and stochastic continuum modelling;
- sensitivity to model parameters, using the adjoint sensitivity method.

The CPM module can be used to model the following features:

- complex lithology distributions;
- conductive and semi-impermeable fracture zones;
- stochastic models of permeability and porosity;
- 3D volumes of enhanced or reduced permeability;
- boreholes, tunnels and shafts both in terms of geometry and as boundary conditions;
- specified value (Dirichlet) and specified flux (Neumann) type boundary conditions;
- non-linear infiltration model of surface recharge/discharge areas and magnitude;
- hydrostatic boundary condition and outflow conditions for vertical boundaries;
- time-varying boundary conditions to model land uplift, or time-dependent contaminant discharge;
- sources of heat, salinity or contaminant at points or in volume.

CPM models and results can be displayed by:

- 3D visualisation system allows 3D rendering of finite-elements, rock types, permeability, variables, fracture zones, flow arrows, pathlines;
- 2D plot output and numerical output includes:
 - plots of the finite-element mesh and its boundaries;
 - plots of contours of a variable on a surface;
 - plots of contours of a variable on a 2D slice;
 - plots of velocity arrows, showing direction and magnitude of the groundwater flow;
 - plots of pathlines either for steady state or for transient groundwater flows;
 - plots of backward pathlines, showing the region of influence of a borehole;
 - graphs of variables along a line;
 - graphs of the evolution of variables at a point;
 - graphs of data;
 - integrals (e.g. flux of groundwater across a plane);
 - variable values at specified points.

CPM models have been used in the following applications:

- Calculations in support of safety assessments for radioactive waste disposal programmes:
 - regional groundwater flow;
 - site investigation;
 - pump test simulation;
 - tracer test.
- Modelling for groundwater protection schemes:
 - aquifer;
 - saline intrusion.
 - Modelling to design and evaluate remediation strategies;
 - aquifer contamination;
 - landfill site.

The CPM module is used in support of the radioactive waste disposal programmes of many countries throughout the world, by both the nuclear regulators and by national disposal organisations and consultants working for these organisations.

The CPM module has a wide range of facilities for specifying the model domain, the properties of the rocks, fluids and solutes within the domain, the equations to be solved and the output options required. An advanced 3D visualisation package is available for a visual display of models and results. In addition to these standard facilities, many options are available that allow the user to customise the functionality of the module for a particular project. For example, it is possible for the user to specify a site-specific relationship between fluid density, solute concentration, fluid temperature and pressure.

1.3 Discrete Fracture Network (DFN) Capabilities

The discrete fracture modelling module has been developed over a period of more than 25 years (since 1992) and has been verified extensively in international comparison exercises (e.g. STRIPA and TRUE block).

Simulation of fluid flow and transport in fractured rock is an essential tool for the study of water resources, oil and gas reservoir management, assessment of underground waste disposal facilities, evaluation of hot dry rock reservoirs, and for the characterisation and remediation of contaminated land management. It can be used to interpret field and laboratory data, to validate conceptual models, to make quantitative predictions, and to develop practical solutions for a range of environmental, reservoir engineering, and civil engineering problems.

The DFN module is a finite-element software package for modelling fluid flow and transport in fractured rock. A discrete fracture network (DFN) approach is used to model fluid flow and transport of tracers and contaminants through the fractured rock. The DFN module incorporates fracture generation, flow simulation, upscaling, transport and 3D visualisation capabilities. The Graphical User Interface allows models to be generated and analysed quickly. A job submission ('batch') facility is included that allows additional options not yet implemented in the GUI to be accessed - these features are indicated below.

The DFN module has a number of sophisticated capabilities including:

Geological modelling:

- the flexibility to model a variety of scales varying from well/borehole scale to the regional/reservoir scales. Detail can be included to model heterogeneity of a single heterogeneous fracture as well as models with many tens to millions of fractures at a regional or reservoir scale.
- the DFN approach allows users to compare aspects of their conceptual geologic models and field observations with simulated models. This comparison includes, fracture orientation, size, transmissivity and flow distribution. An examination of the simulated network can be performed using hypothetical cores, stereonets, fracture maps and connectivity analysis.
- generation of regular and irregular meshes and structural grids (e.g. ZMap, VIP, FEMGEN and a CAD format);
- inclusion of deterministic fractures by specification within the DFN data or by importing a fracture file (e.g. GOCAD Vset, GOCAD Tsurf, Seisworks pointsets and other international formats). Deterministic Faults (or structures) can be used to control populations of stochastic fractures (i.e. proximity or 'Damage Zone' models). For example, the DFN module allows the clustering of fractures around parent fractures, random points or surfaces. It also allows spatially varying fracture densities based on 3D maps of fracture drivers;
- variable distribution laws for stochastic fracture parameters. The DFN module can generate stochastic fractures from a wide variety of probability distribution functions.
- coupling of distributions/parameters to same features i.e. length-aperture relationships.
- areal / volumetric distribution of stochastic fractures can be imported from external map or grid data- e.g. bed thickness, curvature ('strain'), lithological (mechanical) variation.

- dynamic behaviour of ‘production fractures’ and present-day stress can be incorporated.
- all scale ranges, from core observation to seismic scale, can be simulated and integrated into the final model.
- high permeability ‘matrix streaks’ may be incorporated into models as extra flow conduits.
- flow in the matrix can be represented by additional flow channels.

The DFN module is able to:

- simulate steady-state or transient flow in a fracture-network;
- enable steady-state calculations to be performed on very large networks, because it uses an efficient finite-element scheme;
- calculate the full equivalent continuum permeability tensor including off-diagonals, principal values and directions. This is automated to sample flows in several different directions. This can be used for upscaling, analysis of scale dependencies and determination of the representative elementary volume (REV);
- calculate porosity and inter-fracture matrix block size;
- identify connected fracture clusters around wells;
- predict transient pressures and drawdowns at well bores for various types of pump tests;
- calculate steady-state and transient inflows to tunnels and shafts;
- calculate the effects of hydro-mechanical coupling. The hydraulic aperture is coupled to a stress distribution based on an analytical description of the stress field due to either rock overburden or a radial stress around a tunnel;
- simulate tracer transport through the network using a stochastic particle tracking method. Output includes plots of breakthrough curves for many thousands of particles, particle tracks, swarms of particles at specified times or the points of arrival on the surfaces of the model. This can be used to calculate dispersion of a solute transported by the groundwater;
- simulate mass transport for a variable density fluid. This can be used to model coupled groundwater flow and salt transport;
- simulate unsaturated flow in fractured rocks;
- analysis of percolation between surfaces;

The DFN module can be used for the following applications:

- simulation of a range of hydrogeological tests (hydraulic borehole/well tests, including constant, head, pressure and flow tests);
- site and regional scale modelling to determine the effects of various forms of fracture flow to determine, pressure distributions, flows and travel times to discharge points under natural conditions;
- to understand and simulate the behaviour of fracture-influenced sites/reservoirs by being able to parameterise and justify heterogeneous continuum models. For example, the estimation of equivalent parameters for input to conventional dual-porosity simulators;
- simulation of solute transport (tracer) experiments;
- simulation of hydraulic impact of a tunnel or shaft construction;
- simulation of various simple hydromechanical models for the purpose of estimating the impact of rock overburden and in-situ stress.

The DFN module has been used in the following industries:

- water resources for the purpose of hydraulic test and tracer simulation, fractured reservoir estimation and parameterisation, and remediation studies (such as the estimation of fracture flow in dual porosity systems). In addition, it can be used to model saline ingress and unsaturated flow;

- deep radioactive waste disposal, as both a tool useful for site-characterisation and safety assessments (simulation of hydrogeological tests and estimation of flow distributions and travel times to the biosphere);
- oil and gas industry to aid well planning, simulation of various well tests (PBU etc), and the parameterisation of oil simulation software by calculation of up-scaled equivalent continuum parameters (permeability, porosity and matrix block-size and distribution);
- hot-dry rock studies to estimate connectivity and parameters (permeabilities), to help analyse the effectiveness of the fractured reservoir;
- civil engineering projects concerned with construction or remediation in fractured rock. This includes the estimation of water ingress due to excavation of tunnels, studies of underground oil caverns, dam construction in fractured rocks, remediation or containment of contaminated fractured sites.

1.4 Combined (CPM/DFN) Capabilities

The module that allows the construction of a nested CPM/DFN models has been developed over a period of more than 20 years (since 1996).

ConnectFlow can be used to model the following physics and geometries for combined models:

- 3D models only;
- single or multiple DFN sub-regions nested within CPM regions;
- single or multiple CPM sub-regions nested within DFN region;
- stratigraphic layers with DFN representation can be interfaced to layers with a CPM representation;
- models are built up of grids with different patches being assigned to either a CPM or DFN subdomain;
- nesting of detailed DFN models within nested CPM models using embedded ('constraint') grids to represent site-scale and region-scales;
- stochastic DFN and CPM models;
- steady-state and transient constant-density groundwater flow;
- advective transport through a combined DFN/CPM based on a particle tracking approach.

ConnectFlow can be used to model the following features:

- local DFN models to represent the detailed flow in fractures around tunnels, shafts, canisters or boreholes nested within a CPM model that extends the model to appropriate boundaries;
- detailed CPM models of tunnels, shafts and canisters within a DFN model to represent the interaction between flow in a fractured media and backfilled tunnels;
- continuous representation of deterministic faults/fracture zones through the DFN and CPM sub-models using consistent data formats and a combination of explicit fracture planes in DFN regions and an implicit fracture zone (IFZ) method in the CPM region.
- quantifying conceptual uncertainties between DFN and CPM models.

1.5 Quality Assurance

A Quality Assurance (QA) programme defines a set of procedures for carrying out a particular type of work in such a way as to maintain the quality of the work. A well designed QA programme plays an important role in computer program maintenance by ensuring that high standards of coding are adhered to. There are procedures for reporting and fixing program errors and that there is a system for testing and issuing new releases of the program which ensures that the new program gives the correct results for a standard set of test cases.

ConnectFlow is maintained and developed under an appropriate QA programme [e.g. Morris et al., 1996] by Jacobs. The QA programme conforms to the international standard ISO 9000. The Subversion source maintenance program is used to store all source code, documentation and test

data for ConnectFlow. This automatically logs the author and date of each change to the system, and enables previous versions of the code to be accessed and recreated if necessary. All changes are thoroughly tested, and must be approved by the Software Manager before they are accepted. A comprehensive set of test cases is used to test each new release. The verification of the software is described in the ConnectFlow Verification Document. Through the ConnectFlow QA programme, Jacobs seeks to continually improve the quality and reliability of ConnectFlow.

1.6 ConnectFlow Users

ConnectFlow has been used by a significant number of organisations throughout the world, including the following:

- Department of the Environment, UK;
- United Kingdom Nirex Limited, UK;
- RM Consultants, UK;
- British Nuclear Fuels Limited (BNFL), UK;
- Golder Associates, UK;
- Entec, UK;
- British Geological Survey (BGS) Keyworth, UK;
- University of Bath, UK;
- University of Birmingham, UK;
- Gesellschaft fur Reaktorsicherheit (GRS), Germany;
- Federal Office for Radiation Protection (BfS), Germany;
- Federal Institute of Geosciences, Germany;
- Swedish Nuclear Fuel and Waste Management Company (SKB), Sweden;
- Swedish Nuclear Power Inspectorate (SKI), Sweden;
- Kemakta Consultants, Sweden;
- Conterra AB, Sweden.;
- Agence Nationale pour la Gestion des Déchets Radioactifs (ANDRA), France;
- National Co-operative for the Disposal of Radioactive Waste (NAGRA), Switzerland;
- Colenco Power Consulting Ltd, Switzerland;
- Swiss Federal Institute of Technology, Switzerland;
- Diamo, Czech Republic;
- Korea Atomic Energy Research Institute (KAERI), South Korea;
- Korea Electric Power Corporation (KEPCO), South Korea;
- Hyundai Engineering and Construction Company, South Korea;
- Georgia Institute of Technology, USA.

1.6.1 The iCONNECT Club

The **iCONNECT** club (*integrated CONtinuum and NEtwork* approach to groundwater flow and Contaminant Transport) is Jacobs' response to the desire expressed by those involved in radioactive waste management to address a range of generic and site-specific issues related to the evaluation of the geosphere as part of a safety assessment.

The purpose of the **iCONNECT club** is to draw like-minded organisations together into a club in order to dilute the costs of addressing modelling issues, in particular those generic issues faced by organisations wanting to evaluate the performance of the geosphere as part of a repository safety assessment. The **iCONNECT club** acts as a forum for the focused application and enhancement of the ConnectFlow methodology, resulting in wide-ranging benefits to all participants.

2 Concepts within the Continuous Porous Medium model

2.1 Relevant Physical Processes

The aim of this section is to identify a list of physical processes relevant to groundwater flow and transport that can be investigated using a CPM model in ConnectFlow, and then to present the approach to the modelling of the phenomena that is adopted within ConnectFlow. Many other processes that occur in subsurface flows (e.g. those relating to transport of radionuclides in the gas phase or colloidal transport) are not considered further because these processes are not included in the models that have been implemented so far. The processes that can be explicitly modelled in a CPM model are summarised in the rest of this section. The CPM models used are then discussed in subsequent sections.

The following is a list of FEPs (features, events and processes) identified by the NEA as relevant to subsurface flow in the performance assessment of a repository:

- 1.2.5 Hydrothermal Activity;
- 1.3.7 Hydrogeological response to climate
- 1.4.6 Groundwater extraction
- 2.1.6 Hydrogeological changes and response
- 2.1.8 Thermal changes and response
- 2.2.3 Hydrogeological regime
- 2.2.4 Hydrochemical effects
- 2.2.5 Groundwater flow system
- 2.2.6 Solute transport
- 2.2.10 Dilution processes
- 2.2.10 Heterogeneity
- 3.1.1 Radioactive decay and ingrowth
- 3.1.3 Water mediated transport (including advection, dispersion, diffusion and rock matrix diffusion.)
- 3.1.5 Sorption / desorption processes.
- 3.1.10 Dilution processes
- 3.1.11 Transfer by human actions (drilling, mining, excavation, etc.)

In the following sections, the conceptual model to represent these processes is described along with the parameterisation of the models.

In each case, the theoretical and experimental justification for the treatment of the process in the model is presented. In particular, the issue of whether the treatment is conservative or realistic is discussed.

2.2 Groundwater Movement

The soils and rocks that make up the Earth's crust generally are porous, that is they contain empty spaces which can be occupied by groundwater. This empty space is the porosity of the rock, and is defined as the fraction of the volume of the rock that is accessible to groundwater. If the spaces are interconnected then the groundwater may flow under the action of external forces [Jacobson, 1949; Bear, 1972 and 1979; Freeze et al., 1979; De Marsily, 1985]. Generally speaking, groundwater velocities are extremely small.

Nevertheless, flowing groundwater can transport dissolved substances over significant distances if sufficient time is available. In the context of a deep radioactive waste repository, it is important to ensure that groundwater movement does not return unacceptable quantities of radionuclides from the repository to the human environment.

The most common approach to modelling groundwater flow, and the approach used in the CPM module, is the continuum approach. The idea is to treat all the quantities of interest, such as the pressure in the groundwater, as quantities that vary continuously over space. There are two ways of defining these continuous quantities. In the first, the notion of a Representative Elementary Volume (REV) is introduced [Bear, 1972]. This is a volume of rock that is very large compared to length scales characteristic of the microscopic structure of the rock, but small compared to the length scales of interest from the viewpoint of groundwater flow. The continuum quantities are defined as spatial averages over the REV's. In the second, the medium is thought of as being a realisation of a random process [De Marsily, 1985]. The quantities of interest are now defined as ensemble averages. Although the two approaches are philosophically quite different, they lead to virtually the same governing equations for groundwater flow.

In some rocks most of the groundwater actually flows through an interconnected network of fractures. This leads to a quite different approach to modelling groundwater flow known as fracture-network modelling, in which the flow through an explicitly modelled set of fracture planes is calculated [Jacobson, 1949; Bear, 1972 and 1979; Herbert et al., 1991a]. This approach is supported in the DFN module. One potential use of these fracture network models is to determine the appropriate values to use for the effective permeability of a block of fractured rock, if it is to be represented appropriately in a continuum model such as used in the CPM module. Thus, the fact that the CPM module is based upon a continuum-porous-medium approach does not mean that the models described in this document cannot be used to represent flow and transport within a fractured rock. Provided that the scale of interest in the flow and transport calculation is larger than the length scale of the individual fractures and is large enough to include several fractures, it is reasonable to use a porous medium approach to represent flow and transport through the fracture network.

The movement of groundwater is described quantitatively by the specific discharge, \mathbf{q} , sometimes called the Darcy velocity. This is the volumetric rate of flow of water per unit cross-sectional area. The specific discharge, \mathbf{q} , is calculated in the CPM module from Darcy's law [Bear, 1972 and 1979; Freeze et al., 1979; De Marsily, 1985],

$$\mathbf{q} = -\frac{\mathbf{k}}{\mu} (\nabla P^T - \rho_l \mathbf{g}) \quad \text{Equation 2-1}$$

This law is empirical. However, it can be shown that Darcy's law is basically an expression of the law of conservation of momentum for the fluid. The fundamental model for flow of a viscous fluid is embodied in the Navier-Stokes equations [Batchelor, 1967] and in principle these could be used. However, it would be impractical and inappropriate to apply these equations in the geosphere models used in performance assessments. The situation of interest is then the flow of fluid through

the connected void spaces in the rock. In order to apply the Navier-Stokes equations it would be necessary to specify the geometry of the void space. This is clearly impractical. It would also be inappropriate. Such a model would provide far more detail than is actually required. The appropriate expression of the law of conservation of momentum for the fluid in these circumstances is given by Darcy's law, which can be derived from the Navier-Stokes equations of fluid flow for certain simplified models of the microscopic structure of the rock (see e.g. Scheidegger, 1974).

Darcy's law was originally derived from experiments on flow through sand columns. It has since been demonstrated experimentally to apply over a wide range of conditions. Darcy's law also forms the basis for innumerable calculations of groundwater flow in water resources engineering and of the production of oil in oil reservoir models. It can therefore be considered to be a well-validated model, for the circumstances of interest. However, it should always be borne in mind when constructing models based on this approach that deviations from Darcy's law have been observed at very high flow rates, when the flow is not purely laminar [Bear, 1979; De Marsily, 1985; Scheidegger, 1974] (which can occur close to wells, for example). Possible deviations from Darcy's law have also been suggested for very small hydraulic gradients, where in some types of materials the flow may be zero below a critical value of the hydraulic gradient [De Marsily, 1985]. Theoretical considerations suggest that under transient conditions, an additional term will appear in Darcy's law, although in practice this term will be negligible except at short times following a sudden large change in conditions [De Marsily, 1985]. The use of Darcy's law can therefore be regarded as realistic, or at worst to lead to an overprediction of the flow rate, for the types of systems of relevance to a performance assessment.

The question arises of what value to assign for the permeability of the rock, since, in practice, rock properties are rarely, if ever, homogeneous. The approach adopted will depend on the nature of the rock system, and the quality of data available, but essentially it is necessary to assign an effective permeability to the hydrogeological unit, which will lead to the correct flow in an average sense.

In the case of highly fractured rock, it may not be possible to assign an effective property that adequately reproduces the correct average flow behaviour. In this case it may be possible to represent the system as two coexisting continua, one corresponding to the fractures, and one corresponding to the rock matrix [Warren et al., 1963]. In the steady state, this simplifies to a single continuum described by a single effective permeability, but in transient flow, pressure variations can be transmitted through the fractures more rapidly than through the matrix. This type of model is not currently supported in the standard release of ConnectFlow, although a specially modified version has been used to study this type of system in the past. In extreme cases, an explicit fracture-network approach may be better able to represent the groundwater movement.

The groundwater flow depends on the fluid viscosity, through Darcy's law. The viscosity will in general be a function of temperature, and can vary by as much as 50% over the range 10 - 100°C. It may also be a function of salt concentration. In ConnectFlow, this can be modelled by making the viscosity an arbitrary function of temperature and salt concentration.

In unsaturated conditions, the accessible porosity is less than the saturated porosity by a factor called the saturation, S . S is a function of pressure, and in ConnectFlow can be modelled as an arbitrary function of pressure. The permeability is also normally reduced in the unsaturated case by a factor k_r called the relative permeability. The relative permeability can be modelled as an arbitrary function of pressure.

It should be noted that ConnectFlow does not treat the generation or transport of gas, which may influence the movement of groundwater. This approximation is neither realistic nor conservative,

but can be addressed by the use of other models specifically designed to model the effects of gas generation and transport [Agg et al., 1994].

2.3 Groundwater Pressure

In hydrogeology, it is useful to distinguish between two different descriptions of the pressure associated with the groundwater at a given location.

The first description is in terms of the total pressure, P^T , which is the pressure commonly used in other branches of physical sciences and which would be measured using a device such as a manometer. It is measured in units of Pascals. The second description involves the “residual pressure”, P^R , (also referred to as the “non-hydrostatic pressure”). The residual pressure is defined with respect to the selected reference elevation (with respect to which all vertical positions are defined). It is often the case in groundwater studies that the reference elevation lies above the location where the total pressure is measured (because the reference elevation is defined with respect to sea level or a convenient ground surface elevation). The residual pressure, P^R , is then the pressure that is obtained after subtraction from the total pressure of the hydrostatic pressure due to a freshwater column that extends vertically from to the location where the total pressure is measured to the reference elevation (see section 3.1). This explains the name. The residual pressure is also measured in units of Pascals. If the reference elevation lies below the point at which the total pressure is measured then the residual pressure would actually be the total pressure augmented by that of a freshwater column of the appropriate length. The residual pressure is a useful concept, because, according to Darcy’s law, groundwater flow is proportional to the gradient in the residual pressure (see section 3.1).

The familiar concept of groundwater or hydraulic “head” [Bear, 1979] is a quantity closely related to the residual pressure. Hydraulic head is the residual pressure divided by the specific weight of the groundwater (see section 3.1). Hydraulic head is therefore measured in metres. Hydraulic head is useful for two reasons: firstly, Darcy’s law can be conveniently formulated in terms of hydraulic head and hydraulic conductivity (the latter being a quantity depending on properties of both rock and fluid), and, secondly, hydraulic head is very easily measured in the field. For a well that is only open to the formation at a particular level, the height to which water rises in the well is equivalent to the groundwater head at the level of the opening. However, a more general formulation in terms of pressures is more convenient when it is necessary to treat cases in which variations in the groundwater density (e.g. due to variations in groundwater temperature or salinity) have to be taken into account.

The total groundwater pressure, P^T , can be calculated from Darcy’s law (Equation 2-1), together with the equation of conservation of mass,

$$\frac{\partial}{\partial t}(\varphi\rho_l) + \nabla \cdot (\rho_l \mathbf{q}) = 0 \quad \text{Equation 2-2}$$

These two equations lead to a single second-order equation for the total pressure,

$$\frac{\partial}{\partial t}(\varphi\rho_l) - \nabla \cdot \left(\rho_l \frac{\mathbf{k}}{\mu} (\nabla P^T - \rho_l \mathbf{g}) \right) = 0 \quad \text{Equation 2-3}$$

This is the basic equation that is solved in the CPM module. It is straightforward to formulate the pressure equation in terms of total pressure, residual pressure, or pressure head, and all three formulations are supported.

In general, the density and viscosity of the water depend on temperature and on the groundwater chemistry, in particular the presence of solutes, especially salt. Temperature and salt are in turn transported by the groundwater. When the variations in temperature or salt concentration are large

enough to produce significant changes in density or viscosity, it is necessary to couple the solution of the groundwater flow problem to that of the heat or salt transport problem. This is discussed in sections 2.4 and 2.5.

2.4 Groundwater Chemistry

Groundwater chemistry can affect groundwater movement by changing the density or the viscosity of the groundwater. These changes are likely to be dominated by the presence of dissolved salt. This is because salt is the only mineral normally present in rocks in sufficient quantities and with a sufficient solubility to be found in groundwater in concentrations significant enough to affect its physical properties. Salt is therefore normally the only dissolved mineral modelled in the CPM module. This approximation is not necessarily conservative, but is likely to be realistic in all cases of interest. However, it is also possible to represent a wider variety of solutes, either as reference waters or as individual components. For the component representation, it is also possible to carry out chemical reaction calculations.

In CPM models the density of the groundwater is generally modelled using a mass-fraction formulation:

$$\frac{1}{\rho_l} = \frac{c}{\rho_{c0}} + \frac{1-c}{\rho_0} \quad \text{Equation 2-4}$$

However, the user can specify the relationship between the groundwater density and the concentration of total dissolved solids, in order to reflect conditions appropriate to a particular site.

The viscosity of the fluid is generally assumed to be independent of the salt concentration. However, there is no fundamental difficulty in taking account of this effect. Cases in which this has been done have been treated in the past.

The model of the transport of salt by groundwater takes account of the same processes as that for radionuclide transport, i.e. advection, diffusion, hydrodynamic dispersion and anion exclusion. In the conditions prevailing at depth, sorption of the salt ions is not usually considered to be a significant effect. However, chemical effects, such as dissolution/precipitation of minerals or ion exchange processes can be included.

In principle, the groundwater chemistry can affect the transport of radionuclides by modifying the solubility limit of the radionuclides, and by increasing or decreasing the amount of sorption that they undergo. These effects can be taken into account in a CPM model as follows.

For some radionuclides it can be anticipated that the concentration in the repository will be maintained at the solubility limit until sufficient radionuclide has been removed to allow the concentration to fall below the solubility limit, whence the repository concentration becomes inventory limited. The period of solubility limitation can be estimated, based on the groundwater flow rate through the repository (which can be estimated from the CPM model of the site), the repository volume accessible to the radionuclide and the radionuclide inventory. The migration of the radionuclide from the repository, taking account of solubility limitation can then be modelled in a two-stage CPM radionuclide transport calculation. In the first stage, which covers the time period of solubility limitation, the radionuclide concentration at the repository is maintained at the solubility limit. The second calculation then uses the results of the first as an initial condition.

In the CPM model, sorption is modelled by a linear equilibrium model, as described in section 2.6.5. This simple model is effectively characterised by a parameter K_d , the sorption distribution coefficient (equal to literature K_d multiplied by rock density). In the current release of ConnectFlow, K_d is simply specified as a constant for each hydrogeological unit and is not explicitly related to the calculated groundwater chemistry in the unit. However, if appropriate values of K_d are used, that

take into account the prevailing groundwater chemistry in different rock units, then the effect of groundwater chemistry on sorption can be modelled fairly realistically.

2.5 Temperature / Heat

The principal effect of changes in temperature in the far field is to cause changes to the groundwater density and viscosity, which leads to changes in the groundwater movement.

Changes in density as a result of temperature changes are usually no more than a few percent, for any temperature normally encountered in groundwater. The model used in the CPM module to simulate this change is to make the change in density equal to the product of the change in temperature and a constant called the coefficient of thermal expansion. This model may not be valid for large changes in temperature, but the resultant changes in fluid density are sufficiently small for this to be of little significance to the resulting groundwater movement and pressure.

Changes to the viscosity of the groundwater as a result of temperature changes are usually of more importance.

It is also possible that changes in temperature may affect the solubility and sorption of radionuclides. These effects are not modelled in the current release of ConnectFlow. However, the effect of temperature on chemical reactions is modelled when reactive transport is being carried out.

Temperature variations within the far field arise as a consequence of heat sources, and the transport of heat. Various sources of heat are potentially relevant, such as the natural radioactivity of the rock and the radiogenic heating of the repository itself. There are several ways in which these sources of heat can be represented in a CPM model. Regions of specified temperature or specified heat flux can be identified or distributed heat sources can be specified. The processes that result in the transport of heat are the same as or analogous to those that lead to the migration of radionuclides. However, one important difference is that heat energy can be conducted through the solid rock. In many low permeability environments, where the water velocities are low, conduction of heat through the solid rock is the most significant heat transport mechanism.

2.6 Radionuclide Transport

In the following subsections, the processes that can result in transport of dissolved radionuclides by groundwater are described in more detail. These processes can all be treated in the CPM module, albeit to different degrees of accuracy.

2.6.1 Advection

Advection is the process by which the dissolved radionuclides are transported simply by the displacement of the groundwater in rock pores or fractures. The advective flux, F_A , of a radionuclide is related to the specific discharge, q , (Equation 2-1) by

$$F_A = qN_\alpha \quad \text{Equation 2-5}$$

Although q has units of velocity, the actual water velocity in the pores is rather larger because the flow only takes place in the pores rather than over the whole area of the porous medium. The average water velocity in the pores is

$$v = \frac{q}{\phi} \quad \text{Equation 2-6}$$

In some rocks, some water is mobile and some water is immobile, and only the mobile water is directly considered in transport, so ϕ is the proportion of the rock volume taken up by mobile water, and is called the 'transport' or 'flowing' porosity. In fractured rocks, for example, it is often the case that the water in the fractures is mobile and water in the intact rock matrix is much less mobile.

2.6.2 Molecular Diffusion

Even when the driving forces are not sufficient for significant groundwater flow to occur, radionuclides will still migrate through the porewater as a result of molecular diffusion. The flux will be smaller than in free water, both because of the restricted area in the porous medium over which diffusion occurs and because of the tortuous nature of the pores. Fick's Law,

$$\mathbf{F}_D = -D_i \nabla N_\alpha \quad \text{Equation 2-7}$$

links the flux per unit surface area of porous medium, \mathbf{F}_D , to the concentration gradient [Jost, 1960]. Here, the intrinsic diffusion coefficient, D_i , is less than the free water diffusion coefficient and is related to the latter by a scaling factor that depends on the porosity and tortuosity of the rock.

Molecular diffusion in free water is a well-understood process and Fick's law is generally accepted in the scientific community as a valid model of the process. Models of diffusion in the presence of a porous medium are generally based on the application of scaling factors to the fluxes obtained from Fick's law for diffusion in free water. The scaling factors represent the effects of the presence of the solid material and of the tortuous nature of the void spaces. The values of the scaling factors are based on the measurements of the migration of radionuclides in laboratory experiments.

2.6.3 Hydrodynamic Dispersion

Transport of a dissolved species through a porous medium does not simply involve movement along a single well-defined path in the direction of the local velocity. Various processes act to spread the radionuclide about such a path and these processes are collectively termed 'hydrodynamic dispersion'. The hydrogeological properties of the rocks at any site will exhibit variability on all length scales. As a result of this variability, different paths through the medium will have different path lengths and different travel times. This variability in the transport paths is what gives rise to the processes of hydrodynamic dispersion. Qualitatively, dispersion acts in a similar way to diffusion.

Detailed, explicit modelling of the heterogeneity of the rocks at all length scales and of the resulting dispersion of radionuclides is not always practicable. Effective parameters are therefore often used to represent this aspect of the behaviour of the system. In such cases, dispersion is usually represented by a diffusion-like term in the transport equation, with the dispersive flux taken to be proportional to the concentration gradient, by analogy with Fick's law [Bear, 1979]. Different amounts of dispersion are generally observed parallel to and perpendicular to the flow, and the dispersion coefficient is taken to be a tensor. It is usually modelled by a 'geometrical dispersivity', where the coefficient is the product of the velocity and a dispersion length [Bear, 1979]. The dispersion length is generally larger in the direction of flow than transverse to it. Using detailed models of heterogeneity, the dispersion lengths can be shown to be related to the length scale of heterogeneities in the medium [Dagan, 1988 and 1989; Gelhar et al., 1983].

Hydrodynamic dispersion is a very complex process, and the Fickian model is an approximation. In general, very careful choices of the parameters that are used in the Fickian model will be necessary in order to ensure that the model is fit for purpose, or at least conservative. The validity of the model for a particular case depends on the nature of the variability in the rock properties and the relationship between the distance travelled by the radionuclides and the length scale of the variability.

One case that has been extensively studied is that in which the variability in the logarithm of the permeability can be represented by a Gaussian model with a well-defined length scale. In this model the travel distance of interest ranges from values smaller than the length scale of the variability to values greater than the length scale of the variability. Several analytical studies of the dispersive behaviour to be expected in such cases have been performed [Dagan, 1988 and 1989; Gelhar et al., 1983]. The analyses are only valid for cases in which the variance of the log-permeability field is

small (less than 1) and for the conditions of uniform mean flow in an infinite domain. Nevertheless, the analytical studies provide useful insights into the dispersion that is produced by the heterogeneity in the permeability field.

It is found that the dispersive flux is proportional to the concentration gradient, but that the dispersion coefficients are not constant, as assumed in the Fickian model, but depend on the distance travelled. The longitudinal dispersion coefficient, which characterises the dispersive spreading parallel to the mean flow direction, tends to a constant value, which for practical purposes is attained at distances equal to a few tens of the length scale of the variability itself. The length scale of the heterogeneity and the variance of the log-permeability determine the asymptotic value of the longitudinal dispersion coefficient. The transverse dispersion coefficients, which characterise the dispersive spreading transverse to the flow direction, tend to zero, so that, asymptotically, the transverse dispersion is not controlled by the heterogeneity but by the spreading process on a smaller scale than is represented in the Gaussian model, such as molecular diffusion.

In most cases the variance of the log-permeability values for real rocks is greater than 1, so that the approximations made in the analytical studies are not strictly valid. In order to investigate the dispersion produced by the heterogeneity in such cases, numerical Monte-Carlo studies are performed. This means that numerical realisations of spatially correlated random fields are generated to represent the rock properties (generally the log-permeability). Numerical calculations of groundwater flow and particle transport are then performed in each realisation and the results for the particle movements are analysed in order to assess the dispersion produced by the heterogeneity in the permeability.

It is important to ensure that the random fields that are generated have the intended statistical structure. A detailed discussion of this issue lies outside the scope of this document but it is noted that this requires a very careful choice of the parameters in the method that is used to generate the random field (see e.g. [Morris et al., 1997a]). If the permeability field is not generated with sufficient accuracy, then the dispersive behaviour that is obtained from calculations of flow and transport through the field will also be inaccurate. This was demonstrated in a Monte-Carlo study [Morris et al., 1997b] in which many realisations of a permeability field with a relatively small variance were generated.

Calculations of groundwater flow and particle transport through the realisations of the permeability field were performed using the CPM module. The variance of the permeability field had been chosen to be small and the conditions of the flow and transport calculations were set so that the analytical solution for the dispersive spreading of the particles [Dagan, 1988 and 1989] was valid. The results from the CPM calculations were compared with the analytical solution in order to assess the accuracy of the numerical calculations. It was found that the results of the Monte-Carlo study were very sensitive to the choice of the parameters used in the method used to generate the random fields. With an appropriate choice of parameters, good agreement could be obtained between the numerical and analytical results. This builds confidence in the numerical method and its use in circumstances in which the analytical approximations are not valid.

It should be noted that this study also provides a useful and quite stringent test of the groundwater flow and particle transport algorithms used in ConnectFlow. The fact that good agreement could be obtained between the analytical and numerical results for the dispersion of the particles indicates that then CPM model had provided an accurate solution for the groundwater velocities in a case with a heterogeneous permeability field. This case therefore also builds confidence in the validity of ConnectFlow.

ConnectFlow has also been used to perform a Monte-Carlo study of flow and transport in a heterogeneous permeability field at a real potential repository site [Cliffe et al., 1993]. In that case, the statistics of the transmissivity field for the heterogeneous formation were inferred from borehole data at the site. The variance of the log-transmissivity was much greater than 1. The calculations were used to investigate a number of issues associated with the heterogeneity, for example, the impact of different levels of site investigation on the uncertainties in the calculated travel times from the repository.

The validity of the Fickian model of dispersion and the investigation of alternative approaches, including models in which the heterogeneity is modelled explicitly are very active areas of research in many national programmes (e.g. [Baker et al., 1997; SKI, 1996; Norman, 1992]). An appropriate and consistent treatment of heterogeneity on all length scales is an important aspect of performance assessment calculations (e.g. [Jackson et al., 1997]).

2.6.4 Rock Matrix Diffusion

The process of rock-matrix diffusion is potentially significant in many fractured rocks [De Marsily, 1985; Neretnieks et al., 1980]. In such cases, most of the groundwater flow takes place through a network of interconnected fractures, which comprise the 'flowing porosity'. In addition to the flowing porosity, the rock matrix is itself porous. Radionuclides can be transported from the pore water in the flowing porosity into the relatively immobile water in the low permeability rock matrix by diffusion. This process retards the progress of radionuclides. For non-sorbed radionuclides, it is a retardation mechanism, because they would otherwise be transported at a velocity determined by the water velocity and the accessible flowing porosity. For sorbed radionuclides, rock-matrix diffusion also gives access to additional sorption sites away from fractures. Thus rock-matrix diffusion increases radionuclide travel times; it also acts as an additional dispersive process, since radionuclides that have diffused into the rock matrix can diffuse back out over a period of time, increasing the spread of travel times between early and late arrivals.

Understanding of the process of rock-matrix diffusion is developed both by a programme of laboratory experimental work [Baker et al., 1997] and by studies of rock-matrix diffusion in natural systems. A number of approaches exist which allow this effect to be modelled realistically.

2.6.5 Sorption

The migration of radionuclides through the geosphere is retarded by a number of geochemical processes, some of which are grouped together under the label 'sorption'. 'Sorption' is defined as a set of processes, excluding the formation of a discrete phase, by which radionuclides are partitioned between the solution and a solid surface. Of these processes, ion exchange and surface complexation appear to be the dominant processes of relevance in the geosphere. Both of these processes are observed in natural geochemical systems [Baker et al., 1997]. Both ion exchange and surface complexation are rapid processes, with equilibrium being established in a timescale accessible through laboratory experiments. In both cases, a relationship exists between the equilibrium concentration of radionuclide in solution and the concentration adsorbed on the mineral surface. At its simplest, and especially at the very low aqueous concentrations that are relevant for radionuclide transport calculations, it can be assumed that the ratio of 'adsorbed' to 'dissolved' radionuclide is constant and independent of the concentration of radionuclide in the system. This concept is termed 'linear sorption' and is a widely used model of these processes. Radionuclides can also be removed from solution by the incorporation of the radionuclide in the mineral structure.

In the model implemented in the CPM module, the geochemical retardation of radionuclides in the geosphere is represented as a simple linear sorption process characterised by a sorption distribution coefficient, K_d (equal to literature K_d multiplied by rock density). The extent of sorption is measured

in laboratory experiments that are carried out over timescales of the order of months or years in which equilibrium conditions are attained. It is therefore reasonable to assume that a similar equilibrium will be attained during the longer timescales of radionuclide transport through the geosphere. The assumption of equilibrium will be reasonable provided that the timescale of any transients associated with the sorption process is much less than the timescale for radionuclide transport by advection and dispersion.

The linear K_d approach to representing sorption is a simplification, since, for example, the experimentally measured sorption distribution coefficients are commonly observed to decrease at higher aqueous radionuclide concentrations. However, K_d values may be appropriately chosen so that the extent of sorption is adequately approximated over the concentration range of interest. Research in the Nirex Safety Assessment Research Programme (NSARP) confirmed and increased confidence that the linear K_d approach is an appropriate representation for the radionuclides of interest [Baker et al., 1997].

2.6.6 Anion Exclusion

Experimental observations indicate that the porosity of the rock matrix that is accessible by diffusion to some anionic species is less than that accessible to neutral species or to cations. This is believed to be the result of charge effects. Anions are excluded from a portion of the porosity owing to the effect of negatively charged mineral surfaces [Baker et al., 1997]. This effect can be represented in CPM models by using a simple exclusion factor, which is equivalent to the fraction of the porosity that is accessed.

2.6.7 Effect of Organic Complexants

Organic complexants may be present in the geosphere around the repository, although their concentrations will be diluted within the geosphere and they may undergo microbial degradation. The effect of the presence of organic complexants is to reduce sorption. A programme of work in the NSARP has been undertaken to address the impact of such organic complexants [Baker et al., 1997]. The effect of organic complexants can be represented in a CPM model by multiplying the sorption distribution coefficient that would be considered appropriate in the absence of organic complexants by a sorption reduction factor.

2.6.8 Radioactive Decay and Ingrowth

The processes of radioactive decay and ingrowth from parent radionuclides also affect radionuclide concentrations. Models of these processes have the status of widely accepted physical laws. Representations of radioactive decay are easily implemented as a sink term in CPM models of radionuclide transport. Accurate representation of the processes of decay and ingrowth for several members of a decay chain may require the simultaneous solution of models of radionuclide transport for several radionuclides. The CPM module can treat chains with up to 48 members (depending on the options selected) in this way.

2.7 Conceptual Models

In this section we describe the conceptual models used in CPM modelling. Before describing the various models, it is necessary to consider what a conceptual model means. For the purposes of this report we will use the definition put forward by Olsson et al. [Olsson et al., 1994]. According to these authors the ingredients that make up a conceptual model are: the processes modelled, the geometric framework, the parameters required by the model, the method of spatial assignment of the parameters and the boundary and initial conditions required by the model.

ConnectFlow is a very flexible and powerful tool that can be used to model a wide range of flow and transport phenomena in porous media. Any model of a system that is constructed using the CPM module will contain all of the elements of a conceptual model identified by Olsson et al. [Olsson et

al., 1994]. However, it is useful to present these ingredients of the conceptual model in two parts. This is because one of the powerful features of the ConnectFlow program is the way in which the full flexibility of the geometric framework and the method of spatial assignment of the parameters are available to all of the models of physical processes that are implemented. This means, for example, that many different types of finite-element discretisation can be used to represent the different physical processes that can be modelled with ConnectFlow. Thus, for example, if it were appropriate, different finite-element types could be used in the solution of the groundwater flow and the radionuclide transport equations for a particular system.

In the remainder of this chapter, the geometric framework, the method of spatial assignment of the parameters, some general features of the boundary conditions, stochastic modelling and the representation of tabular features are described. In Chapter 3 the physical processes that can be represented, the parameters that must be specified and the initial and boundary conditions required for each model available in the CPM module are presented. The mathematical description of the processes is presented in terms of the governing equations. The scientific basis for these conceptual models has been described in section 2.

2.8 Geometric Framework

The spatial region represented in a CPM model is discretised using the finite-element method. The finite-element mesh used is specified either by importing a mesh from a file or defined explicitly by a patch grid. A patch is a simple region bounded by points in one dimension, straight sides in two dimensions, or planar surfaces in three dimensions. One-dimensional patches are lines, two-dimensional patches may be triangles or quadrilaterals and three-dimensional patches may be triangular prisms, hexahedra or tetrahedra. Patches of different dimensions can be mixed within a single model, for example to represent features such as boreholes by one-dimensional patches within a two- or three-dimensional model. Patches are subdivided into elements and can have different numbers of elements in each direction. The size of the elements within a patch may be constant, or may be assigned arbitrarily. All elements within a single patch are of the same rock type, though this can be changed later in the model creation.

The geometric parameters required to define a grid of patches are the co-ordinates of the corners of each patch, the topology of the patches, and the number of elements and their relative sizes within each patch. The rock type of each patch must also be specified.

Fault zones are also represented either explicitly by patches, with rock types specified in the same way as for ordinary patches, or implicitly by using the Implicit Fracture Zone (IFZ) method to modify the properties of finite-elements intersected by one or more fracture zones. In the explicit case, the fault zones may be defined by specifying a fault line or plane and a fault width vector. In the IFZ case 3D fault zones are defined by a polygon of coplanar points together with a width and properties for the rock within the fracture zone. Both facilities enable the position and thickness of a fault zone to be modified with the minimum of effort.

If required, meshes comprising elements with curved sides in two dimensions, or curved faces in three dimensions can be generated. The curved elements are derived from planar elements by use of a polynomial mapping function. Grids comprising curved elements may be defined by specifying the co-ordinates of the corners of each element, its mapping function, and its rock type.

2.9 Spatial Assignment of Parameters

Physical parameters of the geological regions in a CPM model can be specified as constants, or more usually as constants for a given rock type. Stochastic modelling can be performed by defining permeability as a heterogeneous variable in terms of an exponential variogram with specified mean and standard deviation for each rock type. In this case, and in the case where IFZ is used to model fracture zones, permeability and porosity are calculated for each finite-element and stored in a file. It is also possible for these parameters to be specified as arbitrary functions of space, and sometimes as functions of other parameters, or of variables such as pressure and temperature. This is done through the use of user-supplied Fortran subroutines, which can be interfaced to the program at appropriate places.

In summary, most of the parameters used to specify the properties of the rocks and the fluids represented in the CPM model can be specified in one or more of the following ways:

- To have a constant value throughout the model;
- To have a constant value for a particular rock unit and/or solute species;
- To vary as a function of the variables, for example, the pressure, and certain pre-defined parameters, for example the fluid compressibility, according to relationships built into the CPM module;
- To vary (subject to certain limitations) as a function of the standard parameters, the variables and user-defined parameters in an arbitrary manner specified by the user through a set of Fortran subroutines, which have standard, well-defined interfaces.

2.10 Boundary Conditions

The basic types of boundary conditions available for a CPM model consist of specified value and specified flux conditions for the variables. The boundary conditions may be constant, or spatially varying. Specified value conditions may be constant in time, or can be varying in time for transient calculations. More complex boundary conditions that are non-linear, in that variables or fluxes depend on variables themselves are possible. One example of such a boundary condition is the Recharge-Discharge condition that is a generalised flux condition with the magnitude and direction of flux depending on the difference between the height of the water table and the topographic height. The default (i.e. if nothing is set explicitly) boundary condition for each variable is zero flux. Chapter 3 describes the types of boundary conditions that are available for each physical model in the CPM module. In addition to the conditions described here, more generalised boundary conditions can be specified through user-supplied Fortran subroutines. These allow the value of a variable or its flux to be specified as a function of position and the values of other variables at the boundary.

2.11 Stochastic Modelling

ConnectFlow has the capability to efficiently perform stochastic simulations for both linear systems (e.g. constant-density groundwater flow) and non-linear systems (e.g. coupled variable-density flow and salt transport). For this purpose, the generation of stochastic permeability fields in CPM models has been implemented based on the Turning Bands method. This method has been used and tested extensively in comparisons with HYDRASTAR [Morris et al., 1994] and on the WIPP2 test case [Cliffe et al., 1993]. The stochastic continuum approach requires that calculations be performed on tens or hundreds of Monte-Carlo realisations of essentially the same hydrogeological system. Therefore, care has been taken to ensure that the stochastic continuum method is implemented efficiently.

The methodology allows a good deal of flexibility in the stochastic modelling. The rock mass and individual fracture zone domains can have independent statistical parameters, and the domains can be defined as stochastic or deterministic independently. By treating the rock mass and fracture

zones as independent domains, this method contrasts to HYDRASTAR where the spatial process is continuous and ‘trends’ (scaling of the local conductivity) are used to represent the fracture zones. Currently, simulations are unconditioned. Conditioning of the rock mass or fracture domains would be straightforward to implement numerically, but careful consideration needs to be given to how the data is defined. For example, on what rock volume the data is defined and whether it is associated with a particular zone or just a borehole interval. The stochastic methods for the rock mass are described in the remainder of this section. The stochastic methods for the fracture zones are described in section 2.12.

For the current release, unconditioned realisations of the rock mass are based on an exponential variogram, and can be combined with deterministic fracture zone properties using IFZ (see section 2.12). It may be desired to have different statistical parameters in different parts of the model. For example, a median permeability that decreases with depth. Another important possibility is to have different statistics for the regional- and site-scale domains, since different values will be obtained for upscaling to the different mesh sizes. Generally, the larger the grid size, the higher the median and the smaller the variance until a REV is reached. These requirements are met by having a continuous spatial process in terms of the underlying variogram, but such that the mean and standard deviation can vary spatially by rock type. This approach is therefore appropriate for models whose statistical properties are generally associated with trends rather than absolute discontinuities at lithological boundaries.

The approach is to use a single Gaussian spatial process with a uniform correlation length, and normalised to have zero mean and variance 1.0. This generated normalised field is then rescaled by the mean and variance parameters for the discrete parts of the model. Thus, different upscaled mean and variance parameters can be applied to an embedded regional- and site-scale model, but in a way such that a high permeability in the regional-scale would generally be adjacent to a high permeability in the site-scale near the interface. This avoids having artificial barriers to flow around the boundary of the site-scale model due to discontinuities in the spatial process.

The CPM module also allows anisotropic permeabilities to be defined. For the stochastic case, this is implemented by scaling the normalised spatial process by different factors for the different components of the permeability tensor. Different degrees of anisotropy can be defined for different domains.

2.12 Implicit representation of Tabular Features (Fracture Zones) using IFZ

A method for calculating the effective permeability of a grid block in a model for groundwater flow in a domain containing tabular features has been implemented in the CPM module. The method is based on the IFZ approach [Boghammar et al., 1997], but represents a significant enhancement in the range of structures it can represent, how it handles fracture intersections, and its efficiency. The permeability of the background rock and the features may have arbitrary orientation, and the features may be more or less permeable than the surrounding rock. The approach is simple to implement and has low computational cost.

There are various approaches to modelling groundwater flow in domains containing tabular features. If the features are much more permeable, or more transmissive, than the background rock, the modelling can be undertaken using discrete fracture-network models, as described in the Discrete Fracture Network sections of this document, in which each feature is represented by a planar ‘fracture’, and the background rock is not represented. Such models are easy to set up, and it is easy to change the numbers, positions and properties of the features. However, the features may not be that much more permeable or more transmissive than the background rock, or some features may act as barriers to flow across them, or some features may have a more complicated behaviour in

that they act as barriers to flow across them, but in the directions along their larger extents are more transmissive than the surrounding rock. It may, therefore, be necessary to model the flow through the background rock as well as through the features. This can be done using fracture-network models, but it may be necessary to approximate the background rock in some way in terms of 'fractures'.

Another approach to the modelling is to use continuum porous medium models in which each tabular feature is represented by a group of finite elements chosen so that the boundaries of the feature lie along element boundaries. There are variants of this approach in which, for example, the features are approximated using two-dimensional elements in a grid of three-dimensional elements. All of these approaches represent the flow in both the features and the surrounding rock, and can handle the various types of features discussed above.

However, it is very difficult and time-consuming to set up the grids for such a model in three dimensions, and in general it is very difficult to automate the process of setting up the grid. This is particularly important if one wants to address the uncertainties, which will always exist, in the number and position of the features. This would be done by undertaking Monte-Carlo simulations. Realisations of the features would be generated numerically based on the available information about the features and then the flow would be calculated for each realisation. In this way, the uncertainty about the flow resulting from the uncertainties about the features could be quantified. However, if it were necessary to manually set up the grid for the numerical flow calculation for each realisation, it would only be practicable to undertake calculations for a very small number of realisations, which would limit the usefulness of the Monte-Carlo technique.

An alternative approach to modelling flow in a domain containing tabular features using continuum porous medium models is as follows. The finite-element grid is set up independently of the features. Typically, a simple cubic grid might be used. Then for each element, or grid block, a suitable effective permeability would be determined, appropriate to represent the background rock and all the features crossing the element, or grid block. This approach is often used in finite-difference calculations, because many finite-difference programs can only handle simple cubic grids. Variants of this approach have been proposed by, for example, Svensson [Svensson, 1999] and Lee et al. [Lee et al., 2000]. In fact, the approach is better suited to implementation in finite-element models as they allow an arbitrary direction of hydraulic anisotropy in the effective permeability to be specified. This is important since, in the general case, the principal directions of the permeability tensor will differ from element to element according to the alignment of features that cross them. Another motivation for using simple cubic grids is in undertaking stochastic calculations to address the effects of heterogeneity in the background rock, because the statistical parameterisation may require that all elements or grid blocks have similar sizes.

The approach is particularly flexible. It can be readily automated, which makes it straightforward to undertake Monte-Carlo simulations to address the uncertainties in the number and position of the features. However, for a particular level of grid refinement, the flow calculated for an individual realisation would not be quite as accurate as that calculated using a grid chosen so that each feature is represented accurately by a number of finite elements, although this can be addressed by grid refinement.

An example of the application of the implementation of this method is shown in Figure 2-1.

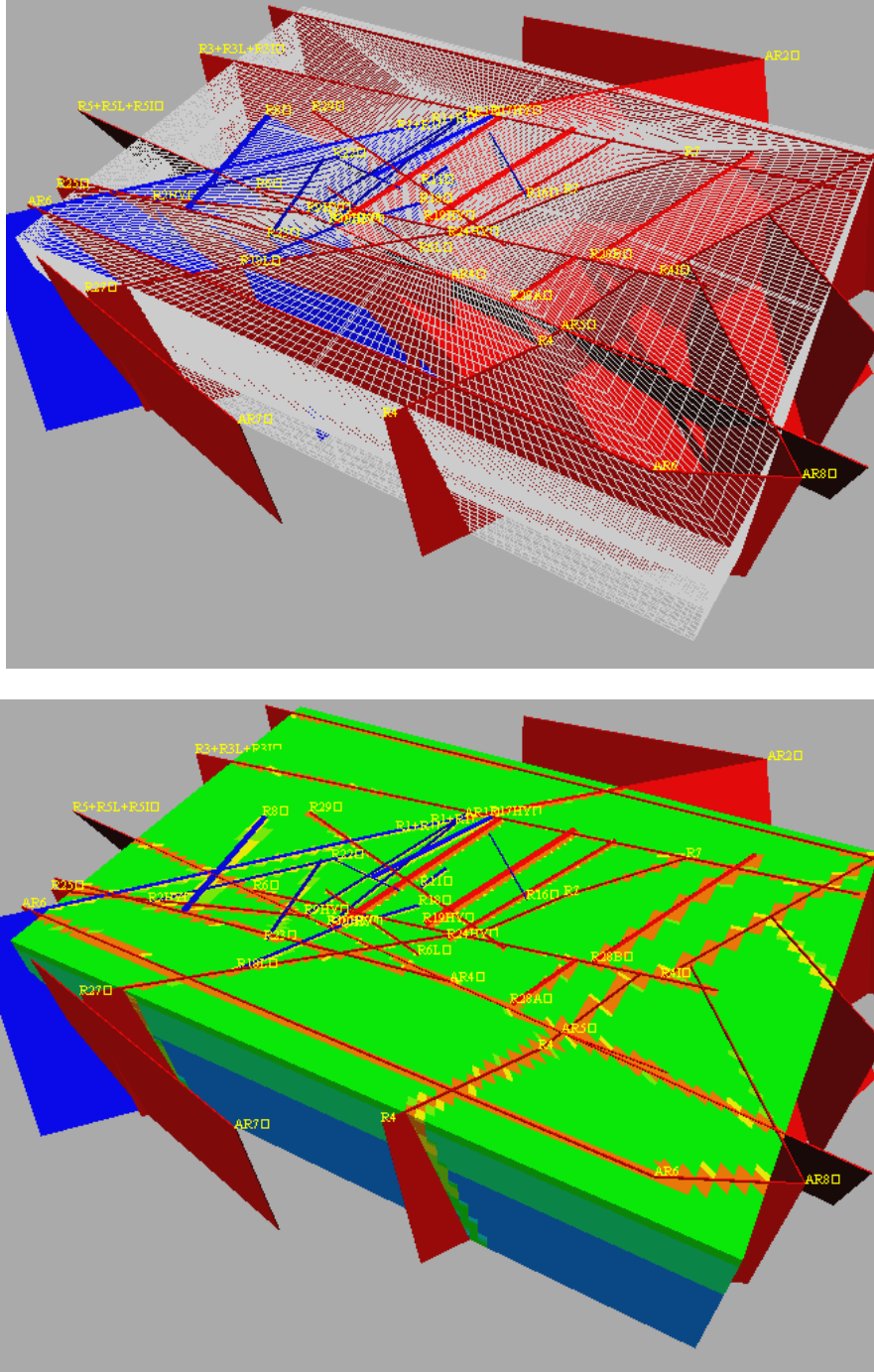


Figure 2-1: Application of CPM IFZ method for representing equivalent permeability of regional-scale fracture zones in a deterministic model. Top: Finite-element grid with fracture zones structures superimposed. Fracture zones that are coloured red have a higher transmissivity than those coloured blue. Bottom: equivalent permeability in each finite-element with fracture zones superimposed. Elements are coloured according to the logarithm of permeability from red (high) to low (blue).

3 Physical processes that can be modelled in Continuous Porous Medium models

The following subsections describe the physical processes, the parameters required, and the initial and boundary conditions for the various equations solved for each CPM model available. Also, the flux term for each equation used is given. This flux is the quantity that is specified by imposing a specified-flux type of boundary condition.

3.1 Groundwater flow

3.1.1 Physical Processes

Groundwater flow in a porous medium is modelled in terms of Darcy's law (Equation 2-1),

$$\mathbf{q} = -\frac{k}{\mu}(\nabla P^R - (\rho_l - \rho_0)\mathbf{g}) \quad \text{Equation 3-1}$$

and the equation of continuity,

$$\frac{\partial}{\partial t}(\phi\rho_l) - \nabla \cdot (\rho_l\mathbf{q}) = 0 \quad \text{Equation 3-2}$$

These are combined to form a single second-order equation for the residual pressure,

$$\frac{\partial}{\partial t}(\phi\rho_l) - \nabla \cdot \left(\rho_l \frac{k}{\mu} (\nabla P^R - (\rho_l - \rho_0)\mathbf{g}) \right) = 0 \quad \text{Equation 3-3}$$

and the flux for this pressure equation is

$$F_p = \rho_l \mathbf{q} \cdot \mathbf{n} \quad \text{Equation 3-4}$$

The residual pressure, P^R , is related to the total pressure, P^T , by the expression

$$P^R = P^T + \rho_0 g(z - z_0) \quad \text{Equation 3-5}$$

The hydraulic head, h , is related to the residual pressure by

$$h = \frac{P^R}{\rho_0 g} \quad \text{Equation 3-6}$$

3.1.2 Parameters Required

The parameters required are as follows:

Parameter	Symbol/definition	Comments
Permeability	\mathbf{k}	A symmetric tensor. Can be constant, or constant for a given rock type, or can be an arbitrary function of position, and can be anisotropic.
Porosity	$\phi = \phi_0 + (P^T - P_0^T) \frac{d\phi}{dP^T}$	P_0^T is a constant. ϕ_0 and $d\phi/dP^T$ can be constant, or constant for a given rock type, or can be arbitrary functions of position and pressure.
Fluid density	$\rho_l = \rho_0 \left(1 + \alpha(P^T - P_0^T) \right)$	α and P_0^T are constants.
Fluid viscosity	μ	A constant.

3.1.3 Initial and Boundary Conditions

The following initial conditions are required:

- Prescribed pressure.

The following boundary conditions can be specified:

- Prescribed pressure;
- Prescribed flux of fluid;
- Non-linear recharge-discharge (see below);
- Hydrostatic for vertical sides (see below);
- Point sinks for abstraction/injection at boreholes.

For the non-linear recharge-discharge condition the discharge of groundwater varies in magnitude and sign as the difference between the watertable, head, and the topographic height, z , such that

$$F_p = \begin{cases} \frac{\rho_l I (h - z)}{L}, & h > z - L \\ -\rho_l I, & h \leq z - L \end{cases} \quad \text{Equation 3-7}$$

for a maximum potential infiltration I . The arbitrary transition thickness, L , is usually set to the soil thickness.

The hydrostatic boundary condition is zero vertical flow:

$$q_z = 0 \quad \text{Equation 3-8}$$

3.1.4 2D Areal Groundwater Flow

It is also possible to model flow in a 2D areal model of an aquifer overlain by a confining layer using a vertically integrated form of Equation 3-2. The resulting equation is

$$\nabla \cdot (b \rho_l \mathbf{q}) = Q \quad \text{Equation 3-9}$$

Here, the effective thickness of the aquifer, b , is given by

$$b = \begin{cases} z_t - z_b, & \frac{P^R}{\rho_l g} \geq z_t \text{ (confined aquifer)} \\ \frac{P^R}{\rho_l g} - z_b, & \frac{P^R}{\rho_l g} < z_t \text{ (unconfined aquifer)} \end{cases} \quad \text{Equation 3-10}$$

The source term, Q , accounts for infiltration when modelling an unconfined aquifer. When modelling a confined aquifer, Q accounts for leakage and is given by

$$Q = \frac{\rho_l k_v}{\mu} \left(\frac{\rho_l g z_s - P^R}{z_s - z_t} \right) \quad \text{Equation 3-11}$$

3.2 Groundwater Flow and Heat Transport

3.2.1 Physical Processes

The CPM module can calculate the non-linear flow due to coupled groundwater flow and heat transport, where the fluid density is dependent upon the temperature. This is modelled using Darcy's law, Equation 3-1, the continuity equation, Equation 3-2, and the heat transport equation [Bear, 1972],

$$(\rho c)_a \frac{\partial T}{\partial t} + \rho_l c_l \mathbf{q} \cdot \nabla T - \Gamma_a \nabla^2 T = H \quad \text{Equation 3-12}$$

The first two of these equations are combined to form a single second-order equation for the residual pressure, Equation 3-3.

The fluxes for the pressure and temperature equations are Equation 3-4 and

$$F_T = -\Gamma_a \nabla T \cdot n \quad \text{Equation 3-13}$$

3.2.2 Parameters Required

The parameters required are as follows:

Parameter	Symbol/definition	Comments
Permeability	k	A symmetric tensor. Can be constant, or constant for a given rock type, or can be an arbitrary function of position, and can be anisotropic.
Porosity	$\phi = \phi_0 + (P^T - P_0^T) \frac{d\phi}{dP^T}$	P_0^T is a constant. ϕ_0 and $d\phi/dP^T$ can be constant, or constant for a given rock type, or can be arbitrary functions of position, pressure and temperature.
Fluid density	$\rho_l = \rho_0(1 + \alpha(P^T - P_0^T) - \beta(T - T_0))$	α, β, P_0^T and T_0 are constants.
Fluid viscosity	$\mu = \mu_0 e^{-\delta_1(T-T_0)}$	T_0, μ_0 and δ_1 are constants.
Average thermal conductivity of the rock and fluid	$\Gamma_a = \phi \Gamma_l + (1 - \phi) \Gamma_s$	Approximated by the thermal conductivity of the rock, Γ_s . Can be constant, or constant for a given rock type.
Average heat capacity of the rock and fluid	$(\rho c)_a = \phi \rho_l c_l + (1 - \phi) \rho_s c_s$	Approximated by the heat capacity of the rock, $\rho_s c_s$. c_l is a constant. ρ_s can be constant, or constant for a given rock type. c_s can be constant, or constant for a given rock type.

3.2.3 Initial and Boundary Conditions

The following initial conditions are required:

- Prescribed pressure;
- Prescribed temperature.

The following boundary conditions can be specified:

- Prescribed pressure;
- Prescribed flux of fluid;
- Hydrostatic for vertical sides (see section 3.1);
- Point sinks for abstraction/injection at boreholes;
- Prescribed temperature;
- Prescribed heat flux.

3.3 Unsaturated Groundwater Flow

3.3.1 Physical Processes

This is modelled in terms of a modified version of Darcy's law (see section 2.2),

$$\mathbf{q} = -\frac{k_r \mathbf{k}}{\mu} (\nabla P^R - (\rho_l - \rho_0) \mathbf{g}) \quad \text{Equation 3-14}$$

and the equation of continuity,

$$\frac{\partial}{\partial t} (\phi S \rho_l) - \nabla \cdot (\rho_l \mathbf{q}) = 0 \quad \text{Equation 3-15}$$

These are combined to form a single second-order equation for the residual pressure,

$$\frac{\partial}{\partial t} (\phi S \rho_l) - \nabla \cdot \left(\rho_l \frac{k_r \mathbf{k}}{\mu} (\nabla P^R - (\rho_l - \rho_0) \mathbf{g}) \right) = 0 \quad \text{Equation 3-16}$$

and the flux for this pressure equation is given by Equation 3-4.

3.3.2 Parameters Required

The parameters required are as follows:

Parameter	Symbol/definition	Comments
Permeability	\mathbf{k}	A symmetric tensor. Can be constant, or constant for a given rock type, or can be an arbitrary function of position, and can be anisotropic.
Relative permeability	k_r	An arbitrary function of saturation, which is related to the total pressure through a specified capillary pressure curve (see below).
Porosity	$\phi = \phi_0 + (P^T - P_0^T) \frac{d\phi}{dP^T}$	P_0^T is a constant. ϕ_0 and $d\phi/dP^T$ can be constant, or constant for a given rock type, or can be arbitrary functions of position and pressure.
Fluid density	$\rho_l = \rho_0 \left(1 + \alpha (P^T - P_0^T) \right)$	α and P_0^T are constants.
Fluid viscosity	μ	A constant.

In the CPM module, the way in which the permeability varies with the saturation, S , is specified using various empirical models for the relative permeability, k_r , and saturation, S .

The Brooks and Corey model is

$$k_r = \left(\frac{S - S_{res}}{1 - S_{res}} \right)^{(2+3\gamma)/\gamma} \quad \text{Equation 3-17}$$

$$S = S_{res} + (1 - S_{res}) \left(\frac{P_E}{-P^T} \right)^\gamma \quad \text{Equation 3-18}$$

The Van Genuchten model is

$$k_r = \sqrt{S_\alpha} \left[1 - (1 - S_\alpha^{\gamma/(\gamma-1)})^{(\gamma-1)/\gamma} \right]^2 \quad \text{Equation 3-19}$$

$$S = S_{res} + (1 - S_{res}) \left(\frac{1}{1 + (-P^T/P_E)^\gamma} \right)^{(\gamma-1)/\gamma} \quad \text{Equation 3-20}$$

where S_α is given by

$$S_\alpha = \frac{S - S_{res}}{1 - S_{res}} \quad \text{Equation 3-21}$$

The Extended Van Genuchten model is

$$k_r = S_\alpha^\beta \quad \text{Equation 3-22}$$

$$S = S_{res} + (1 - S_{res}) \left(\frac{1}{1 + (-P^T/P_E)^\gamma} \right)^{(\gamma-1)/\gamma} \left(1 - \frac{S}{P_D} \right)^{\gamma_1} \quad \text{Equation 3-23}$$

where S_α is defined as in Equation 3-21.

The CPM module default model for k_r is

$$k_r = \begin{cases} \frac{A_{KR}}{B_{KR} + (-P^T)^{S_{KR}}}, & P^T < 0 \\ 1, & P^T \geq 0 \end{cases} \quad \text{Equation 3-24}$$

S is calculated from the capillary pressure curve. The default form used is

$$k_r = \begin{cases} \frac{A_{PC}}{B_{PC} + (-P^T)^{S_{PC}}}, & P^T < 0 \\ 1, & P^T \geq 0 \end{cases} \quad \text{Equation 3-25}$$

A_{KR} , B_{KR} , S_{KR} , A_{PC} , B_{PC} and S_{PC} are constant for a given rock type.

3.3.3 Initial and Boundary Conditions

The following initial conditions are required:

- Prescribed pressure.

The following boundary conditions can be specified:

- Prescribed pressure;
- Prescribed flux of fluid;
- Non-linear recharge-discharge (see section 3.1);
- Hydrostatic for vertical sides (see section 3.1);
- Point sinks for abstraction/injection at boreholes.

3.4 Unsaturated Groundwater Flow and Heat Transport

3.4.1 Physical Processes

This is modelled using a modified version of Darcy's law, Equation 3-14, the equation of continuity, Equation 3-15 and the heat transport equation, Equation 3-12.

The first two of these equations are combined to form a single second-order equation for the residual pressure, Equation 3-16.

The fluxes for the pressure and temperature equations are given in Equation 3-4 and Equation 3-13.

3.4.2 Parameters Required

The parameters required are as follows:

Parameter	Symbol/definition	Comments
Permeability	k	A symmetric tensor. Can be constant, or constant for a given rock type, or can be an arbitrary function of position, and can be anisotropic.
Relative permeability	k_r	An arbitrary function of saturation, which is related to the total pressure through a specified capillary pressure curve (see section 3.3).
Porosity	$\phi = \phi_0 + (P^T - P_0^T) \frac{d\phi}{dP^T}$	P_0^T is a constant. ϕ_0 and $d\phi/dP^T$ can be constant, or constant for a given rock type, or can be arbitrary functions of position, pressure and temperature.
Fluid density	$\rho_l = \rho_0(1 + \alpha(P^T - P_0^T) - \beta(T - T_0))$	α, β, P_0^T and T_0 are constants.
Fluid viscosity	$\mu = \mu_0 e^{-\delta_1(T - T_0)}$	T_0, μ_0 and δ_1 are constants.
Average thermal conductivity of the rock and fluid	$\Gamma_a = \phi\Gamma_l + (1 - \phi)\Gamma_s$	Approximated by the thermal conductivity of the rock, Γ_s . Can be constant, or constant for a given rock type.
Average heat capacity of the rock and fluid	$(\rho c)_a = \phi\rho_l c_l + (1 - \phi)\rho_s c_s$	Approximated by the heat capacity of the rock, $\rho_s c_s$. c_l is a constant. ρ_s can be constant, or constant for a given rock type. c_s can be constant, or constant for a given rock type.

3.4.3 Initial and Boundary Conditions

The following initial conditions are required:

- Prescribed pressure;
- Prescribed temperature.

The following boundary conditions can be specified:

- Prescribed pressure;
- Prescribed flux of fluid;
- Hydrostatic for vertical sides (see section 3.1);
- Point sinks for abstraction/injection at boreholes;
- Prescribed temperature;
- Prescribed heat flux.

3.5 Radionuclide Transport

3.5.1 Physical Processes

This is modelled using the following equation [Bear, 1972 and 1979; Freeze et al., 1979; De Marsily, 1985],

$$\frac{\partial}{\partial t}(\phi R_{\alpha} N_{\alpha}) + \mathbf{q} \cdot \nabla N_{\alpha} - \nabla \cdot (\phi \mathbf{D}_{\alpha} \nabla N_{\alpha}) = -\lambda_{\alpha} \phi R_{\alpha} N_{\alpha} + \lambda_{\alpha-1} \phi R_{\alpha-1} N_{\alpha-1} + \phi f_{\alpha} \quad \text{Equation 3-26}$$

Here, the subscript $\alpha-1$ is used to indicate the parent nuclide of nuclide α .

Normally, since the groundwater flow is not coupled to the radionuclide transport, \mathbf{q} will be calculated from an initial groundwater flow calculation.

The flux for the nuclide equation is

$$F_{N_{\alpha}} = (\mathbf{q} N_{\alpha} - \phi \mathbf{D}_{\alpha} \nabla N_{\alpha}) \cdot \mathbf{n} \quad \text{Equation 3-27}$$

3.5.2 Parameters Required

The parameters required are as follows:

Parameter	Symbol/definition	Comments
Porosity	$\phi = \phi_0 + (P^T - P_0^T) \frac{d\phi}{dP^T}$	P_0^T is a constant. ϕ_0 and $d\phi/dP^T$ can be constant, or constant for a given rock type, or can be arbitrary functions of position and pressure.
Darcy velocity	\mathbf{q}	Obtained from a previous ConnectFlow calculation.
Retardation factors for each nuclide	$R_\alpha = 1 + \frac{(1 - \phi)}{\phi} K_{d,\alpha}$	$K_{d,\alpha}$ is constant for a given rock type and nuclide. (Note The CPM module's definition of K_d differs from the literature definition: i.e. CPM module K_d = rock density multiplied by literature K_d)
Decay constants for each nuclide	λ_α	A constant for each nuclide.
Dispersion tensor for each nuclide	$\mathbf{D}_\alpha = \frac{D_{m\alpha}}{\tau} \delta_{ij} + \alpha_{T\alpha} v \delta_{ij} + (\alpha_{L\alpha} - \alpha_{T\alpha}) \frac{v_i v_j}{v}$	$D_{m\alpha}$ is constant for each nuclide. τ is constant for a given rock type. $\alpha_{L\alpha}$ and $\alpha_{T\alpha}$ are constant for a given rock type. v_i are the components of the porewater velocity, which is given by $\mathbf{v} = \mathbf{q}/\phi$.
Source term for each nuclide	f_α	A function of position and time.

3.5.3 Initial and Boundary Conditions

The following initial conditions are required:

- Prescribed concentration of each nuclide.

The following boundary conditions can be specified:

- Prescribed concentration of each nuclide;
- Prescribed flux of each nuclide;
- Zero dispersive flux for each nuclide (see below).

The zero dispersive flux condition is basically an outflow condition

$$F_{N_\alpha} = N_\alpha \mathbf{q} \cdot \mathbf{n} \quad \text{Equation 3-28}$$

This condition is realistic for surfaces where flow is known to be discharging from the model. Where there is a mixture of recharge and discharge then the boundary condition can be generalised to

$$F_{N_\alpha} = \begin{cases} \frac{(N_\alpha - N_{\alpha 0})\mathbf{q} \cdot \mathbf{n}}{\varepsilon}, & \mathbf{q} \cdot \mathbf{n} \leq 0 \\ N_\alpha \mathbf{q} \cdot \mathbf{n}, & \mathbf{q} \cdot \mathbf{n} > 0 \end{cases} \quad \text{Equation 3-29}$$

This is effectively a mixed boundary condition such that $N_\alpha = N_{\alpha 0}$ at inflows and an outflow condition is applied elsewhere.

3.6 Radionuclide Transport in Unsaturated Flow

3.6.1 Physical Processes

This is modelled using the following equation [Bear, 1972 and 1979; Freeze et al., 1979; De Marsily, 1985],

$$\begin{aligned} \frac{\partial}{\partial t} (\phi S R_\alpha N_\alpha) + \mathbf{q} \cdot \nabla N_\alpha - \nabla \cdot (\phi S \mathbf{D}_\alpha \nabla N_\alpha) & \quad \text{Equation 3-30} \\ = -\lambda_\alpha \phi S R_\alpha N_\alpha + \lambda_{\alpha-1} \phi S R_{\alpha-1} N_{\alpha-1} + \phi S f_\alpha & \end{aligned}$$

Here, the subscript $\alpha-1$ is used to indicate the parent nuclide of nuclide α .

Normally, since the groundwater flow is not coupled to the radionuclide transport, \mathbf{q} will be calculated from an initial unsaturated groundwater flow calculation.

The flux for the nuclide equation is

$$F_{N_\alpha} = (\mathbf{q} N_\alpha - \phi S \mathbf{D}_\alpha \nabla N_\alpha) \cdot \mathbf{n} \quad \text{Equation 3-31}$$

3.6.2 Parameters Required

The parameters required are as follows:

Parameter	Symbol/definition	Comments
Porosity	$\phi = \phi_0 + (P^T - P_0^T) \frac{d\phi}{dP^T}$	P_0^T is a constant. ϕ_0 and $d\phi/dP^T$ can be constant, or constant for a given rock type, or can be arbitrary functions of position and pressure.
Darcy velocity	q	Obtained from a previous ConnectFlow calculation.
Retardation factors for each nuclide	$R_\alpha = S + \frac{(1 - \phi)}{\phi} K_{d,\alpha}$	$K_{d,\alpha}$ is constant for a given rock type and nuclide. (Note The CPM module's definition of K_d differs from the literature definition: i.e. CPM module K_d = rock density multiplied by literature K_d)
Decay constants for each nuclide	λ_α	A constant for each nuclide.
Dispersion tensor for each nuclide	$D_\alpha = \frac{D_{m\alpha}}{\tau} \delta_{ij} + \alpha_{T\alpha} v \delta_{ij} + (\alpha_{L\alpha} - \alpha_{T\alpha}) \frac{v_i v_j}{v}$	$D_{m\alpha}$ is constant for each nuclide. τ is constant for a given rock type. $\alpha_{L\alpha}$ and $\alpha_{T\alpha}$ are constant for a given rock type. v_i are the components of the porewater velocity, which is given by $\mathbf{v} = \mathbf{q}/\phi$.
Source term for each nuclide	f_α	A function of position and time.

3.6.3 Initial and Boundary Conditions

The following initial conditions are required:

- Prescribed concentration of each nuclide.

The following boundary conditions can be specified:

- Prescribed concentration of each nuclide;
- Prescribed flux of each nuclide;
- Zero dispersive flux for each nuclide (see section 3.5).

3.7 Coupled Groundwater Flow and Solute Transport

3.7.1 Physical Processes

The CPM module can calculate the non-linear flow due to coupled groundwater flow and solute transport, where the fluid density is strongly dependent upon the concentration of the solute. This is modelled using Darcy's law, Equation 3-1, the continuity equation, Equation 3-2, and the advection-dispersion equation,

$$\frac{\partial}{\partial t}(\phi\rho_l c) + \nabla \cdot (\rho_l \mathbf{q}c) = \nabla \cdot (\phi\rho_l \mathbf{D}\nabla c) \quad \text{Equation 3-32}$$

The first two of these equations are combined to form a single second-order equation for the residual pressure, Equation 3-3.

The fluxes for the pressure and concentration equations are Equation 3-4 and

$$F_c = (\rho_l \mathbf{q}c - \phi\rho_l \mathbf{D}\nabla c) \cdot \mathbf{n} \quad \text{Equation 3-33}$$

3.7.2 Parameters Required

The parameters required in this case are as follows:

Parameter	Symbol/definition	Comments
Permeability	\mathbf{k}	A symmetric tensor. Can be constant, or constant for a given rock type, or can be an arbitrary function of position, and can be anisotropic.
Porosity	$\phi = \phi_0 + (P^T - P_0^T) \frac{d\phi}{dP^T}$	P_0^T is a constant. ϕ_0 and $d\phi/dP^T$ can be constant, or constant for a given rock type, or can be arbitrary functions of position and pressure.
Dispersion tensor	$\mathbf{D} = \frac{D_m}{\tau} \delta_{ij} + \alpha_T v \delta_{ij} + (\alpha_L - \alpha_T) \frac{v_i v_j}{v}$	D_m is constant. τ is constant for a given rock type. α_L and α_T are constant for a given rock type. v_i are the components of the porewater velocity, which is given by $\mathbf{v} = \mathbf{q}/\phi$.
Fluid density	ρ_l (defined below)	α , α_c , ρ_0 , ρ_{c0} , and P_0^T are constants.
Fluid viscosity	μ	A constant.

The fluid density in the above table is given by

$$\frac{1}{\rho_l} = \frac{1 - c}{\rho_0(1 + \alpha(P^T - P_0^T))} + \frac{c}{\rho_{c0}(1 + \alpha_c(P^T - P_0^T))} \quad \text{Equation 3-34}$$

3.7.3 Initial and Boundary Conditions

The following initial conditions are required:

- Prescribed pressure;
- Prescribed concentration of solute.

The following boundary conditions can be specified:

- Prescribed pressure;
- Prescribed flux of fluid;
- Non-linear recharge-discharge (see section 3.1);
- Hydrostatic for vertical sides (see section 3.1);
- Point sinks for abstraction/injection at boreholes;
- Prescribed concentration of solute;
- Prescribed flux of solute;
- Zero dispersive flux for solute (see below).

The zero dispersive flux condition is basically an outflow condition

$$F_C = \rho_l c \mathbf{q} \cdot \mathbf{n} \quad \text{Equation 3-35}$$

This condition is realistic for surfaces where flow is known to be discharging from the model. Where there is a mixture of recharge and discharge then the boundary condition can be generalised to

$$F_{N_\alpha} = \begin{cases} \frac{\rho_l (c - c_0) \mathbf{q} \cdot \mathbf{n}}{\varepsilon}, & \mathbf{q} \cdot \mathbf{n} \leq 0 \\ \rho_l c \mathbf{q} \cdot \mathbf{n}, & \mathbf{q} \cdot \mathbf{n} > 0 \end{cases} \quad \text{Equation 3-36}$$

This is effectively a mixed boundary condition such that $c = c_0$ at inflows and an outflow condition is applied elsewhere.

3.8 Coupled Groundwater Flow, Solute Transport and Heat Transport

3.8.1 Physical Processes

The CPM module can calculate the non-linear flow due to coupled groundwater flow, solute transport and heat transport, where the fluid density is strongly dependent upon the concentration of the solute and upon the temperature. This is modelled using Darcy's law, Equation 3-1, the continuity equation, Equation 3-2, the advection-dispersion equation, Equation 3-33 and the heat transport equation [Bear, 1972],

$$(\rho c)_a \frac{\partial T}{\partial t} + \rho_l c_l \mathbf{q} \cdot \nabla T - \nabla \cdot (\mathbf{D}' \nabla T) = H \quad \text{Equation 3-37}$$

Note that this equation reduces to Equation 3-12 if the dispersion tensor is a constant diagonal tensor with thermal conductivity Γ_α .

The first two of these equations are combined to form a single second-order equation for the residual pressure, Equation 3-3.

The fluxes for the pressure, concentration and temperature equations are Equation 3-4, Equation 3-33 and

$$F_T = -\mathbf{D}' \nabla T \cdot \mathbf{n} \quad \text{Equation 3-38}$$

3.8.2 Parameters Required

The parameters required in this case are as follows:

Parameter	Symbol/definition	Comments
Permeability	\mathbf{k}	A symmetric tensor. Can be constant, or constant for a given rock type, or can be an arbitrary function of position, and can be anisotropic.
Porosity	$\phi = \phi_0 + (P^T - P_0^T) \frac{d\phi}{dP^T}$	P_0^T is a constant. ϕ_0 and $d\phi/dP^T$ can be constant, or constant for a given rock type, or can be arbitrary functions of position, pressure and temperature.
Dispersion tensor	$\mathbf{D} = \frac{D_m}{\tau} \delta_{ij} + \alpha_T v \delta_{ij} + (\alpha_L - \alpha_T) \frac{v_i v_j}{v}$	D_m is constant. τ is constant for a given rock type. α_L and α_T are constant for a given rock type. v_i are the components of the porewater velocity, which is given by $\mathbf{v} = \mathbf{q}/\phi$.
Fluid density	ρ_l (defined below)	$\alpha, \alpha_c, \beta, \beta_c, \rho_0, \rho_{c0}, P_0^T$, and T_0 are constants.
Fluid viscosity	$\mu = \mu_0 e^{-\delta_1(T-T_0)}$	T_0, μ_0 and δ_1 are constants.
Heat dispersion tensor	$\mathbf{D}' = \Gamma_a \delta_{ij} + \varphi \rho_l c_l \alpha'_T v \delta_{ij} + \varphi \rho_l c_l (\alpha'_L - \alpha'_T) \frac{v_i v_j}{v}$	α'_L and α'_T are constant for a given rock type. c_l is a constant. v_i are the components of the porewater velocity, which is given by $\mathbf{v} = \mathbf{q}/\phi$.
Average thermal conductivity of the rock and fluid	$\Gamma_a = \phi \Gamma_l + (1 - \phi) \Gamma_s$	Approximated by the thermal conductivity of the rock, Γ_s . Can be constant, or constant for a given rock type.
Average heat capacity of the rock and fluid	$(\rho c)_a = \varphi \rho_l c_l + (1 - \varphi) \rho_s c_s$	Approximated by the heat capacity of the rock, $\rho_s c_s$. c_l is a constant. ρ_s can be constant, or constant for a given rock type. c_s can be constant, or constant for a given rock type.

The fluid density in the above table is given by:

$$\frac{1}{\rho_l} = \frac{1 - c}{\rho_0(1 + \alpha(P^T - P^T_0) + \beta(T - T_0))} + \frac{c}{\rho_{c0}(1 + \alpha_c(P^T - P^T_0) + \beta_c(T - T_0))} \quad \text{Equation 3-39}$$

3.8.3 Initial and Boundary Conditions

The following initial conditions are required:

- Prescribed pressure;
- Prescribed concentration of solute;
- Prescribed temperature.

The following boundary conditions can be specified:

- Prescribed pressure;
- Prescribed flux of fluid;
- Hydrostatic for vertical sides (see section 3.1);
- Point sinks for abstraction/injection at boreholes;
- Prescribed concentration of solute;
- Prescribed flux of solute;
- Zero dispersive flux for solute (see section 3.7);
- Prescribed temperature;
- Prescribed heat flux.

4 Numerical methods used for Continuous Porous Medium models

4.1 Spatial Discretisation

4.1.1 Approach

ConnectFlow uses the finite-element approach for spatial discretisation. This is a powerful approach that is particularly suited to numerical modelling in domains that are complicated geometrically, such as domains that represent geological structures with several lithological units or many faults. The basic idea of the approach is that the domain is represented as the combination of ‘finite elements’ that have a simple geometric shape (such as triangles or quadrilaterals in 2D and tetrahedra, triangular prisms or cuboids in 3D). These elements may also be distorted by simple mappings. The possibility of using irregular shaped grids provides much more flexibility in accurately representing the subsurface flow capture area than is possible using the regular blocks of a simple finite-difference method. In particular, triangular and tetrahedral elements allow unstructured meshes to be created.

On each finite element, the quantities of interest, such as the residual pressure, are represented by simple polynomial functions that interpolate between the values at certain special points called nodes. The possibility of using polynomials of higher order than linear enables numerical schemes that have a high order of accuracy to be easily developed.

The CPM module has a library of many different finite elements, including:

- Linear and quadratic triangles in 2D;
- Bi-linear and bi-quadratic quadrilaterals in 2D;
- Linear and quadratic tetrahedra in 3D;
- Tri-linear and tri-quadratic prisms in 3D; and
- Tri-linear and tri-quadratic cuboids in 3D.

The library also includes variants of the so-called ‘mixed elements’ (see section 4.1.3). This provides considerable flexibility in representing the domain.

4.1.2 Grid Generation

Various facilities have been implemented in ConnectFlow to try to make generation of grids of finite elements as simple as possible. Grids can be created within ConnectFlow itself or imported from other software, such as a grid generator, via a formatted file. The principal approach used for generating grids is based on the concept of ‘patches’, which can be subdivided into a number of finite elements. A patch is a region of a simple shape bounded by straight lines, either a triangle or a quadrilateral in 2D and a (possibly distorted) triangular prism or a (possibly distorted) cuboid in 3D. It is specified by the positions of its corners. In two dimensions, an extension of this approach has been developed using the concept of ‘polygons’, which are regions with many sides. These are first subdivided into patches, which are then subdivided into elements.

The use of patches, and polygons in particular, enables grids to be generated with a minimum of input data. It also makes it very simple to change the refinement of a grid, because the user does not have to calculate the locations of all of the individual elements. Figure 4-1, Figure 4-2 and Figure 4-3 illustrate some of the types of grid that can be generated using the standard grid generation facilities available within ConnectFlow. Options are available for representing faults and engineered features, such as boreholes, tunnels and drifts, in the grid.

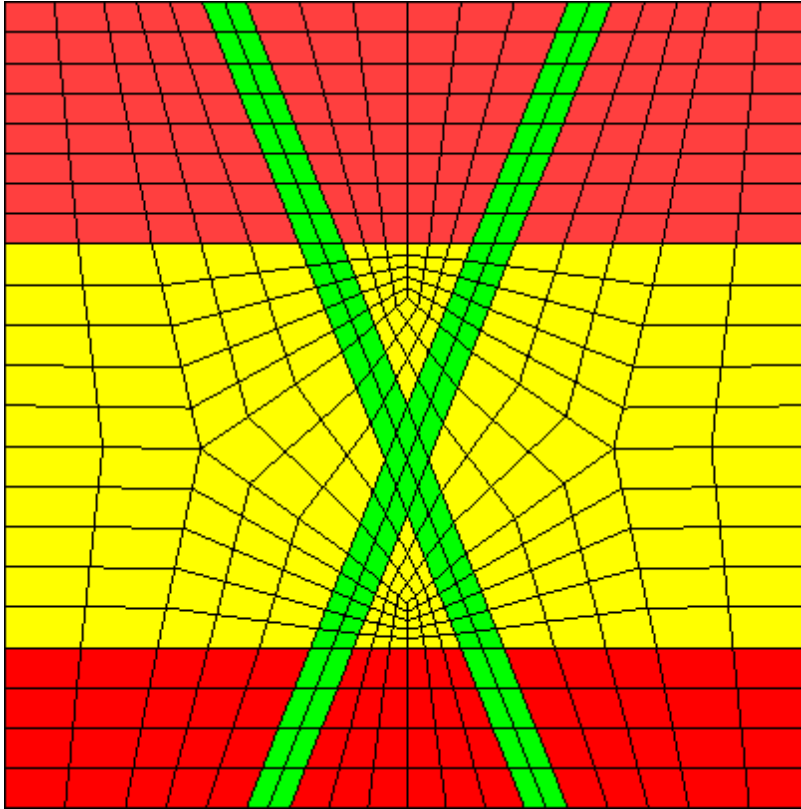


Figure 4-1 A simple 2D grid generated using polygons. The finite elements are coloured according to the rock type.

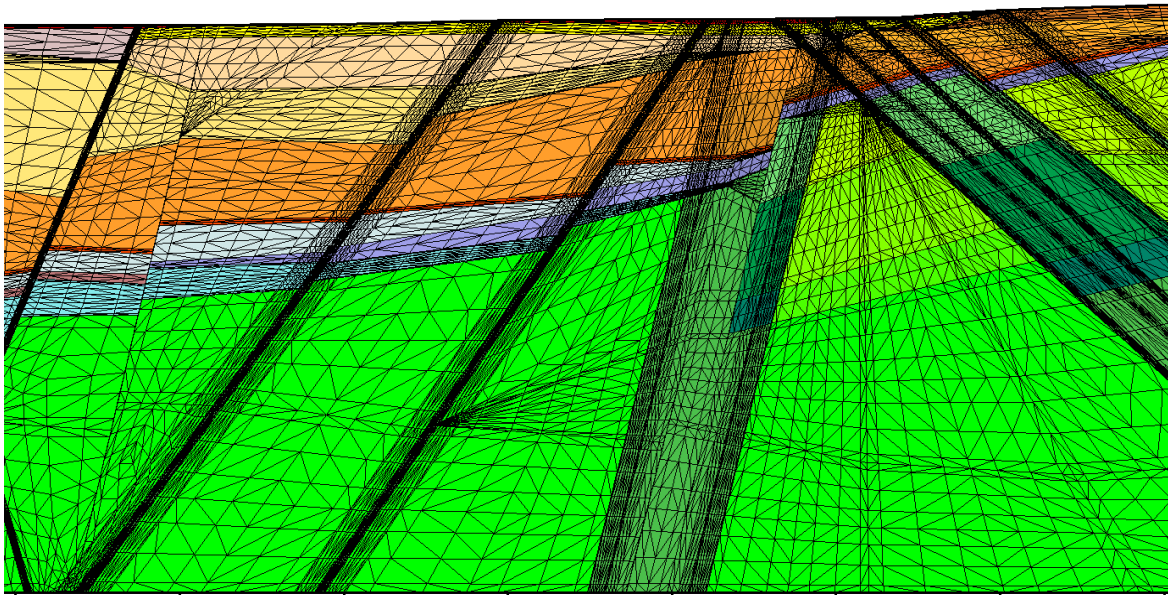


Figure 4-2 An example of part of a complex 2D grid generated using polygons. The finite elements are coloured according to the rock type.

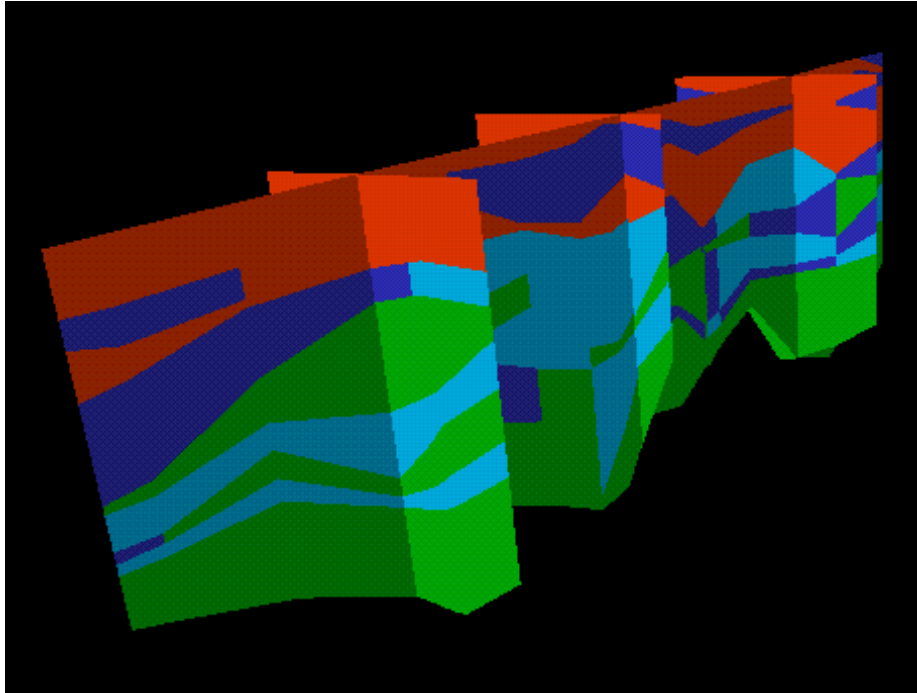


Figure 4-3 Slices through a 3D grid coloured according to rock type. The individual elements are not shown in this picture.

In ConnectFlow, each element is assigned to a rock unit. This assignment associates certain physical properties, for example the permeability, with the element. A rock unit is comprised of one or more finite elements.

ConnectFlow also includes an option for the user to specify the finite-element grid through a user-specified Fortran subroutine. This can be used, for example, to import grids generated using other programs into ConnectFlow.

4.1.3 Formulation of the Equations

There are several approaches to the finite-element method, which all lead to similar equations. In the CPM module, the Galerkin finite-element method [Ciarlet, 1978; Mitchell et al., 1977; Zienkiewicz, 1977] is used to carry out the spatial discretisation of the equations (see [Winters et al., 1984] for a brief ConnectFlow-specific discussion). The finite-element method starts from an integral form of the equations.

The dependent variables in the problem are approximated by functions, which have a simple polynomial behaviour on each of the elements. The discretised equations are a discrete form of the integral equations. The final result is a set of coupled, possibly non-linear, algebraic equations for a steady-state problem, and a set of coupled, possibly non-linear, ordinary differential equations in time for a transient problem (see e.g. [Mitchell et al., 1977]). Temporal discretisation of the equations in the CPM module is described in section 4.2. The equations are solved using the methods described in section 4.3.

Two formulations of the various groundwater flow equations have been implemented in the CPM module. In the so-called standard formulation, the basic quantity that is represented using finite elements is the residual pressure. This formulation is used with the standard elements (linear and quadratic triangles and bi-linear and bi-quadratic quadrilaterals in 2D, and linear and quadratic tetrahedra and tri-linear and tri-quadratic prisms and cuboids in 3D). It is a widely used approach.

In the so-called mixed-element formulation, both the residual pressure and the mass flux are represented using finite elements. This approach is less widely used than the standard formulation.

It has a lower order of accuracy than the standard formulation using bi- or tri-quadratic elements. However, it has one particular advantage. It ensures that the normal component of the mass-flux vector is continuous across any interface within the modelling region, as is the case for the underlying equations, whereas the standard formulation does not preserve this property. This feature of the mixed-element formulation is particularly beneficial when the quantity of primary interest is the velocity field, for example when calculating pathlines or performing transport calculations. In particular, it is sometimes the case that numerically calculated pathlines could become stuck in the flow field obtained using the standard formulation on relatively coarse grids.

A remark must be made about the treatment of advection in CPM modelling. Many authors recommend the use of upstream weighting, the finite-element equivalent of upwinding, which is often used for finite-difference discretisations of advection-diffusion equations. Upwinding often removes the numerical instabilities associated with a straightforward application of the Galerkin method to the advective terms. However, there is a price to be paid - upwinding introduces a numerical dispersion effect which amounts to dispersion with a dispersion length closely related to the mesh spacing. This leads to the total amount of dispersion in the model being a function of the refinement, which may be undesirable. Therefore, in ConnectFlow the amount of dispersion in the calculation is made explicit by using a consistent Galerkin approach for the advective terms [Gresho et al., 1981].

If numerical instabilities appear, the user has two alternatives: either to refine the mesh in the regions of high gradients so that the instabilities disappear or are reduced to an acceptable level, or to increase the physical dispersion lengths to stabilise the calculation.

4.1.4 Use of Constraints

It is often necessary to consider a variety of scales in groundwater flow modelling. For example, a large regional-scale model to understand boundary conditions affecting flow at depth, and a more detailed (or site-) scale around contaminant sources. In ConnectFlow it is possible to nest meshes constructed from elements of different scales using constraints.

An example of how meshes can be nested is illustrated in Figure 4-4. Here a refined (35m element-size) site-scale model is joined to a coarser (105m element-size) regional-scale model. The model is 3D, although only a plan view is shown. Hence, at the interface between the two scales, one element in the regional-scale is adjacent to nine elements in the site-scale, and only every third node in the site-scale mesh is coincident with a node in the regional-scale, the other two nodes being 'pinch' nodes.

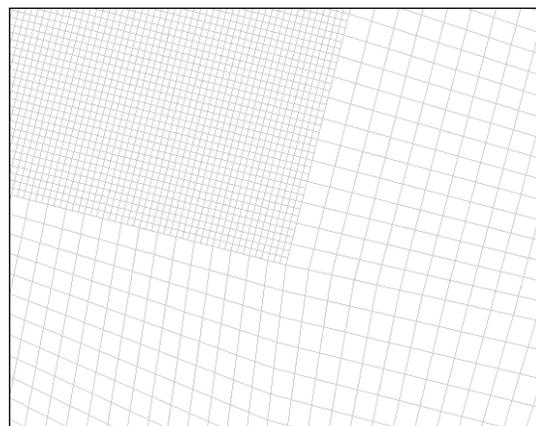


Figure 4-4 Part of a finite-element mesh showing the constraint boundary between a refined site-scale model and a coarse regional-scale model.

To ensure that the physics of groundwater flow is maintained at the interface between meshes, the finite-element equations for elements on the interface are modified using constraint equations.

For pinch nodes in a site-scale element on the interface, the pressure is interpolated from the pressures at the nodes in the adjacent regional-scale element, to ensure continuity in the discrete system. The numerical implementation of this constraint in ConnectFlow is

$$P_{s,i}^R = \sum_j \psi_{r,ij} P_{r,j}^R \quad \text{Equation 4-1}$$

For a regional-scale element on the interface, the flux across the interface is balanced with the sum of the fluxes across the interface for the adjoining site-scale elements, to ensure conservation of mass. The numerical representation of this constraint in ConnectFlow is included implicitly.

Similar principles can be applied to more complex processes, such as salt transport.

4.2 Temporal Discretisation

In the CPM solution, the spatial discretisation is carried out using the Galerkin finite-element method (see section 4.1). For time-dependent problems, the application of this method leads to a set of coupled, possibly non-linear, ordinary differential equations in time. There are two basic methods available in ConnectFlow for integrating these ordinary differential equations:

- The Crank-Nicholson method;
- Gear's method (see e.g. [Byrne et al., 1975]).

The Crank-Nicholson method contains a parameter, θ , that controls the degree of implicitness of the method. The scheme is implicit for all values of θ except 0 (for which it is equivalent to the explicit forward Euler scheme), and first-order accurate for all values except 0.5 for which it is second order accurate. For $\theta = 1$ (fully implicit), the method is a backward-difference scheme (backward Euler). Although this scheme is only first-order accurate, it has the merit of being very stable, and is recommended for use in many cases. Indeed, it often may be unconditionally stable, allowing, in principle, the use of very large timesteps, although this may not give a very accurate description of the time evolution of the system. It may be appropriate for problems with a single time scale such as radionuclide transport in advection dominated flows. The explicit forward Euler scheme ($\theta = 0$) and the second-order accurate scheme ($\theta = 0.5$) are only conditionally stable; that is there are constraints on the size of the timesteps, which depend on the size of the finite elements. If these constraints are exceeded, the numerical solution will diverge.

Three variants of the Crank-Nicholson scheme are included in ConnectFlow:

- A version with a fixed time step size;
- A very fast fully implicit version for linear problems. This is particularly suitable for contaminant transport calculations;
- A version in which the timestep size is chosen automatically at each time step to ensure convergence. This version is particularly recommended for calculations of coupled groundwater flow and transport of salinity (and possibly heat).

Gear's method is a variable-timestep variable-order scheme, based on a predictor-corrector algorithm. At each time step, the size of the time step and the order of the difference scheme are selected to try to maximise the size of the time step subject to a specified accuracy criterion, the error in the step being estimated from the difference between the predictor and corrector. The corrector schemes used are the backward difference schemes of order one to five, which are generally very stable. The scheme is particularly appropriate for use on problems that are 'stiff'; that is, in simple terms the behaviour of the system involves components with a wide range of time scales. For example, Gear's method may be a good scheme to use for modelling coupled

groundwater flow and transport of heat from a radioactive waste repository, which constitutes a decaying heat source.

4.3 Solution Methods and Treatment of Non-Linearities

In general, spatial and temporal discretisation of a problem gives rise to large, non-linear, coupled, algebraic systems of equations. In ConnectFlow, non-linearities are treated using the Newton-Raphson iterative method. This is a powerful technique for solving non-linear equations and converges very rapidly (quadratically) provided the initial guess is sufficiently close to the solution of the equations. Solution of a linear problem is equivalent to using the Newton-Raphson method with a single iteration.

For non-linear transient problems, the solution at the previous timestep is often a sufficiently good initial guess, since one does not want the solution to change too much over a single time step for reasons of accuracy.

For highly non-linear steady-state problems, it is not always easy to find a sufficiently good initial guess. In such cases, parameter stepping may be effective. Parameter stepping is a technique in which the solution of a hard non-linear problem is approached via a sequence of related problems, starting from a problem that is easy to solve. At each step the parameters of the system are changed slightly and the solution at the previous step is used as the initial guess for the Newton-Raphson iterations. Parameter stepping is a very powerful technique.

The Newton-Raphson method requires a linear system of equations to be solved at each stage of the iterative procedure. These linear systems are large and sparse and have a structure that is determined by the underlying finite-element discretisation. In ConnectFlow, both direct and iterative methods are available for solving these systems. The direct method is an efficient implementation of the Frontal Method [Duff et al., 1993; Hood, 1976; Irons, 1975] to solve linear systems. The Frontal Method is a variant of Gaussian elimination that exploits the structure of the equations to solve the system using a relatively small amount of memory, without the need to assemble the full matrix for the system in memory. Gaussian elimination has the advantage of being a very robust method.

However, a direct method can be prohibitively slow for large 3D models, in which case an iterative method may be more appropriate. Two implementations of the Preconditioned Conjugate Gradient (PCCG) are incorporated in ConnectFlow. These are the Generalised Minimum Residual (GMRES) and Biconjugate Stabilised (BicStab) methods. GMRES is suited to non-symmetric systems (e.g. coupled flow and salt transport) and is generally more robust, while BicStab requires less memory.

4.4 Mass-Conserving Particle Tracking

Early methods for calculating pathlines in a CPM model might lead to stuck particles and inaccurate pathlines. One cause of this is the lack of mass balance between elements when using the finite element method. In their paper, Cordes and Kinzelbach [Cordes et al., 1992] propose a method for achieving mass balance between cubic elements by sub-dividing them into tetrahedra and calculating a velocity for each tetrahedron such that mass balance is achieved. Once this is done, more robust pathlines can be calculated.

The mass-conserving method divides a cubic finite element into eight sub-cubes (or hexahedra in the case of a deformed finite element in the general case). These are then further subdivided into five sub-tetrahedra (Figure 4-5). Thus there are 40 sub-tetrahedra per element. Velocities are calculated for each sub-tetrahedra so that mass balance is achieved between elements. This has the effect of a better specified velocity vector field in a given element such that particles do not disappear. The velocity is constant within each tetrahedron.

To calculate the velocities in each tetrahedron, first consider a corner node on the element in Figure 4-5. Assume this node is surrounded by eight other tetrahedra, one from the element shown and seven more from other elements adjacent to the node. The first step is to calculate the fluxes in these 8 tetrahedra surrounding a node (see Figure 4-6). The tetrahedra form an octahedron and the fluxes through the 8 outer surfaces are assumed to be equal to the corresponding “nodal fluxes.”

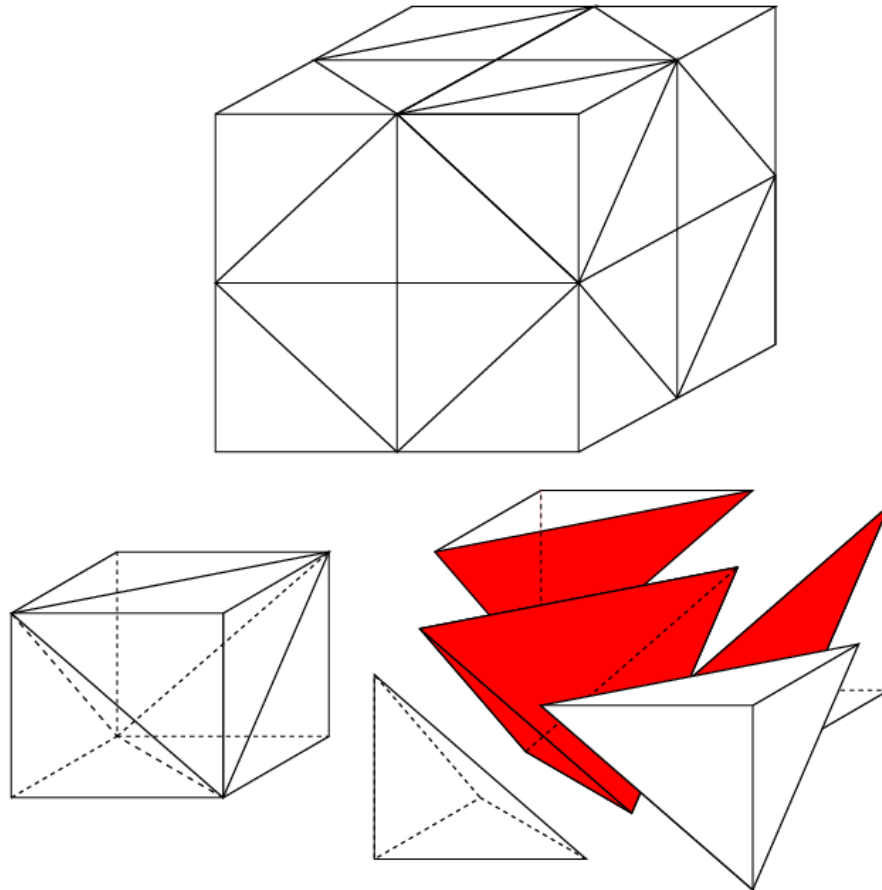


Figure 4-5: A finite element is divided into 8 sub-elements and then further sub-divided into 5 sub-tetrahedra.

The nodal fluxes in finite element theory are conceptually the fluxes from an element, E , towards the nodes, I , on that element. They are derived using Galerkin’s method (the reader is pointed to Cordes et al., 1992 for the derivation of a similar equation for square finite elements) and have the important property that they always sum to zero around a node with no sources or sinks. The nodal flux towards node I on element E is given by:

$$Q_{IE}^N = -\frac{1}{2\mu_E} \int_{V_E} dx \nabla \psi_{IE}(x) \cdot (K_E \cdot \nabla P^R(x)) \quad \text{Equation 4-2}$$

where K_E is the permeability for element E , μ_E is the fluid viscosity inside the element, P^R is the residual pressure, ψ_{IE} is the basis function associated with node I on element E (there are 8 basis functions, one for each node, which are defined such that the pressure inside the element is given by $P^R(x) = \sum_I P_I^R \psi_{IE}(x)$ where the P_I^R are the residual pressures at the nodes) and the integration is over the volume V_E of element E . The factor of $-1/2$ at the beginning is obtained from a simple example for which the solution is known.

Note that the pressure gradient can be rewritten in the form $\nabla P^R(x) = \sum_J P_J^R \nabla \psi_{JE}(x)$ which gives:

$$Q_{IE}^N = -\frac{1}{2\mu_E} \int_{V_E} dx \nabla \psi_{IE}(x) \cdot \left(K_E \cdot \sum_J P_J \nabla \psi_{JE}(x) \right) \quad \text{Equation 4-3}$$

This integral is evaluated using a Gaussian scheme.

The other fluxes in the 8 tetrahedra are calculated using zero-vorticity constraints and mass balance constraints. Once this is accomplished for each of the 8 nodes around an element, the fluxes are then calculated for the tetrahedra in the element not adjacent to a node. This is also accomplished using zero-vorticity and mass balance constraints. Once the fluxes have all been obtained, the flow velocity for each tetrahedron is calculated.

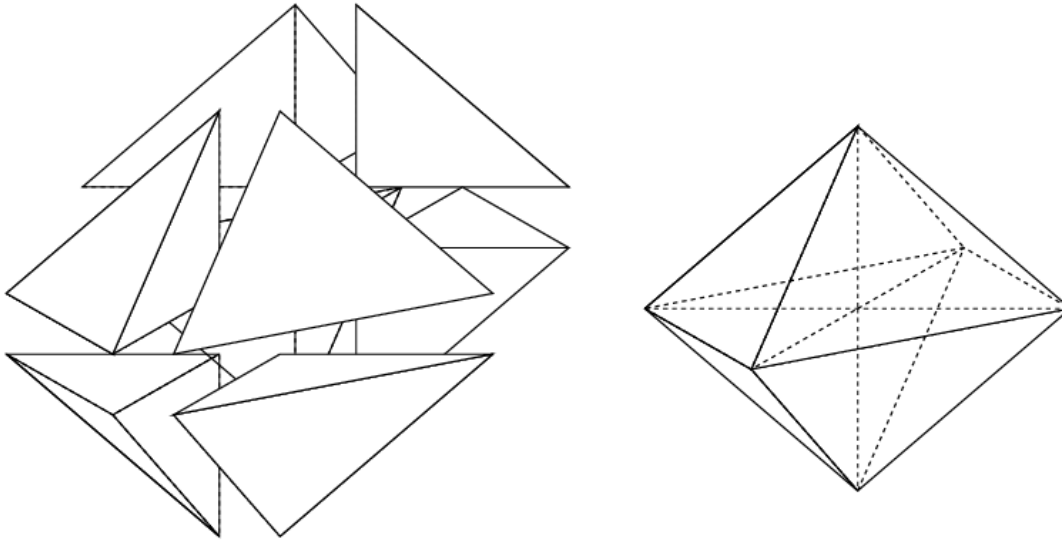


Figure 4-6: The first step of the calculation is finding the fluxes in the eight tetrahedra surrounding each node (which form an octahedron). The fluxes through the 8 outer surfaces are calculated using Galerkin's method, the others are solved using mass conservation & zero vorticity constraints.

The flow velocities are then used to track particles across an element from a start point to an end point. Due to the constant velocity in each tetrahedron, this leads to piecewise pathlines. However, the non-vorticity and mass-balance constraints used in the calculation of the velocity field mean the pathlines rarely get stuck, if at all (some pathlines occasionally still get stuck for numerical reasons).

Mass-conserving pathlines are available in the following CPM models:

- Fully saturated or unsaturated groundwater flow
- Fixed or variable density models
- Hexahedral CB08 or CB81 finite elements (which can be distorted)
- Models with or without nodal quadrature
- Models with regular hexahedral meshes (this means no more than 8 elements per node)
- Models with or without variable mesh refinement (constraint boundaries)

A mass-conserving method is available in the DFN module (see section 6.12.2). This has been coupled to the mass-conserving pathline capability in the CPM module to provide mass-conserving particle tracking for combined DFN-CPM models.

4.5 Using the Mass-Conserving Method to Create a Particle Tracking Library

An alternative approach (still using the mass-conserving method) is to discretise the pathlines or in other words, limit the points a particle can pass through (say 24 per element). By doing so, it is possible to create a “library” file which stores information on all possible particle tracks for a given model. This can then be used to reconstruct any desired particle track the user may wish to consider.

The benefits of this “discrete” scheme are as follows:

1. The library file can easily be used by software other than ConnectFlow to produce particle tracks. It is very convenient to produce particle tracks in the ConnectFlow visualisation package since they can be instantly visualised and quickly modified if necessary.
2. The library file is slow to calculate, but once it has been produced, particle tracking is much faster to accomplish.
3. The library can be constructed in a probabilistic manner so that the particles can take different routes dependent on random numbers generated during the particle tracking.

To understand how the discretisation works, consider a hexahedral finite element. In the mass-conserving method this is broken down into 40 tetrahedra, and a constant Darcy velocity is calculated for each. Particles can then be tracked across the finite element using those velocities. In the continuous scheme, particles are free to enter and exit the element at any point. In the discrete scheme, the entry and exit points are limited to a few fixed points on the element, known as transport nodes. Consider Figure 4-7; this shows 4 and 16 transport nodes arranged evenly on each surface of the element. The number can be increased to 36 or more if required. In general, the number of transport nodes per surface is given by $m=4n^2$, where n is a positive integer chosen by the user.

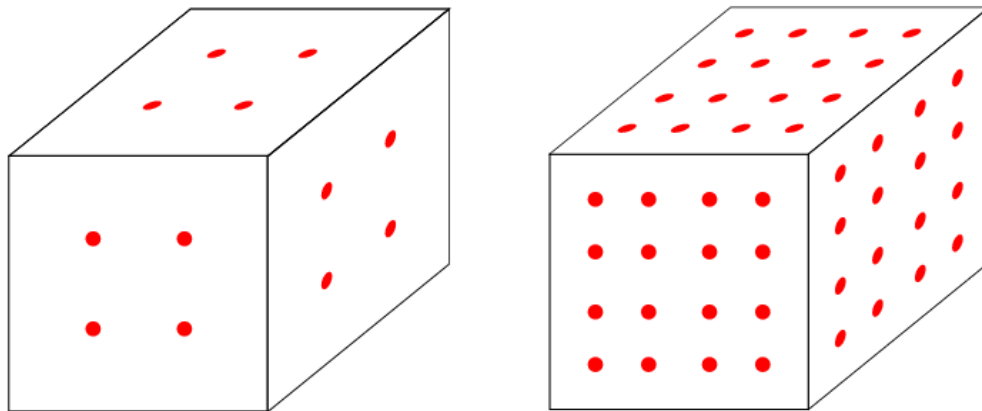


Figure 4-7: Transport nodes are arranged on the surface of each element. The number of nodes per surface (m) is given by $m=4n^2$ where n is an integer chosen by the user

Transport nodes are assigned for every element. When two elements share a surface, the transport nodes on that surface are only stored once, so there are never two transport nodes at exactly the same position (an exception to this is on constraint boundaries, which are discussed later).

Particle tracks are calculated starting from each transport node using the mass-conserving method. These are followed until they leave the element(s) the transport node is located on. The positions the tracks leave the elements are used to select “destination” nodes which are stored in a file. This file then forms a library of the links between transport nodes, and can be used by ConnectFlow to produce particle tracks for a CPM region.

To make the calculation probabilistic, four paths are calculated from each transport node. The start points for each are offset a small distance from the location of the transport node, so that they produce different destinations. There is also a slight offset away from the surface towards the inside of the element. To describe this offset requires a third local coordinate t of range $[-1, 1]$. In that coordinate, the offset is 0.002. (This helps when particles skim along the CPM-DFN boundary in combined models).

A particle is tracked from each of the four start points to the element boundary. The surface quadrants associated with these exit point are used to determine the destination nodes (see Figure 4-8).

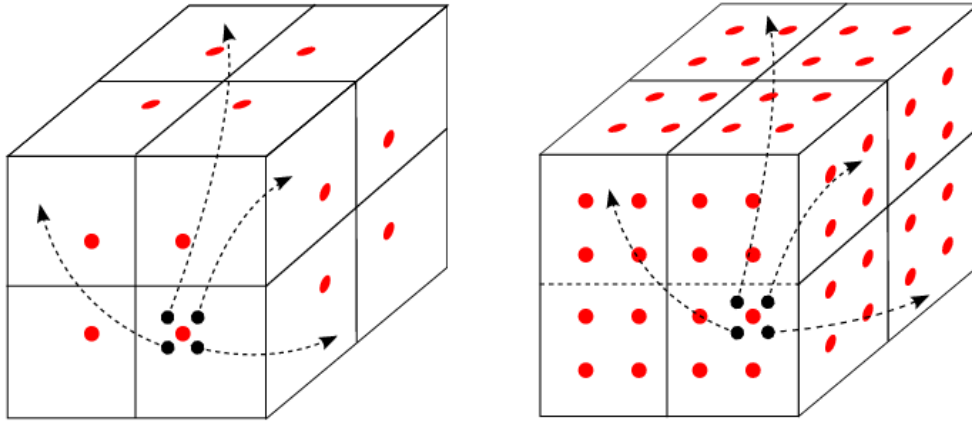


Figure 4-8: The destination nodes are chosen from the surface quadrant the particle leaves from. If $m=4$ (left) then there is only one node on each quadrant but if $m=16$ (right) there are four. In the latter case the four possibilities are assigned probabilities according to how far they are from the exit point.

When $m=4$, the destination node for each start point is the single transport node on the surface quadrant the particle arrives at (note that the flux is constant over the quadrants of a hexahedral surface in the mass-conserving method.) Since there are four start points per destination node and one possible destination for each there are potentially four destination nodes for each transport node. Typically each is assigned a 25% probability. However, if two paths go to the same transport node then that destination has a 50% probability. Also, if the destination node is on the same surface quadrant as the start node then the probability is set to zero for that destination (this also applies if $m>4$). The “good” destinations would then be re-weighted to make sure the total probability was equal to 100%.

Pathline libraries can be calculated for any model appropriate for mass-conserving pathlines (see previous section).

Pathline calculations begin by specifying the starting coordinates for each pathline. The library contains the coordinates of each transport node which are used to find the node closest to each pathline starting point. Each particle is then tracked in the following manner. After the first transport node is determined, all of the possible destination nodes are obtained and a random number between 0 and 1 is calculated and used to select the destination nodes whose total probability should always sum to one. Once the destination node is selected, the destination nodes for that node are obtained, and so on until the particle gets to the boundary and the algorithm stops. Due to this probabilistic approach, 2 particles starting from identical positions can take increasingly different paths the greater the number of steps they take.

4.6 Rock Matrix Diffusion

Rock matrix diffusion (RMD) [Neretnieks, 1980] is the process of diffusion from fracture water into the less mobile water within the rock matrix. The equations for groundwater flow and solute transport in the fracture system for a ConnectFlow equivalent continuous porous medium (ECPM) model on a large scale, with solute diffusion into the rock matrix between parallel equally spaced fractures (see [Hoch et al., 2004], based on [Carrera et al., 1998]), are:

$$\frac{\partial(\phi_f \rho c)}{\partial t} + \nabla \cdot (\rho \vec{q} c) = \nabla \cdot (\phi_f \rho D \cdot \nabla c) + \sigma \rho D_i \left. \frac{\partial c'}{\partial w} \right|_{w=0} \quad \text{Equation 4-4}$$

$$\alpha \frac{\partial(\rho c')}{\partial t} = \frac{\partial}{\partial w} \left(\rho D_i \frac{\partial c'}{\partial w} \right) \quad \text{Equation 4-5}$$

where

- \mathbf{q} is the specific discharge (or Darcy flux) [m/s];
- ρ is the groundwater density [kg/m³];
- t is the time [s];
- ϕ_f is the kinematic porosity due to the fractures carrying the flow [-];
- D_i is the intrinsic diffusion coefficient for diffusion into the rock matrix, which is sometimes referred to as the effective diffusion coefficient, e.g. in the Swedish radioactive waste disposal programme [m²/s];
- σ is the specific fracture surface area, that is the average surface area of the fractures per unit volume [m⁻¹], which is sometimes called the specific flow-wetted surface area, e.g. in the Swedish radioactive waste disposal programme. For smooth planar fractures, σ is given by $2P_{32}$, where P_{32} is the fracture area per unit volume, which is a measure of fracture intensity;
- w is the distance from the fracture surface into the rock matrix [m];
- c' is the solute mass fraction in the groundwater in the matrix [-];
- α is the capacity factor of the matrix [-].

Equation 4-4 corresponds to conservation of solute in the fractures (allowing for diffusion into the matrix) and Equation 4-5 is diffusion within the matrix, based on Fick's second law. The equations have been written in a form that is valid for variable groundwater density, but for the current implementation, the density is taken to be constant.

For non-sorbing solutes, the capacity factor in Equation 4-5 would normally be taken to be equal to the accessible porosity in the rock matrix, ϕ_m . However, it is envisaged that it might also be used to model migration of solutes which might be sorbing. In order to allow for this, Equation 4-5 was written in the more general form using the capacity factor rather than the rock-matrix porosity. For a sorbing solute, the capacity factor would be given by

$$\alpha = R\phi_m \quad \text{Equation 4-6}$$

where R is the retardation due to equilibrium sorption of the solute to the rock matrix [-]. The description in terms of the capacity factor also facilitates modelling possible cases in which a solute is excluded from part of the matrix porosity because of ionic effects.

The equations given above have to be supplemented by appropriate boundary and initial conditions. Suitable boundary conditions for the groundwater flow equations (Equation 2-1 and Equation 2-2) are prescriptions of either the groundwater pressure or the groundwater flux around the boundary of the domain modelled. Suitable boundary conditions for the equation for solute transport (Equation 4-4) are prescriptions of the solute mass fraction in the fractures at the domain boundary or the flux of solute into the groundwater in the fractures. The boundary conditions for Equation 4-5 are that the

solute mass fraction in the groundwater in the matrix at the fracture surface is equal to the solute mass fraction in the groundwater in the fractures locally:

$$c'(w = 0) = c \quad \text{Equation 4-7}$$

and that the flux of solute in the matrix is zero at the maximum penetration depth d into the matrix:

$$-D_i \frac{\partial c'}{\partial w}(w = d) = 0 \quad \text{Equation 4-8}$$

In the original RMD method in ConnectFlow, transport in the rock matrix is modelled analytically and the term for the flux between the rock matrix and the fractures from Equation 4-4

$$\sigma \rho D_i \left. \frac{\partial c'}{\partial w} \right|_{w=0} \quad \text{Equation 4-9}$$

is expressed as

$$A^n + B \frac{(c^n - c^{n-1})}{(t^n - t^{n-1})} \quad \text{Equation 4-10}$$

where c^n is the concentration in the fracture system at the end of time step n and A^n and B do not depend on c^n . A^n and B are calculated from the concentrations in the fracture system at previous time steps. It should be noted that in [Hoch et al., 2004] the definitions of A^n and B are reversed, however the order above matches the actual implementation in ConnectFlow. This RMD method is not compatible with reactive transport as it cannot take into account the changes in solute concentration as a result of chemical reactions.

4.6.1 Finite Volume Implementation of Rock Matrix Diffusion

A finite volume rock matrix diffusion method has been implemented to allow the effects of rock matrix diffusion to be modelled in situations where chemical reactions are being calculated. This method may also be used where no chemical reactions are being calculated. The original method of RMD is still available in ConnectFlow, the equations for which are given above.

The original RMD method uses an expression for the flux into the rock matrix derived from an analytic model. The new method models the diffusion of solutes between cells in the rock matrix using a finite volume method. The flux between the fracture and matrix can then be calculated. This new method more readily provides a detailed description of the distribution of solutes within the rock matrix. It is also straightforward to generalise the approach to handle chemical reactions in the rock matrix. A simplified schematic of the two methods is shown in Figure 4-9. With the new method, the user selects the number of cells that the rock matrix is divided up into per fractured rock finite element and also may choose if these are to be of equal length or have varying lengths. As changes in matrix water composition due to diffusion are greatest closest to the fracture, smaller cell sizes for the first few matrix cells may improve accuracy, whilst larger cell sizes for the other matrix cells will help performance without a significant reduction in accuracy.

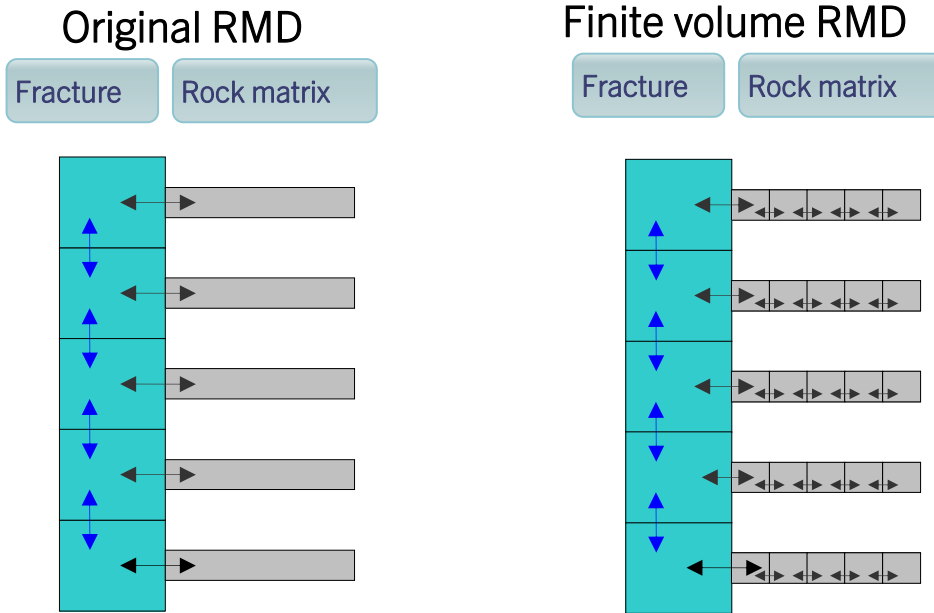


Figure 4-9: Simplified schematic of the original and finite volume rock matrix diffusion methods. The blue arrows show flow within the fractures, the large black arrows show flow between the fractures and the rock matrix, and the small black arrows show flow within the rock matrix.

The finite volume RMD method uses a simple 1D finite-volume discretisation to model the diffusion in the rock matrix. This method provides computational efficiency with reasonable accuracy for a given level of refinement. The rock matrix is discretised into N cells of length Δw_i . The user may choose whether to set all the cells to the same size or whether to define the length of each cell separately by rock type. With constant-density assumed, for a general cell, a simple fully implicit discretisation in time (backward Euler) leads to the equation

$$\alpha \frac{(c_i^{n+1} - c_i^n)}{\Delta t} = \frac{D_i}{\Delta w_i} \left\{ \frac{(c_{i+1}^{n+1} - c_i^{n+1})}{\frac{1}{2}(\Delta w_i + \Delta w_{i+1})} - \frac{(c_i^{n+1} - c_{i-1}^{n+1})}{\frac{1}{2}(\Delta w_{i-1} + \Delta w_i)} \right\} \quad \text{Equation 4-11}$$

where D_i is the intrinsic diffusion coefficient [m^2/s], α is the capacity factor of the matrix [-] and c_i^n refers to the discretised value of c' at time $n\Delta t$ for the cell i . The backward Euler scheme is first-order accurate and is often unconditionally stable, but can be inaccurate for large time steps.

Rearranging, this can be written as

$$E_i c_{i-1}^{n+1} + F_i c_i^{n+1} + G_i c_{i+1}^{n+1} = H_i \quad \text{Equation 4-12}$$

where E_i , F_i , and G_i are constants (i.e. independent of c_i^n)

$$E_i = -\frac{2D_i \Delta t}{\alpha \Delta w_i} \frac{1}{(\Delta w_{i-1} + \Delta w_i)} \quad \text{Equation 4-13}$$

$$F_i = 1 + \frac{2D_i \Delta t}{\alpha \Delta w_i} \left(\frac{1}{(\Delta w_{i-1} + \Delta w_i)} + \frac{1}{(\Delta w_i + \Delta w_{i+1})} \right) \quad \text{Equation 4-14}$$

$$G_i = -\frac{2D_i \Delta t}{\alpha \Delta w_i} \frac{1}{(\Delta w_i + \Delta w_{i+1})} \quad \text{Equation 4-15}$$

$$H_i = c_i^n \quad \text{Equation 4-16}$$

The coefficients in this equation are modified at the ends of the grid to represent the specified boundary conditions. At the left hand end of the grid, where matrix concentration equals the fracture concentration,

$$E_1 = 0 \quad \text{Equation 4-17}$$

$$F_1 = 1 + \frac{D_i \Delta t}{\alpha \Delta w_1} \left(\frac{2}{\Delta w_1} + \frac{2}{(\Delta w_1 + \Delta w_2)} \right) \quad \text{Equation 4-18}$$

$$G_1 = -\frac{2D_i \Delta t}{\alpha \Delta w_1} \frac{1}{(\Delta w_1 + \Delta w_2)} \quad \text{Equation 4-19}$$

$$H_1 = c_1^n + \frac{2D_i \Delta t}{\alpha \Delta w_1} \frac{c^{n+1}}{\Delta w_1} \quad \text{Equation 4-20}$$

and at the right-hand end of the grid, where there is a zero concentration gradient,

$$E_N = -\frac{2D_i \Delta t}{\alpha \Delta w_N} \frac{1}{(\Delta w_{N-1} + \Delta w_N)} \quad \text{Equation 4-21}$$

$$F_N = 1 + \frac{2D_i \Delta t}{\alpha \Delta w_N} \left(\frac{1}{(\Delta w_{N-1} + \Delta w_N)} \right) \quad \text{Equation 4-22}$$

$$G_N = 0 \quad \text{Equation 4-23}$$

$$H_N = c_N^n \quad \text{Equation 4-24}$$

The discretised equations form a tridiagonal system, which can be readily solved using the Thomas algorithm [Thomas, 1949].

The case of interest is slightly more complicated than this because the equations involve the unknown c , which is the value of the solute mass fraction in the fracture system at the end of the time step. However, this can be readily handled as follows. Equation 4-12 can be written in the form

$$E_i c_{i-1}^{n+1} + F_i c_i^{n+1} + G_i c_{i+1}^{n+1} = H1_i + C^{n+1} H2_i \quad \text{Equation 4-25}$$

where, from Equation 4-16 and Equation 4-20,

$$H1_i = c_i^n \quad \text{Equation 4-26}$$

and

$$H2_i = \begin{cases} \frac{D_i \Delta t}{\alpha \Delta w_1} \frac{1}{\Delta w_1} & i = 1 \\ 0 & \text{else} \end{cases} \quad \text{Equation 4-27}$$

Equation 4-25 is a linear equation for c^{n+1} and so the solution is given by

$$c_i^{n+1} = c_{1,i}^{n+1} + c^{n+1} c_{2,i}^{n+1} \quad \text{Equation 4-28}$$

where $c_{1,i}^{n+1}$ and $c_{2,i}^{n+1}$ are the solutions of the linear system for right-hand sides $H1_i$ and $H2_i$ respectively, i.e.

$$E_i c_{1,i-1}^{n+1} + F_i c_{1,i}^{n+1} + G_i c_{1,i+1}^{n+1} = H1_i \quad \text{Equation 4-29}$$

$$E_i c_{2,i-1}^{n+1} + F_i c_{2,i}^{n+1} + G_i c_{2,i+1}^{n+1} = H2_i \quad \text{Equation 4-30}$$

Then the contribution to solute transport in the fracture system from the matrix

$$\sigma \rho D_i \left. \frac{\partial c'}{\partial w} \right|_{w=0} \quad \text{Equation 4-31}$$

is given by

$$\frac{2\sigma \rho D_i}{\Delta w_1} (c_1^{n+1} - c^{n+1}) = \frac{2\sigma \rho D_i}{\Delta w_1} (c_{1,1}^{n+1} + c^{n+1} c_{2,1}^{n+1} - c^{n+1}) \quad \text{Equation 4-32}$$

which can be written in the form shown in Equation 4-10.

Once an expression for the flux has been found (in terms of A^n and B) then the transport calculation can be performed to calculate a value of the fracture concentrations at the latest time step. This can be used in Equation 4-28 to calculate equivalent values of the matrix concentration at that time step.

4.7 Reactive Transport

ConnectFlow is able to combine groundwater flow and transport calculations with geochemical calculations (reactive transport) [Joyce et al., 2014]. At each time step, the mass fractions of solute components are updated based on the results of chemical reaction calculations. The chemical reactions are calculated by the iPhreeqc software library [Charlton et al., 2011], which encapsulates and provides access to the widely respected PHREEQC geochemical software [Parkhurst et al., 1999]. The data produced by iPhreeqc are used to update the mass fractions of components for the next time step in ConnectFlow. Chemical reactions are calculated for both the equivalent continuous porous medium (ECPM) representation of fractures and the rock matrix. The chemical calculations are based on a set of thermodynamic constraints defined in a separate, user-specified, database file in PHREEQC format.

In order to perform calculations of chemical reactions, groundwater transport must be carried out in terms of the transport of solute components since the quantities of each individual component may be changed by the chemical reactions. PHREEQC expresses all chemical equations in terms of master species, with one master aqueous species associated with each element, e.g. Ca^{2+} , or element valence state, e.g. Fe^{2+} and Fe^{3+} . Therefore, each transported component represents a master species from the user-specified PHREEQC thermodynamic database that defines the reactions. Only those master species present in the groundwater under consideration or are produced as a consequence of the chemical reactions need to be included for transport. The transported quantities are the total amounts of each element master species. However, to fully define the chemical state of the system, three additional components must always be defined, namely H (total hydrogen not included in water molecules), O (total oxygen not included in water molecules) and E (charge balance). It is necessary to know the quantity of H and O , since they are constituents of some species involved in chemical reactions, but since the quantity included in H_2O is known from the quantity of water, it is not necessary to transport the H and O included in water molecules and it is more accurate not to do so. The charge balance, E , should be zero for a physical

system, but due to numerical rounding it is typically in the range $1.0 \cdot 10^{-18}$ to $1.0 \cdot 10^{-12}$. Transporting E prevents numerical charge imbalances arising from the chemistry calculations accumulating due to transport.

Transport of solutes is calculated using multi-component solute transport. However, for the transport of many components it is not usually practicable to solve the full set of coupled equations simultaneously. In this case, sequential iteration can be used as an operator splitting method to decouple the equations and solve each groundwater flow and transport equation separately within each time step. Multiple iterations of the sequence of equations can be carried out for increased accuracy at the expense of computational time, but normally a single iteration is sufficient for a system that is evolving slowly relative to the time step size. The boundary conditions and initial conditions can either be defined in terms of the individual components or they can be defined in terms of reference waters. Each reference water defines a particular solution composition and is often associated with water of a particular origin, e.g. sea water. Reference waters can be pre-reacted and charge balanced. Figure 4-10 shows a flow diagram describing the reactive transport system in ConnectFlow.

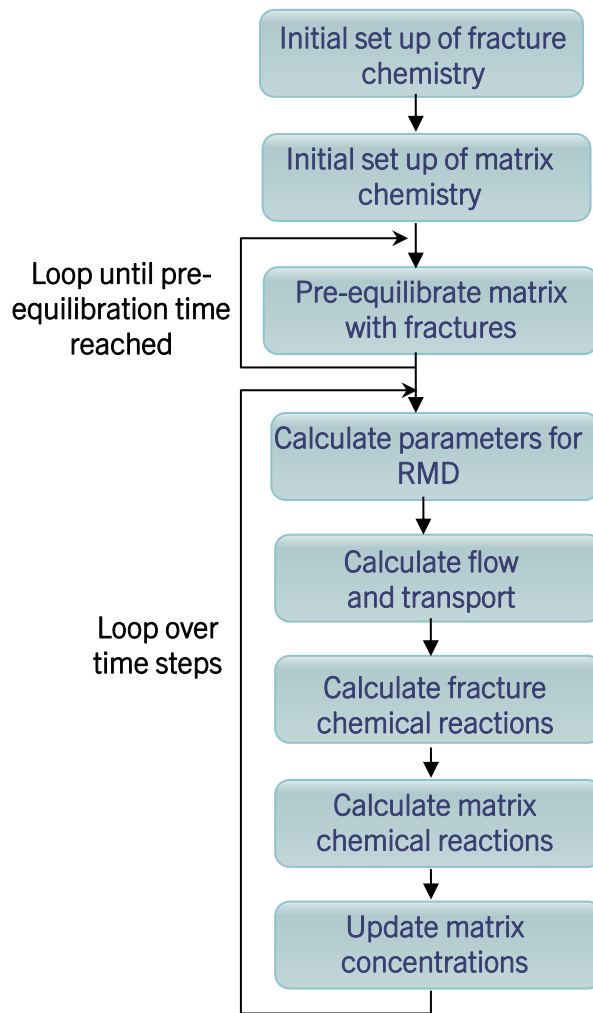


Figure 4-10. Flow diagram showing the stages of a reactive transport calculation.

The following reactive transport features are implemented in ConnectFlow:

- Mineral equilibration reactions;
- Ion exchange reactions;
- Surface complexation reactions;
- Kinetic reactions;
- Spatially varying minerals (uniform, by rock type or by finite element);
- Formation of secondary minerals (minerals not initially present, but generated by chemical reactions) and their equilibration with solutes;
- Pore clogging.

Reactions at equilibrium are governed by a mass-action equation:

$$K_i = a_i \prod_{m=1}^{m=M_{aq}} a_m^{-\nu_{m,i}} \quad \text{Equation 4-33}$$

where K_i is the temperature-dependent equilibrium constant of species i , a_i is the activity of species i , M_{aq} is the total number of master species in its formation reaction, a_m is the activity of master species m , $\nu_{m,i}$ is the stoichiometric coefficient of master species m in the chemical equation forming species i . Terms on the right-hand side of the reaction equation are given negative coefficients and terms on the left-hand side are given positive coefficients. A master species is associated with each element, e.g. Ca^{2+} , or element valence state, e.g. Fe^{2+} or Fe^{3+} .

The activity of a species, a_i , is related to its molality, m_i , [moles per kg of water] by

$$a_i = \gamma_i m_i \quad \text{Equation 4-34}$$

where γ_i is the activity coefficient of species i .

Reactions that do not reach equilibrium within the timescales of interest are kinetically controlled. The changes in concentrations of solutes associated with the dissolution of non-equilibrium solids are given by the rate equation:

$$\frac{dm_i}{dt} = \nu_{i,k} R_k \quad \text{Equation 4-35}$$

where m_i is the molality of species i [moles per kg water], t is time [s], $\nu_{i,k}$ is the stoichiometric coefficient of species i for substance k , and R_k is the overall reaction rate [mol/kg/s] for the dissolution of solid k . The changes in solute concentrations are calculated by integrating over time using a Runge-Kutta scheme with up to six intermediate evaluations of the derivatives. The integration time is adjusted to maintain an error estimate to within a user-specified tolerance. The overall reaction rate, R_k , for solid, k , is:

$$R_k = r_k \frac{A_0}{W} \left(\frac{m_k}{m_{0k}} \right)^n \quad \text{Equation 4-36}$$

where r_k is the specific rate [mol/m²/s], A_0 is the initial surface area [m²] of the solid, W is the mass of solution [kg], m_{0k} is the initial number of moles of solid, m_k is the number of moles of solid at a given time and the term $(m_k/m_{0k})^n$ is a factor to account for changes in A_0/W during dissolution and ageing of the solid.

The actual reactions available will be those present in the thermodynamic database supplied by the user. If the model has temperature variation then this will be reflected in the reaction temperatures, if supported by the thermodynamic database. Typically the reactions will be valid up to ionic strengths of around 3 moles per litre for thermodynamic databases with appropriate ionic strength treatments and parameters (such as SIT), but only to 0.3 moles per litre when the Davies equation is used. Rate expressions for kinetic reactions are also given in the thermodynamic database.

Treatment of spatially varying minerals and secondary minerals allows minerals to be created and depleted across the model and their quantities to be initially specified in a flexible way and the evolution of the quantities to be monitored. The pore-clogging facility allows the permeability and porosity of the rock to be modified due the volume changes in minerals as a result of precipitation or dissolution. The change in permeability as the porosity changes is calculated as:

$$K = \left(\frac{\phi}{\phi_0}\right)^3 K_0 \quad \text{Equation 4-37}$$

where K is the updated permeability [m^2], K_0 is the original permeability, ϕ is the updated porosity [-] and ϕ_0 is the original porosity. Changes in porosity in the rock matrix due to chemical reactions are not currently included.

Various output options are available to export the chemical composition at selected locations in the model as mass fractions of chemical components, pH and pe. Also there is a facility to carry out additional chemistry on solute compositions at selected times, which provides access to the quantities of different chemical forms, e.g. bicarbonate and carbonate in the case of carbon.

A finite volume method for rock matrix diffusion (RMD) is provided within Connectflow (see section 4.6.1) that allows a flexible discretisation of the rock matrix and is compatible with chemical reactions (unlike the original RMD method). The method allows chemical reactions to be carried out for each cell in the rock matrix, and the full solute composition, including its distance dependence, can be output for analysis. The temperature is also needed for the chemistry calculations so this is assumed to be the same for the rock matrix as at the centre of the associated fractured rock finite element. For cases where the density is needed (where the water compositions are given in the form of concentrations, rather than mass fractions), the rock matrix pore water density is calculated using the rock matrix pore water salinity along with the pressure and temperature at the centre of the associated fractured rock finite element.

The sequential iteration transport calculations and the chemistry calculations have been parallelised to provide improved run-times on multi-processor computers and compute clusters via the Message Passing Interface (MPI) approach. Additional improvements in performance can be achieved by specifying a threshold for chemistry calculations. This threshold specifies a minimum relative change in the mass fraction of any component at each location that needs to occur, since the last time chemistry was calculated at that location, before chemistry is calculated again at that location. The use of a calculation threshold reduces the number of chemistry calculations in parts of a model where the groundwater composition is evolving very slowly. However, calculation thresholds cannot be used with kinetic reactions.

5 Concepts within the Discrete Fracture Network model

In many geological formations, the primary flow is through a connected network of discrete fractures (DFN). This provides a very heterogeneous system, and the fracture-network geometry can lead to dispersion of any solute being transported through the formation. It is often necessary to show sufficient understanding of the flow system to give confidence that predictions of the large-scale properties of the flow system can be made from the results of field-scale investigations. In order to build confidence, it is important to show a very detailed understanding of field experiments that are generally on scales at which the influence of the fracture-network geometry is significant. The geometry and connectivity of the fracture system and the possibility of hydraulically important pathways through the network can play an important role in determining the scale dependence of the effective properties of the system. Indeed, one of the early motivations for the development of the DFN approach was to develop an understanding of the scale dependence of the effective dispersion parameters for radionuclide transport through fractured rock, which had been inferred from field data ([Smith et al., 1984] for example).

In the DFN approach, the geometry of the fracture-network is accounted for explicitly. The approach is needed to describe or predict aspects of the performance of the fractured system where the geometry of the fracture-network plays a significant role. Some examples of such circumstances are:

- representations of any flow experiments where the fracture connectivity is important, which in practice means almost all interpretations of field experiments where a detailed understanding is needed;
- prediction of the effective flow properties of the fracture-network system and of the scale dependence of effective properties;
- prediction of the effect of the fracture-network geometry on the effective dispersion for solute transport;
- prediction of the effect of the fracture-network geometry on the effective hydraulic diffusivity of the pressure field in response to a pressure change and the inferred radius of influence of pressure tests.

From the above list, it can be seen that an understanding of the role of the fracture geometry can be important in almost all aspects of an investigation of a fractured rock system. The two main reasons that such discrete models are not more commonly used are the complexity of the models and the fact that stochastic models inevitably require uncertainty to be addressed formally.

The complexity means that many data are required to characterise fracture systems adequately. Whilst there are still issues to be resolved in the experimental characterisation of fracture-network flow geometry, a number of research projects for the radioactive waste industry have demonstrated the feasibility of collecting suitable basic input data [Bolt et al, 1995; Geier et al., 1992; Herbert et al., 1991b, Olsson et al., 1995]. Understanding fracture channelling and the extent of the flow wetted surface of the fracture are still research tasks, but simple assumptions can be made and the other data interpreted consistently so that the resulting fracture-network geometry reproduces key features of the physical network. In many cases, however, there will be a balance between the benefits of a more detailed representation of the system, and the increased cost of collecting data for which there may be significant uncertainty.

The second reason why the discrete fracture-network approach is not more widely used is the need to treat predictions in a probabilistic framework and consider the uncertainty due to the details of the fracture geometry directly. Fracture-network models are necessarily stochastic since it is not possible to determine the location and extent of each flow-conducting or mechanical break in the rock. Instead a stochastic approach is used, in which the statistics of the fracture system are

determined and realisations of the fracture-network geometry that exhibit the same statistics as the physical system are generated and used for simulation. This means that a discrete fracture-network approach does not predict the result of a given experiment. Instead, it predicts a probability distribution of equally likely results given the stochastic description of the fracture geometry and properties. This realisation-dependent uncertainty corresponds to a lack of knowledge of the precise fracture geometry. In many respects this is an advantage of the approach over deterministic models since the uncertainty is real and unavoidable. Conventional approaches often make single-valued predictions, however this is simply not facing up to the reality of uncertainty.

Applications of DFN modelling include:

- interpreting site characterisation data;
- modelling of flow and transport in regional fracture-network systems;
- obtaining effective properties as data input to large-scale effective porous medium models.

In site characterisation programmes, DFN modelling has been used to validate the fracture network approach by comparing data from hydrogeological experiments in fractured rock (e.g. well tests) against model predictions. As part of the assessment of post-closure performance of potential deep repositories, discrete fracture-network models have been used to predict the groundwater pathways by which radionuclides released from a repository might return to the environment. Effective properties have been obtained using ConnectFlow's DFN capabilities for input into large-scale 3-D porous medium models or reservoir simulators (for example [Scafer et al., 1995]).

DFN modelling can be broken up into two phases:

- Creation of a DFN model.
- Performing calculations on this model, such as solving for groundwater flow, upscaling of properties for use in a CPM model, solute transport and various analyses.

The creation of a DFN model will be discussed in subsequent sections and involves:

- definition of the model domain;
- fracture generation;
- inclusion of engineered features (boreholes, tunnels or shafts);
- calculation of fracture intersections.
- provision of boundary conditions;

The calculations that can be performed are detailed in Chapter 6.

5.1 Model Domain

The model is defined within a domain formed from the union of a number of (possibly irregular) hexahedra or “region elements”. The region elements are defined by supplying a list of the coordinates of the vertices belonging to each element. Where the faces of two region elements are joined, the four corners of the adjacent sides must be coincident. The faces of the region elements need not be planar. In general, they form bilinear surfaces. An example of a complex flow domain is shown in Figure 5-1.

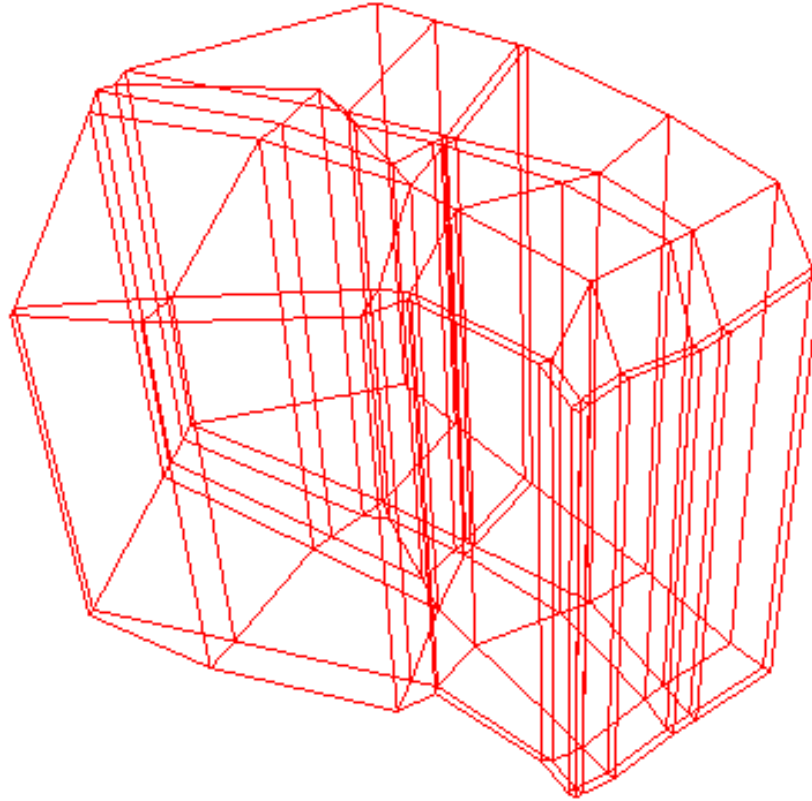


Figure 5-1: An example of a complex flow domain built from 37 irregular hexahedra.

5.2 Fracture Generation

An individual planar fracture is completely defined by:

- the location of its centre;
- three orientation angles (dip angle, ψ , dip direction, α , and orientation, ω);
- the lengths of each side (or in the case of square fractures, a single length);
- an effective hydraulic aperture or transmissivity (and possibly the variation of aperture within the fracture).

The definition of the orientation angles (ψ , α , ω) relative to the Cartesian coordinate system (x , y , z) is shown in Figure 5-2. It is usual to orient the axes such that x is east, y is north, and z is vertically upwards.

Fractures can either be “known” (deterministic) in which case the above properties are specified explicitly, or “random” in which case the fracture properties can be sampled from a wide range of statistical distributions.

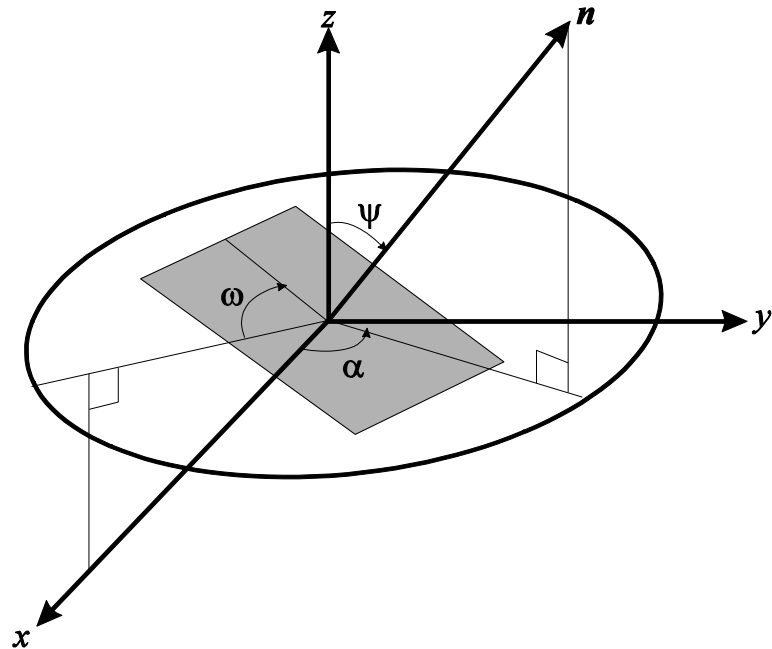


Figure 5-2: The angles describing the orientation of a fracture, in relation to the coordinate axes and the normal to the plane, n : ψ : the dip angle, α : the dip direction, ω : the orientation angle.

5.3 Fracture Network Characterisation

This section describes the main methods for inferring fracture-network geometries from field measurements of the fracture-network properties [Dershowitz, 1984; Herbert et al., 1990]. This is the first major task the user faces in three-dimensional simulations. Analogous methods are used in the derivation of appropriate two-dimensional equivalent networks.

The key parameters used to characterise a fracture-network are:

- identification of independent fracture sets;
- the distribution of fracture orientations;
- the statistical process for generating the fracture locations in space;
- the fracture density;
- the distribution of fracture lengths;
- and the distribution of fracture transmissivities.

When characterising the fracture orientation distribution, it is generally found that the fractures can be divided into a number of distinct fracture sets. These sets of fractures comprise fractures that can be characterised by common distributions of parameters, and which have a common origin and history.

These fracture sets are often defined in terms of their orientation distributions that tend to be clustered around preferred orientations of the normals to each fracture plane projected on to a lower hemisphere. This definition of the characteristic orientation is best achieved by using conventional statistical methods to identify distinct clusters. The fractures can then be separated into their distinct sets and further parameters inferred for each set independently.

The distribution of fractures has commonly been assumed to be uniform in space with just a single fracture density being used to specify how many fractures to generate. An equivalent approach to using a fracture number density is to generate fractures up to a specified area density of fracture surfaces per unit volume. Sampling the various distributions of the parameters generates the

fractures. The positions of the fracture centres are generated assuming a Poisson process. Care must be taken to avoid edge effects, and this is usually accomplished by generating the fracture-network in a larger region than that to be simulated.

The fracture density may be obtained from the spacing of fractures along a scan line on a mapped exposure, or from a fracture log along a borehole or core. Each distinct set of fractures has its own characteristic distributions of properties, and the density of each of these fracture sets is usually determined independently. For a given fracture set, the number density, ρ , is given in terms of the mean spacing of intersections along a straight line, \bar{s} , by:

$$\bar{s} = (\rho \bar{X})^{-1} \quad \text{Equation 5-1}$$

where \bar{X} is the mean projected area of the fractures onto a plane perpendicular to the measurement line.

The fracture set length distribution is one of the more difficult parameters to infer since we have only one- or two-dimensional data from which to infer a length distribution that will only be fully determined by a three-dimensional description. A number of assumptions need to be made at this stage. First, it is difficult to characterise the shape of the transmissive area of the fracture plane. It is generally assumed that this surface has a simple geometry. In the DFN module of ConnectFlow, it is assumed to be rectangular.

Once the fracture shape has been fixed, then one can use analytical results giving the relationship between the distribution of fracture lengths to the distribution of fracture trace lengths as measured on a large two-dimensional trace plane intersecting the network. For example, for square fractures of side length distribution, L , the moments of the length distribution, L_i , are related to the moments of the corresponding distribution, t , of fracture traces measured on a large trace mapping plane by:

$$t_1 = \frac{\pi L_2}{4 L_1} \quad \text{Equation 5-2}$$

$$t_2 = \left[\ln(1 + \sqrt{2}) - \frac{\sqrt{2} - 1}{3} \right] \frac{L_3}{L_1} \quad \text{Equation 5-3}$$

where L_i are the i -th moments of the length distribution and t_i are the i -th moments of the trace length distribution. Similar formulae can be obtained for higher moments. A common approach is to make an assumption as to the mathematical form of the distribution of fracture lengths and then either use these simple formulae between the means and second moments of the distribution, or to simply calibrate against statistics from a specific trace map. In fact, the trace length to fracture length relationship is quite insensitive to the precise shape assumed for the fractures and there is relatively little difference between the results for circular or square fractures. A more significant assumption is the choice of the mathematical form of the fracture length distribution. Typically, log-normal or power law distributions are used. Although these often result in a good fit between the main parts of the simulated and measured trace length distributions, the goodness-of-fit of the tails of the two distributions is often less good. A poor match in the tail of the distribution may result in the existence of extreme, unphysical fractures with very long traces. These are quite unimportant to many of the statistics used to infer parameters but may have a much more important role in the network flow.

Finally, the hydraulic properties of the fractures need to be defined. The usual assumption is that some form of the parallel plate law for plane fracture flow applies, but rather than measure a distribution of apertures directly, a more reliable approach is to infer a distribution of fracture transmissivities. This too, generally relies on an assumption as to the form of the probability

distribution of fracture transmissivities. Generally the log-normal distribution is used. With this distribution and a specified fracture spacing, then the mean and standard deviation of fracture transmissivities can be related to the mean and standard deviation of short interval packer tests in boreholes so long as it is assumed that the transmissivities of fractures intersecting the test section add to give the transmissivity of the test section. Strictly, fracture connectivity away from the borehole will affect the packer test results, but for short tests, the radius of influence of the test will be small and the measurements can be taken to correspond to the summation of local transmissivities. The fitting process involves typically using maximum likelihood estimators and in general will require numerical evaluation of the best estimates. Again, the results of the fracture property interpretation should be checked by simulation of the measurement process and it may be appropriate to infer the parameters of the distribution by calibrating directly against the experimental data (see [Herbert et al., 1990] for more detail).

An alternative approach to generating the fracture-network, which is often used, is to generate fractures using an initial approximation and test the resulting network by simulating the experimental measurement procedures. Then the network is modified to improve the correspondence between, for example, the numerically simulated log and the physical log. This calibration procedure is particularly appropriate when simulations are made based on more complex statistical descriptions of the fracture properties and spatial densities. Such simulated measurements should in any case be used to check the validity of the interpretation of the network parameters.

5.4 Known Fractures

For known (or deterministic) fractures, all properties are specified either within the ConnectFlow input or imported from a formatted file. There are several instances when the use of known fractures is appropriate. Firstly, when large-scale fracture zones are defined. The appropriate transmissivity for such zones may be obtained from hydraulic tests or by calculating an effective transmissivity based on a local scale stochastic model of the fracturing around the zone.

Secondly, where the network has been well characterised, the stochastic network may be replaced by the set of fractures that have been measured. For example, a stochastic network of fractures may be generated based on a statistical analysis of the data from several boreholes. The random fractures around each borehole can then be replaced by the observed fractures at the borehole. This is a simple method of conditioning random simulations.

5.5 Random Fractures

Separately parameterised sets of random fractures can be defined in a ConnectFlow DFN model. The locations of the centres of the fractures are distributed uniformly within a cuboidal region whose boundaries are set by the user. This region should be sufficiently larger than the flow domain, bearing in mind the expected size of the fractures, so that there is no reduced density of fractures near the edge of the flow domain. For each of the other fracture properties, the user specifies the distribution type and its parameters.

In the DFN module, the following distributions are available:

- constant;
- uniform;
- normal;
- log-normal;
- two parameter negative exponential;
- triangular;
- log-triangular;
- univariate or bivariate Fisher (for dip angles and dip directions only);
- truncated log-normal;
- power-law (for fracture lengths only).

Given this information, fractures are generated randomly up to a user-prescribed density. A typical generated fracture-network is shown in Figure 5-3.

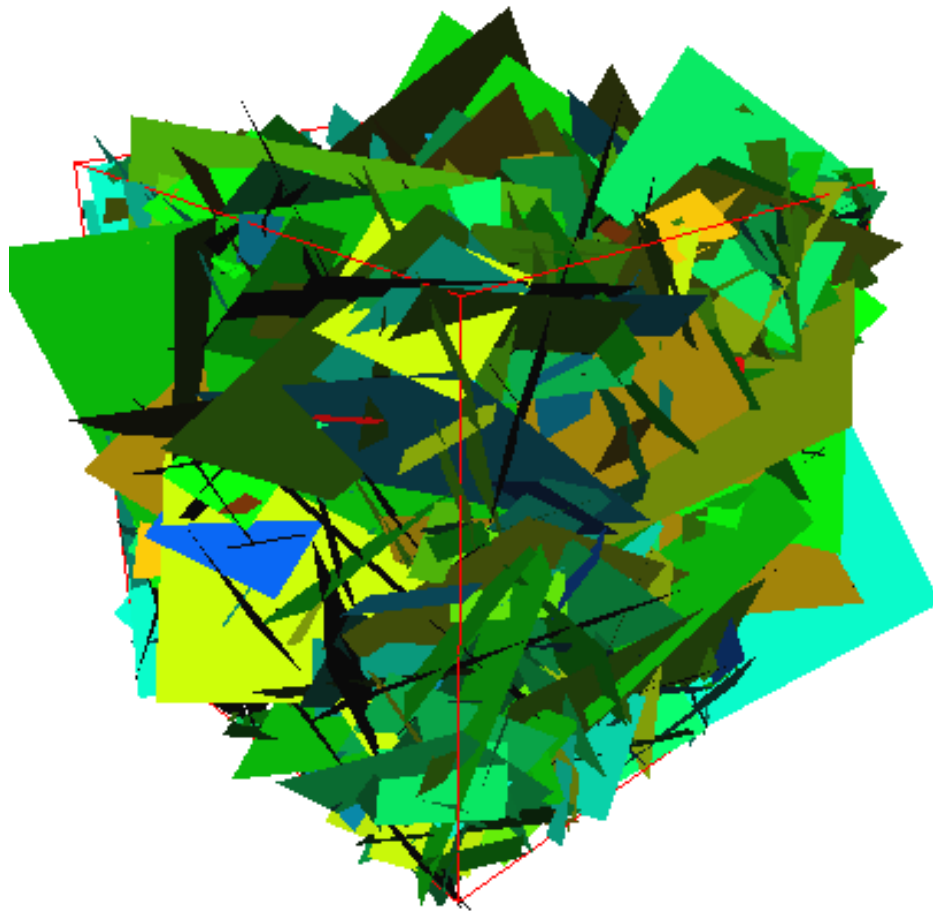


Figure 5-3: An example of a fracture-network generated within a cuboid flow domain. The fractures are coloured according to the logarithm of transmissivity: red for high transmissivity, blue for low.

5.5.1 Variable Apertures on Fractures

As well as fractures each having a uniform aperture, ConnectFlow can represent the random variations of aperture within a given fracture. This option may be specified for some or all of the sets of random fractures, and also on a known fracture. The local values of the aperture are generated from a log-normal distribution with standard deviation prescribed by the user. With a known fracture, the mean value of the distribution is simply the aperture given by the user.

In the case of a random fracture, a value is first randomly sampled in the same way as for a uniform fracture, but this value is then used as the mean aperture about which the local aperture distribution on the fracture is generated. Note that the standard deviation of the aperture distribution for a single fracture need not be the same as the standard deviation of the mean apertures of the fracture set.

In reality, the apertures at nearby points on the same fracture may well be correlated to some extent. To represent this, the DFN module provides the user with the facility to specify a correlation length scale and one of 3 correlation functions (note that these are correlations for the distribution of the logarithm of the aperture):

$$\rho_1(\xi) = \begin{cases} 1 - \frac{2\xi}{2l} - \frac{\xi^3}{2l^3}, & \xi < l \\ 0, & \xi \geq l \end{cases} \quad \text{Equation 5-4}$$

$$\rho_2(\xi) = \exp\left(\frac{-\xi}{l}\right) \quad \text{Equation 5-5}$$

$$\rho_3(\xi) = \begin{cases} 1 - \frac{\sqrt{(2\xi l - \xi^2)}}{l}, & \xi < l \\ 0, & \xi \geq l \end{cases} \quad \text{Equation 5-6}$$

where ξ is separation and l is the correlation length scale. If uncorrelated apertures are required, this may be achieved by using either correlation function 1 or 3, with a zero correlation length.

5.5.2 Fracture Subdivision (“Tessellation”)

A simpler method of generating a variable transmissivity on each fracture (tessellated fractures) is to sub-divide the fractures into smaller fractures (sub-fractures) according to an approximate correlation length, and generate the transmissivity on each sub-fracture independently. In this way fractures are generated according to a specified length distribution, but then sub-divided such that no sub-fracture is longer than the correlation length. Hence, the number of fractures increases but the fracture area density is maintained. This method is more appropriate for large random networks.

Another reason for sub dividing fractures is one of discretisation. The number of finite elements used to discretise each fracture is similar on every fracture, irrespective of the fracture length. If fracture lengths vary by orders of magnitude then large fractures may be under-refined, and small ones over-refined. Hence, tessellation can be used to split large fractures into a network of sub-fractures of a more uniform size, and consequently a more uniform discretisation. In this case, the transmissivity of the sub-fractures is inherited from the transmissivity of the tessellated fracture from which it was created.

5.6 Engineered Features

Since field experiments in fractured rock usually involve boreholes, a model feature (“borehole”) is provided to facilitate their incorporation in simulations. There is a further feature (“shaft”) to represent engineered features of larger radii such as tunnels or shafts. Both types of feature are specified by the coordinates of the two ends and a radius. Both models add extra flow connections to the network where the engineered features intersect fractures. Generally, if the radius of the engineered feature is small compared to the length of fractures then the borehole submodel is adequate, otherwise greater accuracy is gained by using the shaft model. For a borehole, only the fractures intersecting a line joining the two ends are hydraulically joined to the borehole. For a shaft, all fractures intersecting a cylinder with the specified radius and axis are hydraulically joined to the shaft. The axial hydraulic conductance (units of m^3s^{-1}) of the feature is calculated from the radius or from a specified permeability. The properties of a skin layer due to grouting or skin effects can be specified to limit radial flow. Section 6.9 gives more details on the simulation of flow around engineered features.

Any two engineered features may be joined hydraulically. Hence, curved boreholes can be represented by several joined boreholes of varying inclination. Figure 4 gives an example of a complex model with many sections of engineered feature joined together to form a spiral tunnel. Two vertical shafts are also shown.

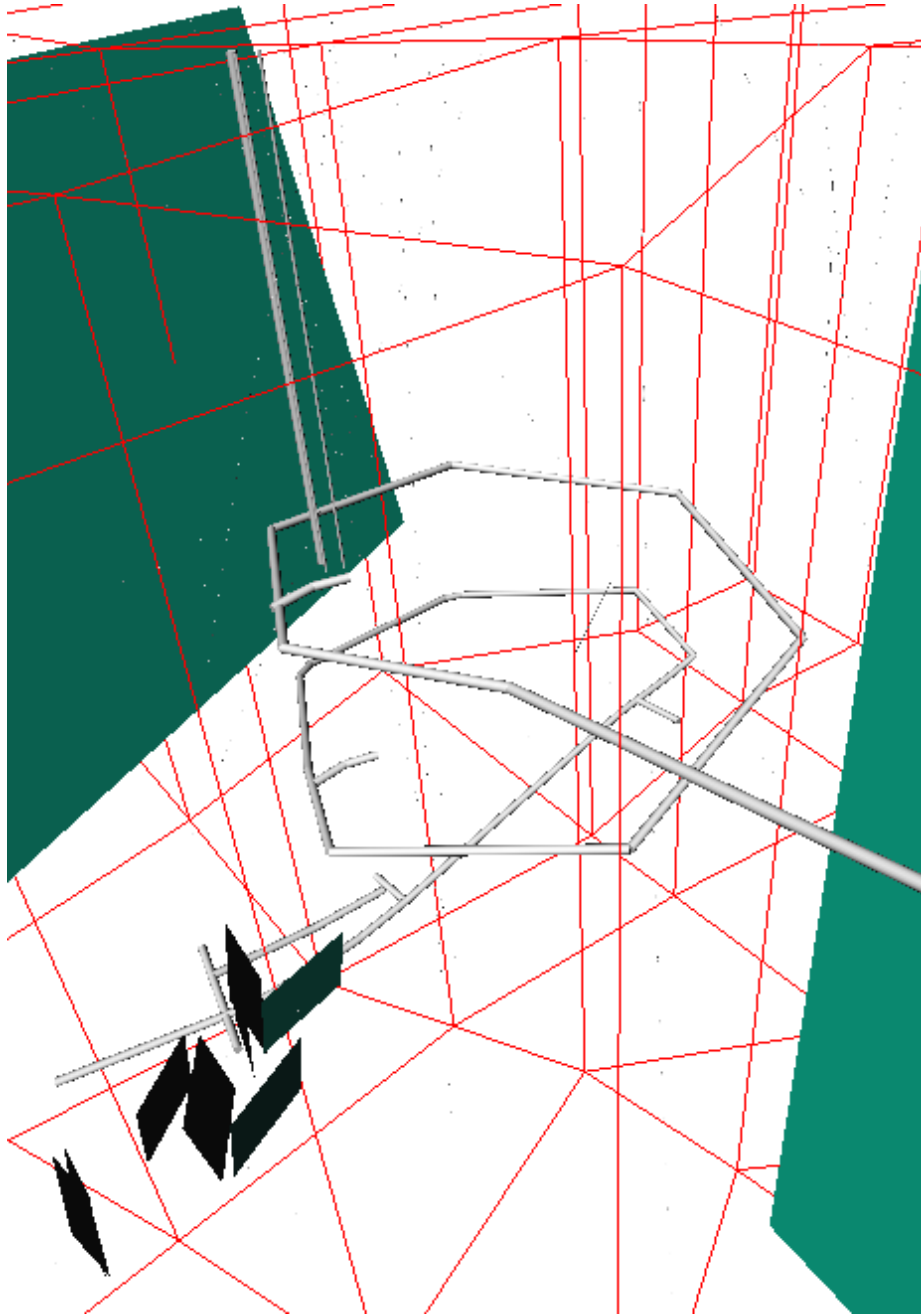


Figure 4: An example representation of a complicated system of tunnels (spiral) and shafts (vertical). Some region element edges, two large deterministic fractures, and a few random fractures are also shown.

5.7 Fracture Intersections

Once the fracture-network has been generated, the next step is to calculate all the fracture intersections. This allows an interpretation of the fracture-network connectivity. Intersections between the fracture planes and the boundaries of the flow domain are calculated, and part or all of a fracture falling outside the flow domain is discarded.

The intersections are determined by solving the equation for the intersection of the two fracture planes using elementary geometry. In order that large networks can be handled, the search for intersections is optimised by dividing the overall region into subregions and determining the planes wholly or partly within each subregion, and then only testing planes in the same subregion for

intersections. In this way, the asymptotic cost of the calculation of the intersections is proportional to the number of planes rather than the square of the number of planes. The flow field is discretised by assigning a number of nodes, referred to as the global flow nodes, to each intersection.

5.8 Boundary Conditions

Boundary conditions are set on the boundaries of the flow domain. By default, ConnectFlow treats any boundary for which no condition is set as impermeable. For a permeable boundary, either a pressure distribution or a fluid mass flux can be specified. A pressure distribution can be defined in five ways:

- a constant value may be set over the whole surface;
- a linear pressure variation may be specified over the whole surface;
- interpolated (bilinearly) from a set of pressure values at the region element vertices, the pressure values are specified in the input data file;
- interpolated (bilinearly) from a regular mesh with pressure values that is read from a file;
- assuming the pressure is equal to a specified initial condition (current value).

For flux boundary conditions, a uniform fluid mass flux in units of $\text{kgm}^{-2}\text{s}^{-1}$ is specified over a boundary surface. A mass flux enters each fracture that intersects the surface. The amount of flux entering a particular fracture is weighted according to the length of the fracture's trace, such that the total mass-rate entering the surface equals the mass flux value specified multiplied by the area of the surface.

In addition to the boundary conditions set on the flow domain boundaries, the user may specify the pressure or flux on individual engineered features.

For mass transport, the salinity can be specified on selected surfaces in the following ways;

- setting a constant concentration boundary condition over the whole surface;
- setting a linearly varying concentration boundary condition over the whole surface;
- setting a zero dispersive flux (an outflow condition);
- setting an inflow concentration (where inflow occurs), where there is outflow a zero dispersive flux is automatically applied;
- assuming the concentration is equal to a specified initial condition (current value).

6 Numerical Methods used for Discrete Fracture Network Models

This chapter details the various types of calculations that can be performed on DFN models by ConnectFlow.

6.1 Geometric Analysis

Prior to a flow calculation, useful information can be gained by analysis of the fracture intersections. One of the main characteristics of a fracture-network that controls the behaviour of the flow is the connectivity of the network.

6.2 Percolation Analysis

The most basic measure of connectivity is whether the fracture-network has a connection across the region or not. This depends on the fracture density and the change from unconnected to connected networks is predicted by the percolation threshold. The percolation threshold gives the density at which the size of connected clusters of fractures suddenly increases from a relatively small typical cluster size to the existence of a percolating cluster that spans the region. The percolation threshold is quite a sharp transition: a small increase in fracture densities will change the network from one for which no realisations have connections across the model region to one for which all realisations are well-connected [Robinson, 1984]. This percolation threshold depends upon the statistical properties of the network, but for random networks there is a much more significant dependence on the dimension of the network geometry. Three-dimensional networks become well connected at much lower fracture densities than two-dimensional networks.

The ConnectFlow percolation option builds the network one fracture at a time. As each individual fracture is included, a list of fracture clusters is maintained and updated. If the fracture intersects any fracture belonging to an existing cluster it is added to the appropriate cluster list. If it intersects with two or more disjoint clusters, then the cluster lists are combined. If it is isolated, then a new cluster list is started. When a single cluster connects all the relevant boundary surfaces, percolation has occurred, and any remaining fractures in the original network may be discarded, if required.

6.3 Steady State Constant Density Groundwater Flow

Steady-state constant-density groundwater flow in a fracture network can be modelled in the current version of ConnectFlow. The basic approach is very simple. Groundwater flow in each fracture is modelled numerically. Then the flow in the overall network is obtained by combining the flows in the different fractures, using the conditions that

1. the groundwater pressure is continuous between two intersecting fractures;
2. groundwater is conserved at an intersection, so that groundwater which flows out of one fracture flows into the other.

The DFN module uses a Galerkin finite-element approach to modelling. The Galerkin approach starts from the weak form of the governing equation, which is derived by multiplying the governing equation by an arbitrary test function in a suitable function space, and integrating over the domain, integrating by parts terms involving high-order derivatives (see Equation 6-4 below). The benefit of this manoeuvre is that the weak form is equivalent to the original equation for sufficiently smooth functions, but it is also applicable to functions that are not as smooth, such as the functions derived by finite-element discretisation.

In the finite-element method, the domain is discretised into ‘finite elements’ of simple shape. On each element, a quantity of interest is approximated by a simple function, such as a polynomial, determined by the values at a small number of points, or nodes on the element. This is equivalent to approximating the quantity of interest as a linear combination of certain basis functions that are associated with the nodes; the basis function associated with a node taking the value 1 at the node and 0 at all the other nodes. The discretised equations are obtained by taking the test functions in

the weak form to be the set of basis functions for nodes where the value of the quantity is not specified by a Dirichlet boundary condition. These equations are supplemented by the Dirichlet boundary conditions.

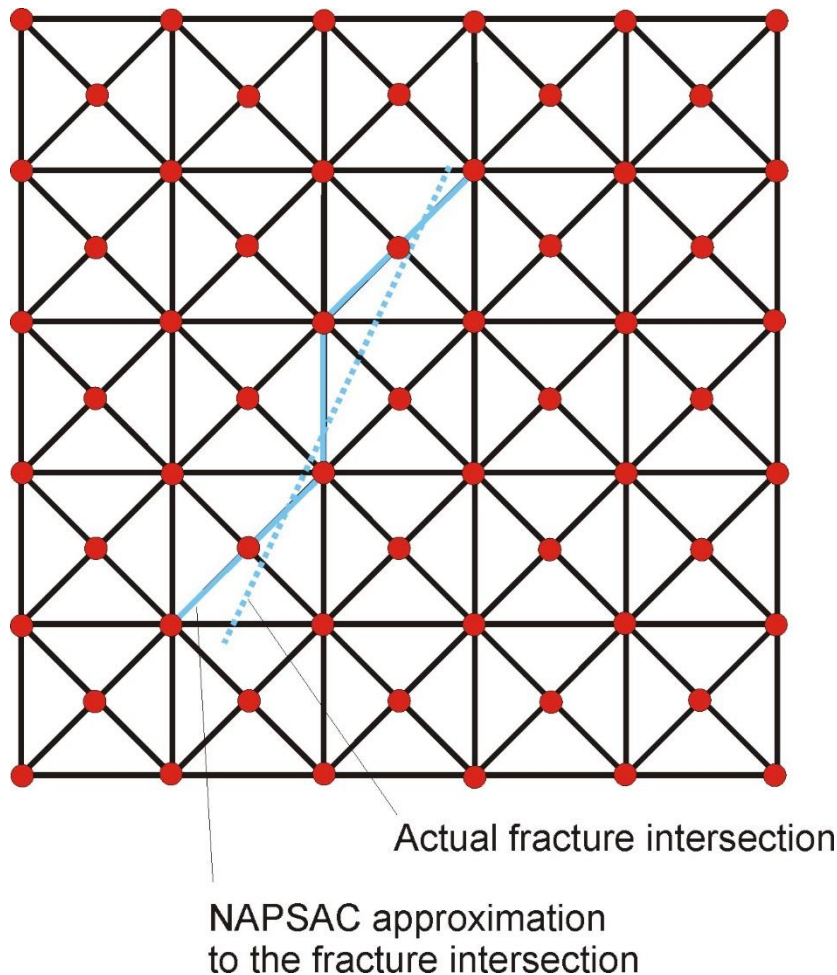


Figure 6-1: The finite element discretisation of a fracture in ConnectFlow (NAPSAC) and the approximation of intersections with other fractures by lines along finite-element boundaries.

In the DFN module, the finite-element method is applied on two levels: individual fractures and fracture intersections. Individual fractures are discretised into triangular elements as shown in Figure 6-1. On each element, the residual pressure

$$P^R = P + \rho_0 g(z - z_0) \quad \text{Equation 6-1}$$

is approximated as a linear function. Here

- P is the groundwater pressure;
- ρ_0 is a reference value of the groundwater density;
- z is the elevation;
- z_0 is a reference elevation.

As noted above, this is equivalent to approximating the residual pressure on the fracture as a linear combination of the ‘local basis functions’.

On the scale of the overall network, the residual pressure is characterised by its values at certain ‘global nodes’ associated with the fracture intersections, which are approximated by lines along the boundaries of the elements representing the fracture (see Figure 6-1). On a fracture, the global

basis function Ψ_I corresponding to a global node I on one of the intersections with other fractures is taken to be the finite-element solution for steady-state groundwater flow on the fracture in the case in which the residual pressure is specified to be 1 at global node I and 0 at all the other global nodes on the fracture.

The steady-state groundwater-flow equation in the fracture is

$$-\nabla \cdot \left(\frac{e^3}{12\mu} (\nabla P^R) \right) = 0 \quad \text{Equation 6-2}$$

where

- e is the hydraulic aperture;
- ρ is the groundwater density;
- μ is the groundwater viscosity;
- ∇ denotes the two-dimensional gradient operator in the fracture.

The possibility that the fracture aperture, and hence fracture transmissivity, may vary over the fracture surface is allowed. The transmissivity T is generally taken to be related to the fracture aperture e by the cubic law

$$T = \frac{\rho g e^3}{12\mu} \quad \text{Equation 6-3}$$

on the basis of flow between parallel plates [Snow, 1968].

The weak form of Equation 6-2 is

$$\int_F \nabla w \cdot \frac{e^3}{12\mu} \nabla P^R + \int_B w \mathbf{n} \cdot \mathbf{f} = 0 \quad \text{Equation 6-4}$$

where

- F is the fracture;
- B is that part of the boundary of the fracture on which the flux is specified. Note that B includes both sides of intersections with other fractures;
- \mathbf{n} is the unit normal to the boundary directed out of the domain;
- \mathbf{f} is the groundwater flux density on B ;
- w is a test function.

The approach used in ConnectFlow allows considerable flexibility in the number and location of the global nodes. This allows highly refined models to be used for accuracy or coarser models to be used in order to keep computational costs down, as appropriate. However, the details of the method are quite complicated in the most general case. Therefore, the basis of the approach is first presented in the case in which the global nodes are identical to the local nodes on the intersections (see Figure 6-2), and then the modifications for more complicated cases are indicated. In the simplest case, the finite-element equations that characterise the global basis function for node I (denoted ψ_I in this case) are

$$\int_F \nabla \varphi_n \cdot \frac{e^3}{12\mu} \nabla \psi_I = 0, \text{ for local nodes } n \text{ not on intersections;} \quad \text{Equation 6-5}$$

supplemented by the boundary conditions

$$\psi_I = \begin{cases} 1 & \text{for } j = \text{local node } i \text{ corresponding to } I \\ 0 & \text{else} \end{cases}, \quad \text{Equation 6-6}$$

for local nodes j on the intersections.

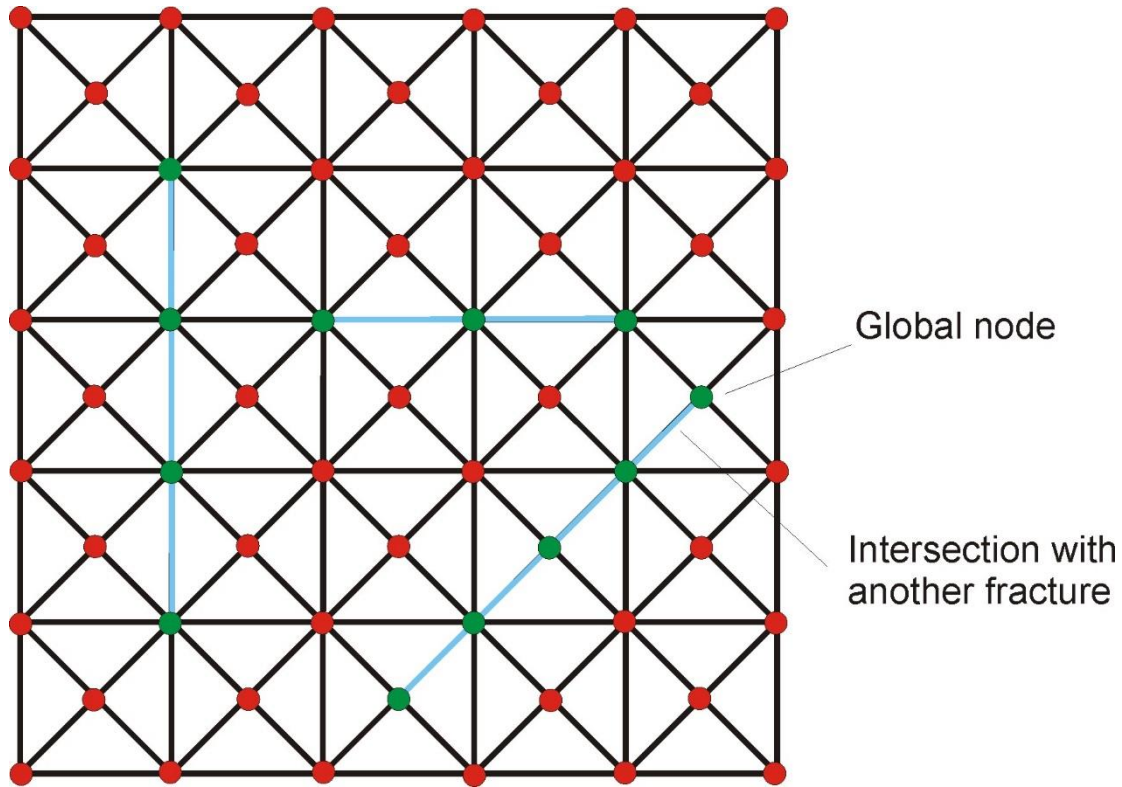


Figure 6-2: Intersections on a fracture in the case in which they lie along finite-element boundaries and the global nodes correspond to the local nodes on the intersections.

These equations can be readily solved using a suitable numerical scheme. In ConnectFlow, a direct solver, which employs a variant of Gaussian elimination, is used. The solver is purpose-built to exploit the structure of the numerical equations resulting from the regular form of the finite-element grid used in ConnectFlow. Essentially, the equations for the nodes at the centre of each rectangular block (see Figure 6-1) are eliminated first, to give a matrix with the same form as that for a regular rectangular discretisation. This matrix is then solved using straightforward Gaussian elimination. This is a very efficient approach.

It can easily be seen that the global basis function for global node I is equal to the local basis function for the local node i corresponding to I plus a linear combination of local basis functions for local nodes n not on intersections, that is

$$\psi_I = \varphi_i + \sum_n b_{In} \varphi_n \tag{Equation 6-7}$$

for certain constant coefficients b_{In} (which depend on the geometry of the fracture and its intersections).

Because of the linearity of the flow equation, the finite-element solution for steady-state flow on a fracture in the case in which the residual pressure has values P_I^R at the global nodes is given by a linear combination of the global basis functions:

$$\hat{p}^R = \sum_I P_I^R \psi_I \tag{Equation 6-8}$$

It is easy to see that this ensures that the residual pressure is continuous between intersecting fractures (condition (i) above), because on each fracture the residual pressure on the intersection is given by the same interpolation between the global nodes on the intersection.

In accord with the basic Galerkin approach, condition (ii) above is imposed in a weak way:

$$\sum_{\text{intersecting fractures}} \int \psi_I(\alpha) Q_{fracture}(\alpha) d\alpha = 0 \quad \text{Equation 6-9}$$

where

- α is a coordinate along the intersection;
- $Q_{fracture}(\alpha)$ is the flux to the intersection on the fracture.

A key issue is how the flux to a fracture intersection is calculated. In fact, in order to impose the constraint of Equation 6-9) it is not necessary to calculate the flux itself, but only the integrals that appear in Equation 6-9. These are calculated from the following quantities

$$Q_i = - \int_F \nabla \varphi_i \cdot \frac{e^3}{12\mu} \nabla \hat{P}^R \quad \text{Equation 6-10}$$

As can be seen from Equation 6-4, if, rather than specifying a Dirichlet boundary condition on an intersection, the flux to the intersection were specified to be Q , then the finite element equation for a local node i on the intersection would be

$$- \int_F \nabla \varphi_i \cdot \frac{e^3}{12\mu} \nabla \hat{P}^R = \int_{\text{Intersection}} \varphi_i Q \quad \text{Equation 6-11}$$

The left hand-side of this equation is just Q_i so that it can be seen that it is natural to call this the flux to node i on the intersection.

Now, from Equation 6-6,

$$\psi_I = \varphi_i \text{ on the intersection containing } i \quad \text{Equation 6-12}$$

where i is the local node corresponding to global node I .

(This is because all the other local basis functions appearing in Equation 6-5 are zero on the intersections.) Thus, the integral that appears on the right-hand side of Equation 6-9 can also be written as

$$\int_{\text{Intersection}} \psi_I Q \quad \text{Equation 6-13}$$

Therefore, the quantities Q_i give the natural way to evaluate the integrals appearing in Equation 6-9. Further, it should be noted that Q_i can be expressed as

$$Q_i = - \int_F \nabla \psi_I \cdot \frac{e^3}{12\mu} \nabla \hat{P}^R \quad \text{Equation 6-14}$$

Because

$$- \int_F \nabla \psi_I \cdot \frac{e^3}{12\mu} \nabla \hat{P}^R = - \int_F \nabla \left(\varphi_i + \sum_n b_{In} \varphi_n \right) \cdot \frac{e^3}{12\mu} \nabla \hat{P}^R = - \int_F \nabla \varphi_i \cdot \frac{e^3}{12\mu} \nabla \hat{P}^R \quad \text{Equation 6-15}$$

using Equation 6-5.

The flux on a fracture to a node on an intersection calculated as described above is a linear combination of the residual pressures at the global nodes on the fracture. The equations for the conservation of groundwater at a fracture intersection therefore give linear relations between the residual pressures at the global nodes on the intersecting fractures. These equations, together with any boundary conditions on the fracture-network model provide the overall set of discretised equations for the residual pressures at the global nodes. In ConnectFlow, these equations can be solved using either a direct solver or a preconditioned conjugate gradient method.

It is worth noting that the approach described above leads to the equations that would be obtained were the finite-element approach to be applied directly to all the fractures together, with the basis functions for a node on an intersection being taken to be defined on both intersecting fractures in the obvious way. That is, on each fracture, the basis function would have the form of the basis function for the appropriate local node. This result is almost trivial because the equation for the conservation of groundwater for a global node on the intersection would then just be the sum of the contributions to the finite-element equation for the basis functions for the corresponding local node on each fracture, which is exactly what is obtained for the corresponding overall basis function defined as above. This is exactly the same as Equation 6-9. Thus the approach is a very natural one.

In the discussion above, the approach used in ConnectFlow has been presented for the simplest case in which global nodes are identical to local nodes on fracture intersections. However, ConnectFlow allows considerable flexibility about the number and position of global nodes on intersections. (This means that highly refined models can be used for accuracy or coarser models can be used in order to keep computational costs down, as appropriate.) The flexibility about the global nodes complicates the analysis slightly.

First, there may be fewer global nodes along an intersection than local nodes. This can readily be handled by a minor extension of the approach previously described. It is simply necessary to take the global basis functions to be the appropriate linear combinations of the global basis functions described above. In fact

$$\Psi_I(\alpha) = \sum_j \Psi_I(\alpha_j) \psi_j(\alpha) \quad \text{Equation 6-16}$$

This is illustrated in Figure 6-3.

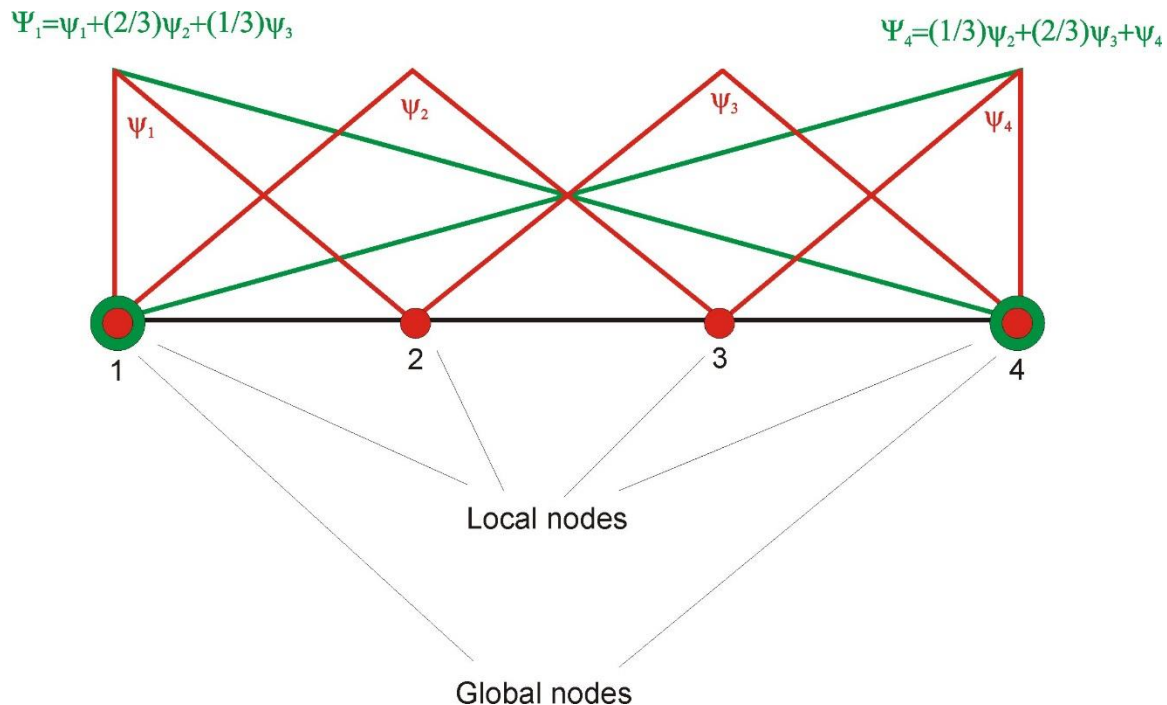


Figure 6-3: The relation of local and global basis functions on an intersection in a case in which there are fewer global nodes than local nodes on the intersection

Second, it is possible that two (or more) fracture intersections may themselves intersect. (Although the probability of more than two intersections intersecting is vanishingly small for the physical

fractures, it is quite possible that this may occur in the DFN model with fractures approximated to lie along element boundaries.) Provided that there are global nodes at the ‘multiple intersection points’ where two (or more) fracture intersections, then the discussion above applies unchanged. However, if global nodes are not present at multiple intersection points, then the residual pressure and the groundwater flux are effectively double counted at the multiple intersections, because there are separate contributions to the residual pressure (or flux) from each intersection. In order to avoid this double counting, the global basis functions are modified by reducing the contributions from the local node associated with a multiple intersection point. The contribution to each affected global basis function is divided by the number of fracture intersections crossing the local node, that is

$$\Psi_I(\alpha) = \sum_j \frac{1}{N_j} \Psi_I(\alpha_j) \psi_j(\alpha) \quad \text{Equation 6-17}$$

where N_j is 1 if there is a global node at local node j , and the number of fracture intersections intersecting at node j otherwise. This is illustrated in Figure 6-4. The approach introduces an approximation, which was tested during the development of the DFN module and found to be acceptable.

The fluxes to the global nodes are calculated from

$$Q_I = - \int_F \nabla \Psi_I \cdot \frac{e^3}{12\mu} \nabla \hat{p}^R = - \sum_J \int_F \nabla \Psi_I \cdot \frac{e^3}{12\mu} \nabla \Psi_J \hat{p}_J^R \quad \text{Equation 6-18}$$

which is a straightforward extension of Equation 6-14. These fluxes are used, for example, in the approximate particle tracking calculations.

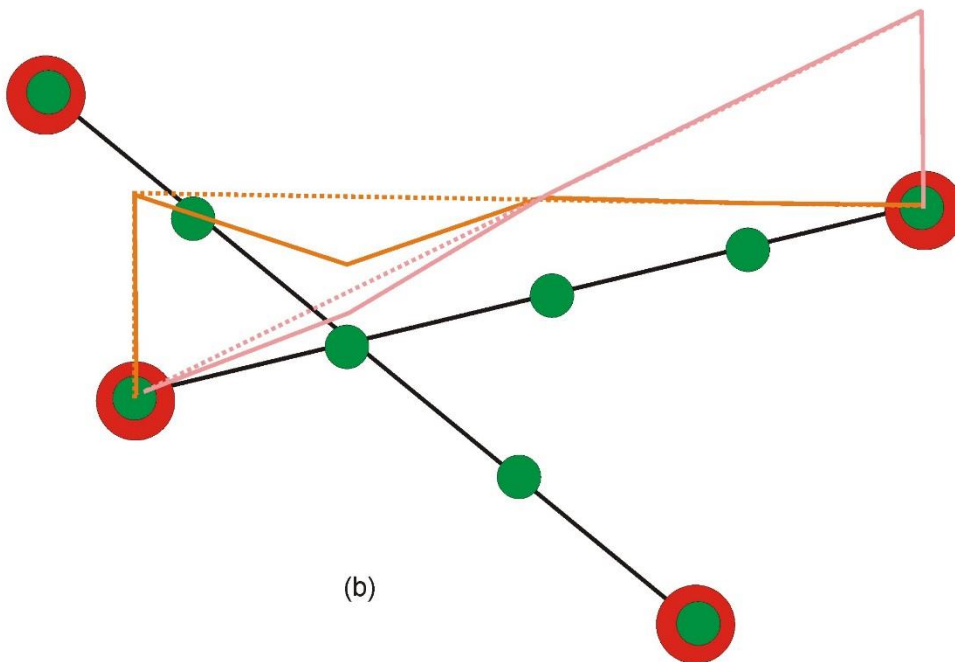
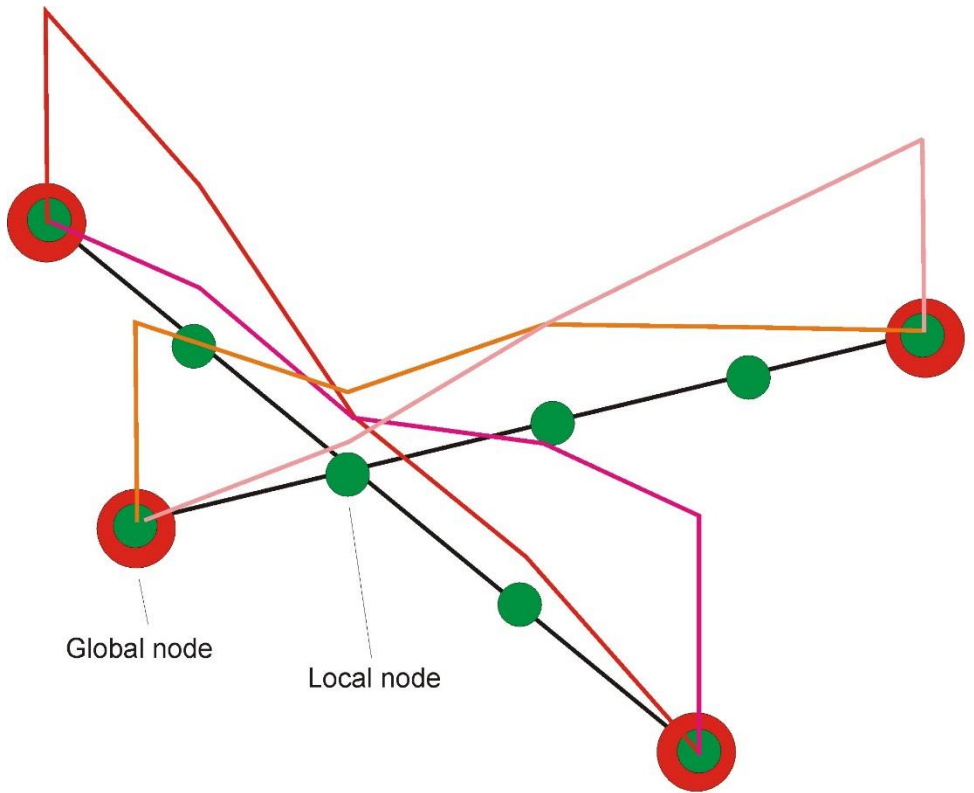


Figure 6-4: The global basis functions for a case in which fracture intersections intersect. (a) the basis functions for the global nodes (b) the construction of the basis functions on fracture intersections from the basis functions for local nodes

The calculation of steady-state groundwater flow is illustrated in Figure 6-5 and Figure 6-6. Figure 6-5 shows an example of the pressure distribution on the network scale for a network of 12,601 random fractures. Figure 6-6 gives an example of the pressure distribution on the finite-element scale for a network of 8 known fractures.

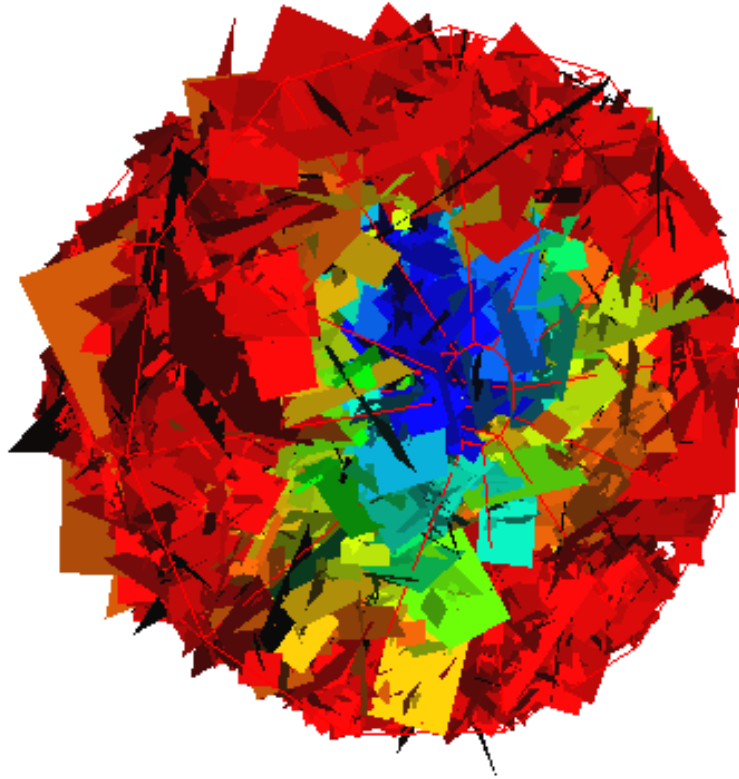


Figure 6-5: The pressure distribution on the network scale. Each fracture is coloured according to the mean pressure on the plane. Red indicates high pressure, blue low pressure. The flow domain is an annular region built from 12 hexahedra. Flow is from the external surface to the internal surface to model inflow to a tunnel.

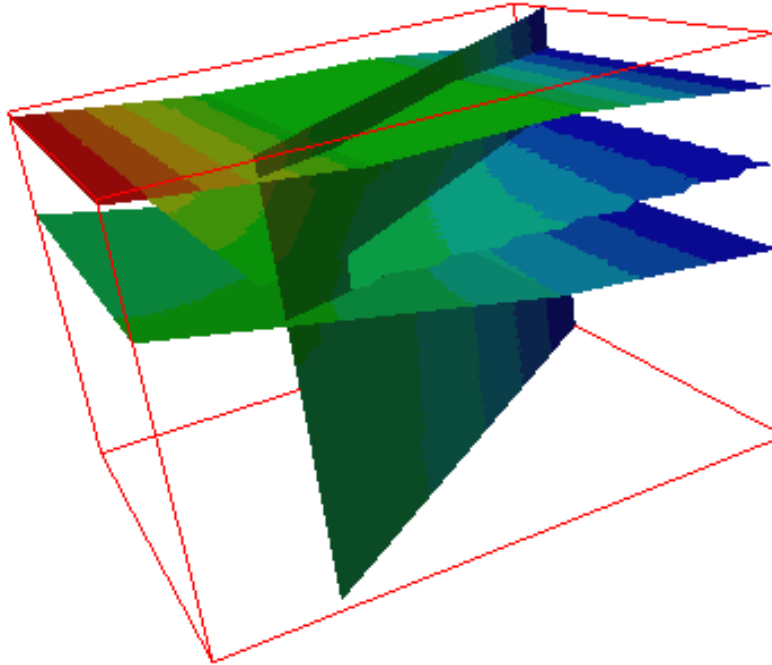


Figure 6-6: The pressure distribution on the scale of the finite-elements for a network of 8 fractures. Red indicates high pressure, blue low pressure.

6.4 Full Permeability Tensor (Upscaling)

The approach adopted to the calculation of the full permeability tensor, that is, all six independent components, k_{xx} , k_{yy} , k_{zz} , k_{xy} , k_{yz} , k_{zx} for a specified volume, is as follows. Consider a rectangular block of a continuum porous medium with an anisotropic permeability tensor with components k_{ij} . For a given head gradient with components G_i , the specific discharge would be

$$q_i = - \sum_j k_{ij} G_j \quad \text{Equation 6-19}$$

The fluxes through the faces of the block are given by

$$Q_\alpha = A_\alpha \sum_i n_{\alpha i} q_i = A_\alpha \sum_j n_{\alpha i} k_{ij} G_j \quad \text{Equation 6-20}$$

where $n_{\alpha i}$ are the components of the normal to face α with area A_α . These fluxes vary in a simple way with the imposed head gradient.

Now consider a similar block composed of fractures. Using ConnectFlow, the fluxes through the faces of the block can be calculated for a specified head gradient imposed as a boundary condition on the block. These fluxes will vary with the imposed head gradient. The variation is unlikely to be as simple as the variation of the fluxes through the faces of a block composed of an anisotropic continuum porous medium. However, one can look for the best fit to the variation of the fluxes through the block composed of fractures in terms of the variation of the fluxes through an anisotropic continuum porous medium. The corresponding permeability tensor provides, in an average sense, the effective permeability tensor for the block composed of fractures.

In practice, rather than fitting to the variation of the fluxes through the faces of the block as continuous functions of the imposed head gradient, the fit is made to the fluxes for a modest number of directions of the imposed head gradient. In the current implementation in ConnectFlow, the head gradients may be specified by the user, or their directions may be chosen automatically in the following manner, which is designed to avoid directional bias, as far as possible. A number of

randomly oriented regular icosahedra centred on the origin are chosen. Then the directions of the head gradients are taken to be along the lines from the centre to the mid-points of the sides of each icosahedron. (There are 15 such lines for each icosahedron.) This gives a uniform coverage of direction.

Thus the components of the effective permeability tensor are obtained by minimising

$$f = \sum_{\beta, \alpha} \left(q_{\beta\alpha} + A_{\alpha} \sum_{i,j} n_{\alpha i} k_{ij} G_{\beta j} \right)^2 \quad \text{Equation 6-21}$$

where $Q_{\beta\alpha}$ is the flux through face α for imposed gradient $G_{\beta\alpha}$. (Here β indexes the imposed head gradients.)

This leads to the “normal equations” (see for example [Press et al., 1986])

$$\frac{\partial f}{\partial k_{ii}} = 0 = 2 \sum_{\beta, \alpha} \left(Q_{\beta\alpha} + A_{\alpha} \sum_{k,l} n_{\alpha k} k_{kl} G_{\beta l} \right) A_{\alpha} n_{\alpha i} G_{\beta i}; \quad i = 1, 2, 3 \quad \text{Equation 6-22}$$

$$\frac{\partial f}{\partial k_{ii}} = 0 = 2 \sum_{\beta, \alpha} \left(Q_{\beta\alpha} + A_{\alpha} \sum_{k,l} n_{\alpha k} k_{kl} G_{\beta l} \right) (A_{\alpha} n_{\alpha i} G_{\beta j} + A_{\alpha} n_{\alpha j} G_{\beta i}); \quad i < j \text{ and } i = 1, 2, 3 \quad \text{Equation 6-23}$$

(It should be noted that only six components of the permeability tensor are independent, namely k_{xx} , k_{yy} , k_{zz} , $k_{xy} = k_{yx}$, $k_{yz} = k_{zy}$, $k_{zx} = k_{xz}$)

Equation 6-22 and Equation 6-23, which are a system of linear equations, are solved by Gaussian elimination. The quantities $A_{\alpha} n_{\alpha i} G_{\beta i}$ and $(A_{\alpha} n_{\alpha i} G_{\beta j} + A_{\alpha} n_{\alpha j} G_{\beta i})$ are called the basis functions. The inverse of the matrix for the system is called the covariance matrix and is closely related to the uncertainties in the parameter estimates obtained by the least-squares fitting.

6.5 Efficient Implementation

It is important to make the effective permeability calculations as efficient as possible.

In fact, the calculation of the full permeability tensor is implemented in such a way that its computational cost is little more than that of computing the flow through the block for a single set of boundary conditions.

The reason for this is as follows. The discretised flow equations for the network can be written in matrix notation as

$$\mathbf{Ax} = \mathbf{b} \quad \text{Equation 6-24}$$

where

- \mathbf{x} is the vector of unknowns, that is the residual pressures (or effectively heads) at the internal nodes of the model;
- \mathbf{b} is the right-hand side vector of specified residual pressures (heads) on the boundary.

ConnectFlow uses a direct Gaussian algorithm to solve these equations. The method is equivalent to making a decomposition of \mathbf{A} into the product \mathbf{LU} of a lower triangular matrix \mathbf{L} and an upper triangular matrix \mathbf{U} followed by successively solving

$$\mathbf{Ly} = \mathbf{b} \quad \text{Equation 6-25}$$

$$\mathbf{Ux} = \mathbf{y} \quad \text{Equation 6-26}$$

The computationally expensive step in this procedure is the determination of the LU-decomposition. Relatively speaking, Equation 6-25 and Equation 6-26 are very cheap to solve. Once the LU-decomposition has been made, it is therefore possible to solve the matrix equations for a number of different right hand sides very cheaply. This is exactly what is required to calculate the flows for the different imposed head gradients. The various gradients are defined by specifying the corresponding distribution of head around the boundary of the block. In this way, a very efficient method for calculating the full effective permeability tensor is obtained.

6.6 Calculation of Effective Permeabilities for Many Blocks

One application of this facility is the calculation of effective permeabilities in a study of upscaling. Such studies require the calculation of the distribution and correlation structure of the effective permeabilities. An option is therefore available to generate a realization of a fracture-network in a specified region, and then automatically calculate effective permeability tensors for each block in a subdivision of the region. It is then possible to analyse the statistics of the data obtained using this option in order to estimate the correlation structure of the effective permeability.

6.7 Effective Permeability of an Internal Block

The facility to calculate the permeability for many blocks provides a very powerful tool. However, the issue of boundary short-circuits needs to be considered. As discussed above, the algorithm is based on calculating the flows through the block of interest for a number of different imposed head gradients, which are specified in terms of imposed heads on the boundaries of the block. However, it is possible that there are one, or more, highly transmissive fractures within the block directly connecting an inlet face with an adjacent outlet face (see Figure 6-7)

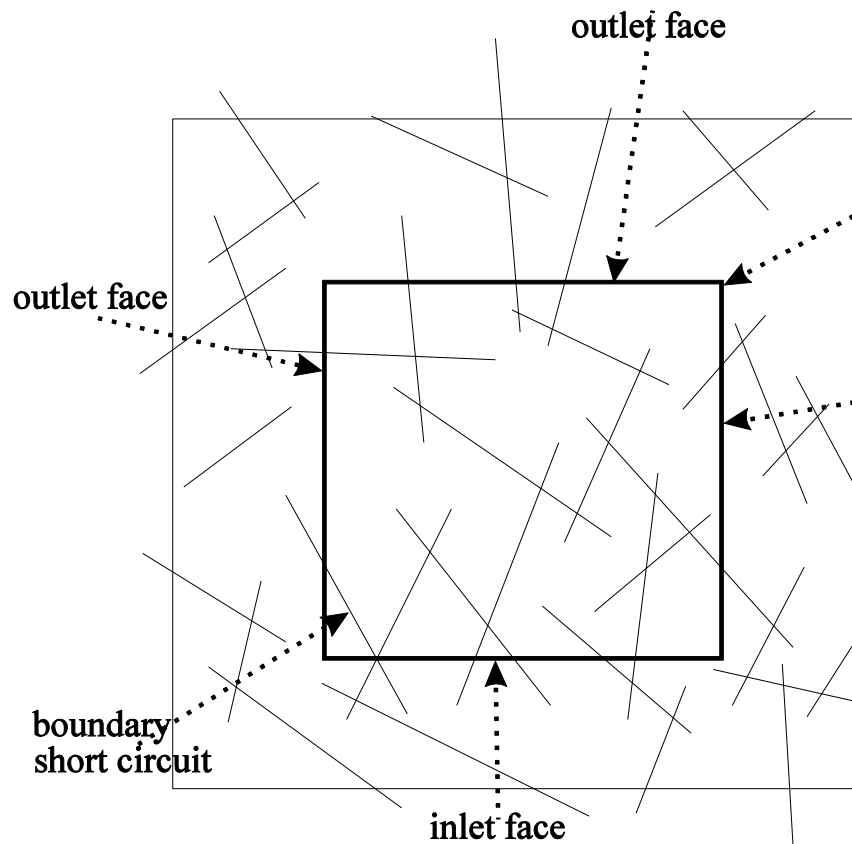


Figure 6-7: Schematic of short circuits in a two-dimensional case.

Because of the imposed head boundary conditions there are large flows through such fractures. This leads to an estimate of the effective permeability that is biased towards high values. The problem arises because of the interaction of such short circuits with the imposed boundary conditions. Consider the behaviour of the block in question in the context of the surrounding network. It is unlikely that the imposed head would be present across such a short circuit.

Rather, because of its high transmissivity, the head drop across the short circuit would be small, with most of the head drop being taken up by other fractures. One limiting case, which is shown in Figure 6-7 is that of a short circuit that is not connected beyond the block in question. In the case shown in Figure 6-7, when the surrounding network is taken into account the head in the short circuit would actually be constant, and there would be no flow in the short circuit, whereas if the block was considered in isolation, the short circuit might well completely dominate the flows through the block and hence the calculated effective permeability. In order to address this problem, it is necessary to modify the procedure for calculation of the effective permeability tensor. This modification introduces a “guard zone” around the block of interest. This allows the effective permeability of the block to be calculated in the context of the surrounding network, so the effect of short circuits is restricted to the guard zone. In practice, it is necessary to choose a guard zone of a sensible size, which depends on the distributions of the fracture properties.

6.8 Transient Flow Modelling

As the field experiments from which the data to generate fracture-networks are derived usually involve transient flows, a transient flow modelling capability has been developed in ConnectFlow. An approach consistent with the steady-state approach is adopted. This ensures that the code is applicable to the complex networks that the steady-state code is able to handle. The equation describing constant-density transient flow through a fracture-network is

$$\frac{S}{\rho g} \frac{\partial P^R}{\partial t} = \frac{e^3}{12\mu} \nabla^2 P^R \quad \text{Equation 6-27}$$

where S is the fracture storativity which is dependent both on fluid and rock compressibility. The choice of a suitable model for fracture storativity is important for an accurate transient flow model. Three models for fracture storativity are available in the DFN module:

$$S = \rho g A e \quad \text{Equation 6-28}$$

$$S = \rho g \left[\frac{1}{RKN} + e C_f \right] \quad \text{Equation 6-29}$$

$$S = \alpha T^\beta \quad \text{Equation 6-30}$$

Here A , RKN , C_f , α and β are constants that can be specified by the user.

The fracture-network is discretised in the way described in section 3.2 and a backward difference is used to approximate the time derivative. The finite-element equation to be solved for the pressure values at the global flow nodes becomes

$$\sum_j \left(\frac{S}{\rho g \Delta t} \int_{\Omega} \psi_I \psi_J P_j^{R,n+1} + \frac{e^3}{12\mu} \int_{\Omega} \nabla \psi_I \nabla \psi_J P_j^{R,n+1} \right) = \sum_j \frac{S}{\rho g \Delta t} \int_{\Omega} \psi_I \psi_J P_j^{R,n} \quad \text{Equation 6-31}$$

This equation is solved for a fixed timestep Δt to give $P^{R,n}$ the residual pressure solution at time $t = n\Delta t$. The second term on the left-hand side of this equation is simply the flux term,

$$\sum_j F_{IJ} P_j^{n+1} \quad \text{Equation 6-32}$$

that appears in Equation 6-18, and the first term on the left-hand side of this equation will be referred to as the storativity term

$$\sum_j S_{IJ} P_j^{R,n+1} \quad \text{Equation 6-33}$$

The second step of a transient groundwater flow calculation is analogous to that in the steady-state calculation. The contributions from the individual planes to the global matrix are calculated. As before, the contributions to the flux term from each plane are evaluated by solving the mass conservation equation on each plane subject to a number of different boundary conditions. In addition, the contributions to the storage term are evaluated for each fracture plane.

These contributions are then assembled into the global matrix, ready to start timestepping. In order to simplify generating the right-hand sides of Equation 6-31 for each timestep, two global matrices are assembled, one containing the flux term, F_{IJ} , and the other containing the storativity term, S_{IJ} . It is assumed that the boundary conditions are fixed with respect to time, and therefore can be imposed by deleting terms from the storativity matrix and changing the flux matrix in the same way as for the steady-state model. A boundary condition vector is constructed at this point. The two global matrices are added together, component by component, to form one global matrix. The resulting global matrix and the boundary condition vector are unchanged for all timesteps of the same size, since they depend on time only through the timestep size Δt .

The third stage of the transient groundwater flow calculation is to solve the matrix equations for each timestep. The right-hand side of Equation 6-31, for the first timestep, is evaluated by multiplying the storativity matrix by an initial solution which is prescribed by the user. This initial solution may be a constant pressure, a linearly varying pressure or an existing solution previously found by ConnectFlow. The contribution from the boundary conditions is added to this right-hand side and the matrix Equation 6-31 is solved using the same direct frontal solver as for a steady-state calculation to produce the pressure solution at the first timestep. This solution is used to evaluate the next right-hand side and the timestepping loop is repeated producing a sequence of solutions P^{n+1} which define the flow field at the $(n+1)$ -th timestep.

As with steady-state problems, this method allows quite coarse meshes to be used on very large systems. However more detailed refinement might be required for smaller networks, or near sources and sinks. To deal with this, the transient model permits optional local refinement for significant fractures. This option involves solving the transient mass conservation equation on the fracture and then adding this contribution to the refined matrix. At each timestep, the local pressure solution is saved on the finite-element mesh of the refined plane and this solution is used to calculate the next solution to the transient mass conservation equation on the refined plane.

6.9 Engineered Features

Close to a point where an engineered feature intersects a fracture, the pressure field behaves like that within a parallel plane having a single sink:

$$P^R = P_w \frac{12\mu Q}{2\pi e^3} \ln\left(\frac{r}{r_w}\right) \quad \text{Equation 6-34}$$

where P_w is the wall pressure, r is the distance from the engineered feature, r_w is the engineered feature radius and Q is the volumetric flow rate from the engineered feature into the fracture.

This logarithmic behaviour is poorly approximated by a regular linear finite-element discretisation, and so a correction is applied to the residual pressure calculated by the finite-element method at the engineered feature, P_{PE} , using the analytical solution in Equation 6-34, to obtain the wall pressure, P_w

$$P_w = P_{PE} + \frac{Q}{\Gamma} \quad \text{Equation 6-35}$$

where Γ is a productivity index, which is dependent on the size of the finite element mesh, the feature radius and the transmissivity of the fracture. Although this model is based on a steady-state analytical solution, tests have shown that the correction factor to be reasonable when modelling transient flow.

6.10 Two-Dimensional Networks

For formations with very high aspect ratios, a simplification to a two-dimensional network may be justified. Alternatively when approaches to complex physics are being developed it may be necessary to simplify the geometry by approximating a three-dimensional network by a two-dimensional one. A two-dimensional version of the DFN module was developed that uses much of the existing three-dimensional code. The flow model and the approach used to solve the equations are analogous to the three-dimensional version. The network can be considered as a slice through a three-dimensional network in the x - z coordinate plane, with constant flow in the y -direction, and mass conservation governing flow through the fracture. The fractures are represented as straight-line segments, and are defined by an orientation angle, a length and an effective aperture. As in three-dimensional simulations, the parameters describing each fracture may be sampled from statistical distributions. A more physical way of generating a two-dimensional network, and the one usually adopted, is to generate a three-dimensional fracture-network and to map traces onto a plane.

The flow solution in the two-dimensions is less complicated than in three-dimensions. The flow field is discretised by assigning one global flow node to each intersection between fractures. Linear basis functions, which are zero outside the fractures, are defined at each node J by

$$\Psi_J = 1 \text{ at node } J \quad \text{Equation 6-36}$$

$$\Psi_J = 0 \text{ at node } I \neq J \quad \text{Equation 6-37}$$

and are defined by linear interpolation along fractures between nodes. The contributions to the matrix equations for each plane are calculated directly without needing to calculate the response functions on each plane. Boundary conditions are imposed and the resulting matrix equation is solved using the direct frontal solver.

6.11 Modelling the Effect of Stress on a Fracture Network

The DFN module is designed to deal with complex fracture-networks, and as a consequence it is only practical to incorporate relatively simple models for the effect of stress on flow (hydro-mechanical coupling). The effect on the flow of a change in stress caused by disturbing the surrounding fracture-network, for example by drilling a repository tunnel, can be calculated. The network is assumed initially to be in hydro-mechanical equilibrium, with the apertures of the fractures being those that apply to the in-situ network under the specified equilibrium stress field. ConnectFlow does not calculate the stress field directly. An analytical solution may be used to determine the changed stress field, or the results of field experiments can be used to obtain an empirical specification of the changed stress field. Thus the normal stress acting at any point on a fracture may be calculated.

Having calculated the change in normal stress, a stress-aperture coupling is used to change the fracture aperture. In three-dimensions, the change in aperture for each finite-element is computed from the value of the normal stress at the centre of the finite-element.

In two-dimensions, the change in normal stress acting on the fracture is calculated at the centre point of each section of fracture between intersections.

There are several stress-aperture couplings available. Three that have been used in DFN modelling [Wilcock, 1996] are

$$T = \text{constant} \quad \text{Equation 6-38}$$

$$\frac{T}{T_0} = \left(\frac{\sigma_n}{\sigma_{n0}} \right)^{-\alpha} \quad \text{Equation 6-39}$$

$$e = \max\left(e_0 - \left(\frac{\sigma_n - \sigma_{n0}}{RKN} \right), e_{min} \right) \quad \text{Equation 6-40}$$

In the first coupling, the transmissivity, T , of each fracture is assumed to be unchanged by the excavation of the tunnel. The DFN module directly converts transmissivities into apertures using the parallel-plate law, as defined by Equation 6-3, and so the apertures remain constant. The second coupling is a compliance law relating the change in fracture transmissivity, T , to changes in normal stress, σ_n through a power law with exponent α . The value of α is obtained from laboratory tests carried out on the rock. For fractured rock α typically has values between ~ 0.1 and ~ 1.0 . The third law relates the change in aperture, $e - e_0$ directly to the change in stress and the fracture normal stiffness, RKN . It is necessary to define a minimum aperture, e_{min} to ensure that all apertures remain positive, and to reflect the physical reality that fractures can only be compressed so far. Again, the results of laboratory tests are used to determine the value of RKN .

6.12 Tracer Transport

The tracer transport option in the DFN module is designed to calculate the migration and dispersal of tracer through a discrete fracture-network. Within the groundwater, it is assumed that tracer transport is dominated by advection, so that molecular diffusion can be ignored, and the major cause of dispersion is due to the existence of a number of different paths through the fracture network. It is also assumed that the fracture apertures are small enough that the tracer diffuses quickly across the aperture.

The transport calculations are based upon a particle-tracking algorithm. The problem is split up into the calculation of single fracture responses followed by the calculation of the transport of a particle swarm through the network. For each fracture plane, a representative number of pathlines between

the intersections on the plane are calculated. Intersections are discretised by transport nodes and pathlines are calculated from each transport node. There are two algorithms available for calculating these pathlines, ‘exact particle tracking’ (with standard and mass-conserving methods) and ‘approximate particle tracking’. Each algorithm is described in the following sections.

6.12.1 Exact Particle Tracking (Standard Method)

For each fracture, the flow field is discretised in terms of linear triangular finite-elements. The flow is determined by the pressure field, and since the pressure varies linearly over each triangle, the groundwater velocity,

$$\mathbf{v} = \frac{\mathbf{q}}{e} = -\frac{e^2}{12\mu} (\nabla P^R - (\rho - \rho_0)\mathbf{g}) \quad \text{Equation 6-41}$$

is constant on each element. The pathlines are calculated on each fracture by stepping the path across the mesh, one element at a time. On reaching a fracture intersection, the path is complete. Once the pathlines from the transport nodes on each fracture plane have been calculated, the possible connections for that node are determined. A list of possible destinations, travel-times, distances and relative probabilities for a particle leaving each node are calculated. In this way, a library of paths is created for every transport node in the network. The model relies on the calculation of a very accurate flow solution. If a low accuracy solution is used, then problems with local flow sinks on fractures may occur, resulting in the loss of a significant fraction of the particle swarm.

6.12.2 Exact Particle Tracking (Mass-Conserving Method)

The standard method of exact particle tracking using the finite-elements does not guarantee conservation of mass in the flows between elements. Effectively there are sinks or sources at finite-element boundaries and nodes. This can cause problems for particle tracking calculations because particles can become ‘trapped’ or ‘lost’ at the sinks. However, the mass-conserving method (introduced with ConnectFlow version 9.3 as the default) does conserve mass between elements. It does this by using a method proposed by Cordes and Kinzelbach [Cordes et al., 1992]. This method takes each DFN fracture triangular finite-element and sub-divides it into four sub-triangles. The velocity within each sub-triangle is then calculated in such a way as to conserve mass between elements and sub-triangles. The set of sub-triangles around each finite-element node is termed a patch. The velocity calculations are carried out patch by patch, with the calculations for each patch independent of those of the others. The velocities for the middle sub-triangles that are not part of any patch can be calculated from the finite-element pressures. This keeps the scale of the calculations small and velocities only need to be calculated for those patches or middle sub-triangles that particles enter.

Figure 6-8 shows the sub-triangle patch for a non-boundary, non-intersection node. The black lines are the element edges and the red lines are the sub-triangle edges. The purple arrows are the fluxes across the sub-triangle edges and the green arrows are the velocities for the sub-triangles.

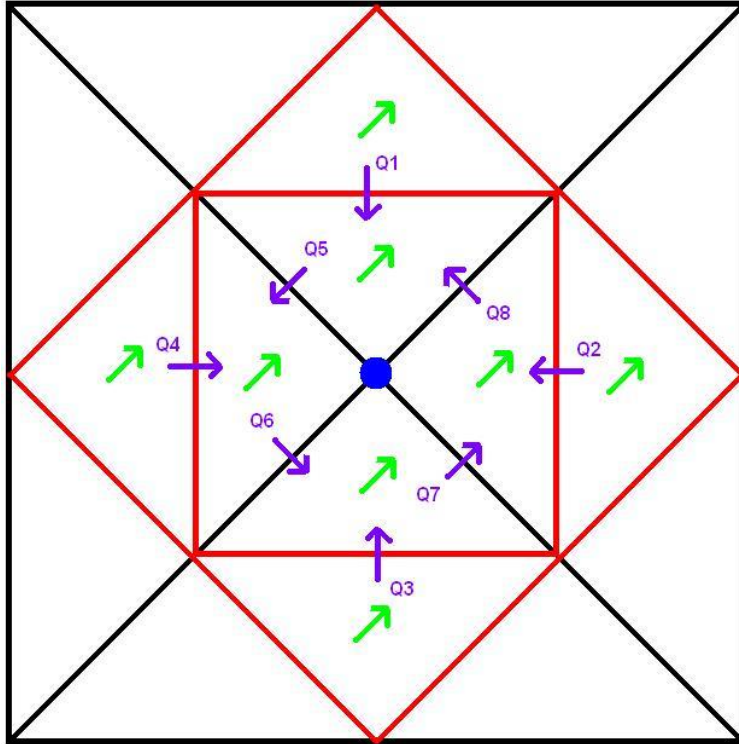


Figure 6-8: A sub-triangle patch for a non-boundary, non-intersection node.

The fluxes entering or leaving the patch ($Q1$ to $Q4$) can be calculated directly from the finite-element pressures. The fluxes through the edges connected to the node can be calculated by applying the following constraints:

1. There is no net flux into or out of a sub-triangle, e.g. $Q5 = Q1 + Q8$;
2. The fluxes entering or leaving the patch sum to zero, i.e. $Q1 + Q2 + Q3 + Q4 = 0$;
3. The integral of the head gradient around the node is zero (the irrotationality constraint).

The velocity in each sub-triangle can be calculated directly from the fluxes entering or leaving it. Note that for the middle sub-triangles (those not connected to an element node), the fluxes, and hence velocities, can be calculated directly from the finite-element pressures.

Figure 6-9 shows a boundary node on the edge of a DFN fracture. There is no flow across the boundary and so fluxes $Q5$ and $Q9$ will be zero. Fluxes $Q1$ to $Q4$ can be calculated from the finite-element pressures. Since flux is preserved between sub-triangles, this enables fluxes $Q6$ to $Q8$ to be calculated and hence the sub-triangle velocities.

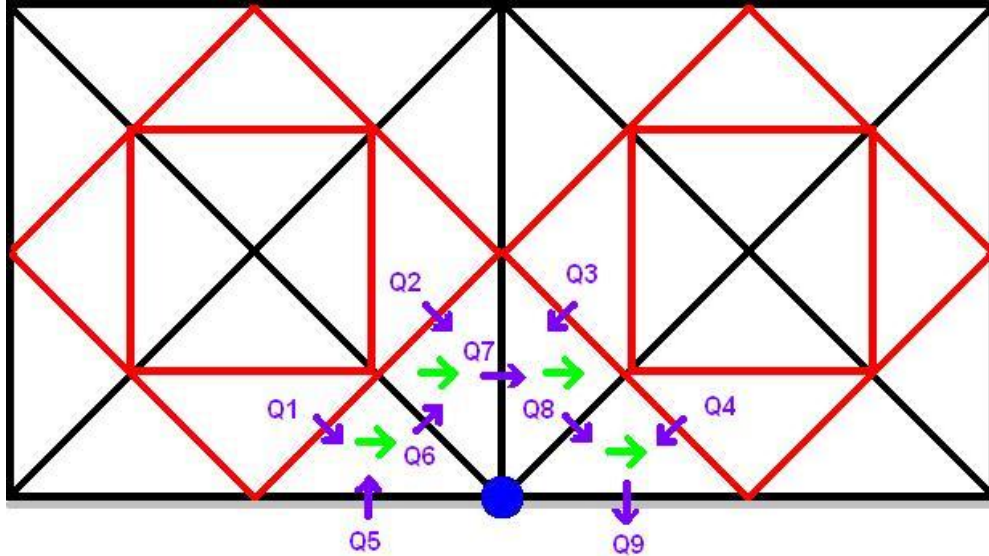


Figure 6-9: A sub-triangle patch for a boundary node. Figure 6-10 shows a node on a fracture intersection, with the intersection edges highlighted in blue.

Because flow can be entering or leaving the fracture through the intersection then constraints b and c above are no longer true. In this case, the patch is split into segments, with each segment being the sub-triangles between a pair of intersection edges. Then each segment is treated separately, since the fluxes on each side of the intersection are not necessarily equal, e.g. $Q7$ may not equal $Q8$. For each segment, the sum of the fluxes entering or leaving the patch through sub-triangle edges, e.g. $Q1 + Q4$, must equal the sum of the fluxes entering or leaving the intersection, e.g. $Q5 + Q7$. The fluxes entering the patch through the sub-triangle edges can be calculated from the finite-element pressures and it is possible to assign this flux to the intersection edges. This enables the remaining fluxes, and hence the velocities, to be calculated. A similar approach is taken for very short, i.e. point, intersections and for boreholes, but in this case the flux is assigned to the node itself and the radial flow component is taken into account.

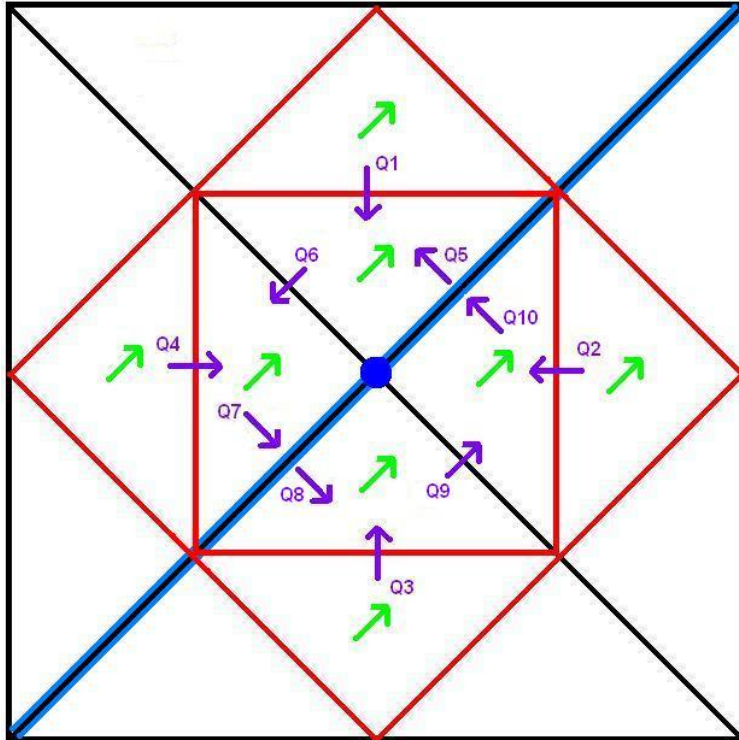


Figure 6-10: A sub-triangle patch for an intersection node.

Once the velocities have been calculated, the particle paths between the transport nodes can be calculated using a stepping method, where each step is between a sub-triangle edge. In the case of a point intersection or borehole node, a radial flow component is present in the sub-triangles around the node, which requires a time-stepping approach within those sub-triangles. Information on the paths is stored in the same way as for the standard method.

6.12.3 Approximate Particle Tracking

The DFN module is able to create a database that records the net flux between all the intersections for a flow solution. This network of flux connections links the centre of every intersection on a given fracture with every other intersection centre on the fracture. A transport option has been developed that is based on this flux database in which particles are transported between intersections. This is a more robust method than exact particle tracking as it does not need a highly accurate flow solution, just a good flow balance at the network intersections. It is also more computationally efficient. One disadvantage is that this model cannot accurately model dispersion on a single fracture. However, where dispersion is dominated by the different paths through the network rather than dispersion on an individual fracture plane, these inaccuracies may be small and so this method is most appropriate for large networks. The accuracy of the calculation for transport across any fracture can be improved by tessellating fractures which effectively increases the discretisation. Figure 6-11 shows 30 particle tracks based on approximate particles tracks for a simple random network. The paths clearly demonstrate the heterogeneities in flow due to variations in network connectivity and fracture transmissivity.

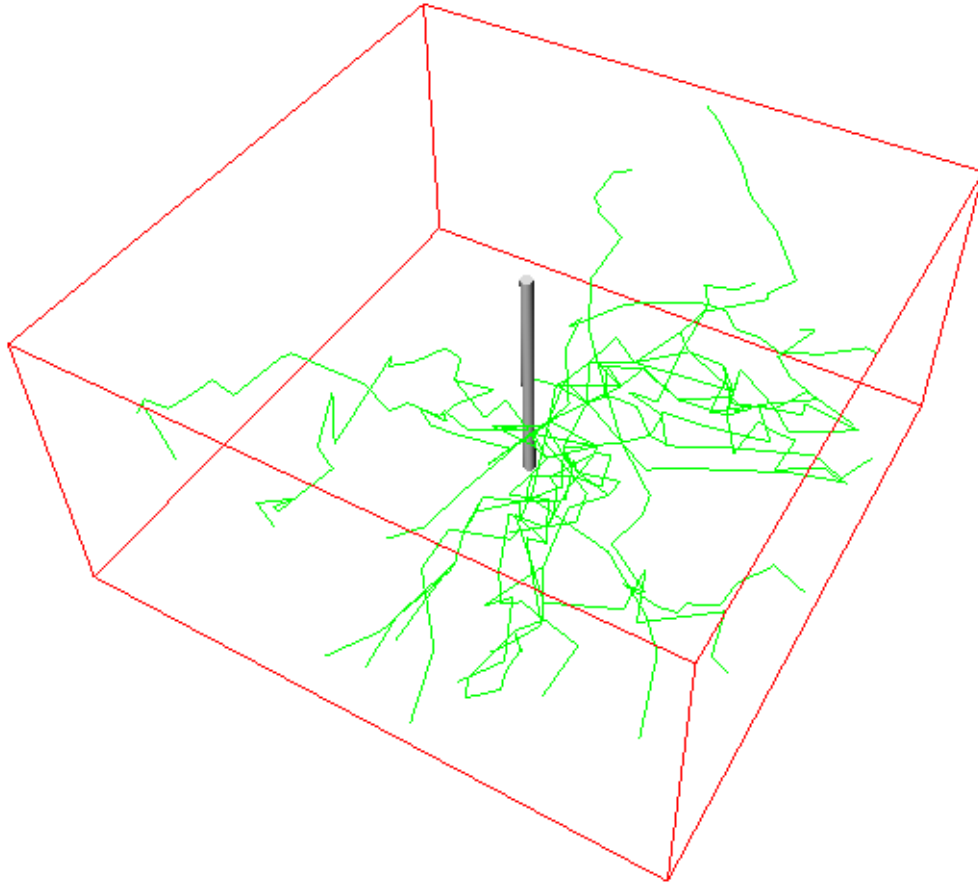
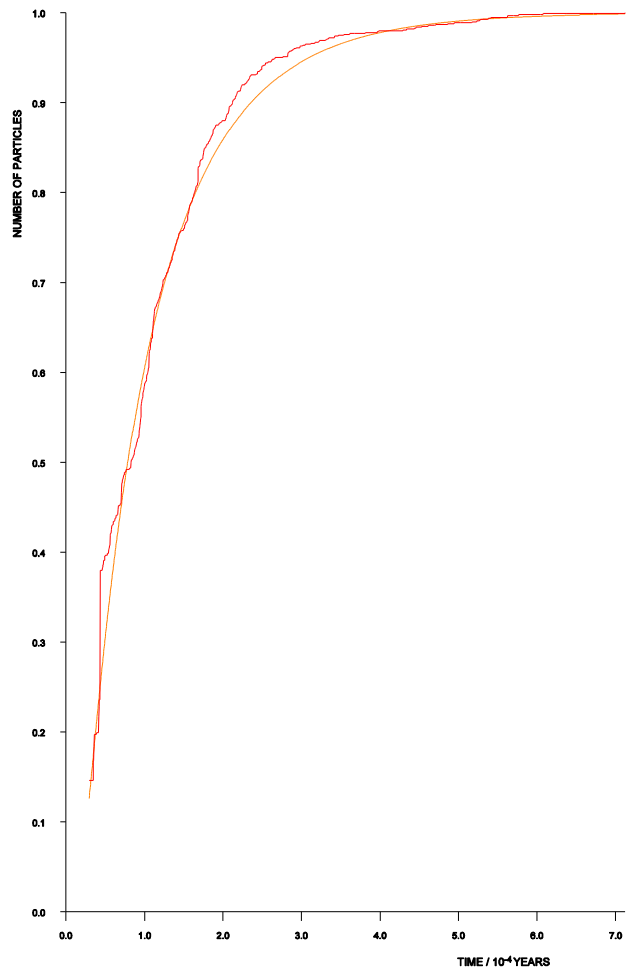


Figure 6-11: An example of a particle tracking calculation for 30 particles starting at the same injection borehole interval (located centrally and vertical) and dispersing outward toward the vertical boundaries. Flow is radially outward from the injection borehole.

The next step in the transport calculation consists of following a large swarm of particles across the network. Particles can be started on any surface of the fracture-network region where there is an inflow or from any number of engineered features. Particles are tracked through the network from node to node, building up the path taken by each of the particles using the information calculated in the first step. Figure 6-12 is an example of a breakthrough curve for particle tracking across a simple cuboid region.

SMALL TRACER TRANSPORT MODEL



CUMULATIVE ARRIVAL CURVE



Figure 6-12: An example of a breakthrough curve based on 1000 particle tracks through a small random network. The jagged line is the cumulative curve based on the particle tracks. The smooth curve is a fit to the data based on a two-parameter advection-dispersion curve.

6.13 Coupled Groundwater Flow and Salt Transport

The DFN module includes an option for modelling coupled groundwater flow and salt transport. Both steady-state and transient modelling can be undertaken.

The equations characterising transient coupled groundwater flow and salt transport in an individual fracture are:

$$\frac{\partial(e_t \rho)}{\partial t} + \nabla \cdot (\rho \vec{q}) = 0 \quad \text{Equation 6-42}$$

$$\frac{\partial(e_t \rho c)}{\partial t} + \nabla \cdot (\rho \vec{q} c) = \nabla \cdot (e_t \rho D \cdot \nabla c) \quad \text{Equation 6-43}$$

$$\vec{q} = \frac{e^3}{12\mu} (\nabla P_R - (\rho - \rho_0)\vec{g}_f) \quad \text{Equation 6-44}$$

$$\frac{1}{\rho} = \frac{1-c}{\rho_0(1+\alpha_f(P_T - P_{T0}))} + \frac{c}{\rho_s(1+\alpha_s(P_T - P_{T0}))} \quad \text{Equation 6-45}$$

The other variables referred to here are:

- e is the effective hydraulic aperture of a fracture, which may vary within the fracture and between fractures;
- e_t is the transport aperture of a fracture, i.e. the effective aperture of a fracture accessible to mobile water, which may vary within the fracture and between fractures;
- c is the fraction of the saline water and $(1 - c)$ is the fraction of fresh water.
- ρ is fluid density;
- ρ_s is the saline fluid density; ρ_0 is the reference fluid (fresh water) density;
- α_s is the compressibility of saline water; α_f is the compressibility of fresh water;
- P_T is the local total pressure;
- P_{T0} is the reference pressure;
- μ is fluid viscosity (constant);
- P_R is the local residual pressure: $P_R = P_T - P_{T0} + \rho_0 g(z - z_0)$, where g is the magnitude of gravitational acceleration, z is the elevation and z_0 is the reference elevation.
- \vec{q} is Darcy flux;
- t is time;
- D is the dispersion tensor. This includes contributions from diffusion and from hydrodynamic dispersion. The latter is usually taken to be proportional to D with different values along and perpendicular to the flow;
- ∇ is the two-dimensional gradient operator within the fracture;
- \vec{g}_f is the acceleration due to gravity in the plane of the fracture.

The equations for the overall network comprise these equations for each fracture, together with the conditions at a fracture intersection that the pressure and salinity are continuous across the intersection and the rates of flow of water and salt per unit length out of one fracture are equal to the rates of flow of water and salt per unit length into the other fracture.

Transients are handled by expressing the time derivatives as finite differences. Generally, fully implicit differences are used in ConnectFlow.

The equations are non-linear. The straightforward and most accurate way to generalise the approach described in section 6.3 to deal with this would be simply to use an iterative approach such as Newton-Raphson iterations to handle the non-linearity for both the global nodes and for the local nodes within fractures. At each iteration, updates for the residual pressure and the salinity at the global nodes would be determined. This would be done by solving the equivalents of Equation 6-9. This would take into account the non-linearity. Then updated versions of the global basis functions on each element would be determined by solving the equivalents of Equation 6-5 and Equation 6-6. This would take into account the non-linearity of the equations for each fracture. This would be repeated until satisfactory convergence was achieved.

However, this approach would be very costly computationally. The calculation of the global basis functions for each time step would cost about two orders of magnitude more than the calculation of the global basis functions for the case of steady-state constant density groundwater flow. (Twice as many basis functions would have to be calculated, twice as many cases would have to be considered in the determination of the global basis functions, the matrices in the calculation of each basis function would be twice as large, so the calculation for each basis function might cost about eight

times as much and the calculations would have to be done for say five Newton-Raphson iterations for each time step.) Further, the calculation of the global basis functions would have to be repeated for each timestep.

Therefore an approximate approach is adopted that is much less expensive computationally. The basic idea of the approach is as follows. The global basis functions derived for the case of steady-state constant-density groundwater flow effectively provide a set of basis functions that can be used directly in the Galerkin approach for the calculation of the residual pressure at the global nodes. The key point is that for steady-state constant-density groundwater flow, the discretised equations for the residual pressure at the global nodes can be expressed in terms only of the global basis functions without directly involving the local basis functions (see Equation 6-8). In the approximate approach, the salinity is also represented as a linear combination of these global basis functions.

Thus

$$\hat{p}^R = \sum_I p_I^R \psi_I \quad \text{Equation 6-46}$$

$$\hat{c}^R = \sum_I c_I^R \psi_I \quad \text{Equation 6-47}$$

The discretised equations for coupled flow and transport of salinity are then

$$\sum_F \int_F \psi_I \frac{\partial(e\rho)}{\partial t} + \sum_F \int_F \nabla \psi_I \cdot \frac{e^3}{12\mu} (\nabla \hat{p}^R - (\rho - \rho_0) \mathbf{g}_f) = 0 \quad \text{Equation 6-48}$$

$$\sum_F \int_F \psi_I \frac{\partial(e\rho\hat{c})}{\partial t} + \sum_F \int_F \nabla \psi_I \cdot (\hat{q}\rho\hat{c} + e\rho D\nabla\hat{c}) = 0 \quad \text{Equation 6-49}$$

Together with the boundary conditions on the overall boundary of the network.

The key benefit of this approach is that, as indicated, it is much less expensive computationally than the straightforward approach. The approach involves an approximation. Effectively the variation of salinity within a fracture is represented using functions with a small number of degrees of freedom (the number of global nodes), whereas in the straightforward approach the variation of salinity would be represented using functions with a much larger number of degrees of freedom (the number of local nodes). However, in many cases, the variation of salinity over individual fractures may be relatively small, and in such cases the approximate method is likely to provide a good approximation. If some fractures are sufficiently large that the salinity varies significantly over the fractures then the fractures can be tessellated, so that the variation over each tessellate is relatively small.

Figure 6-13 and Figure 6-14 show the distributions of residual pressure and salinity calculated for a steady-state case (a variant of the so-called Henry test case [Simpson et al., 2004]). The results are physically reasonable and in reasonable accord with the results for the Henry test case.

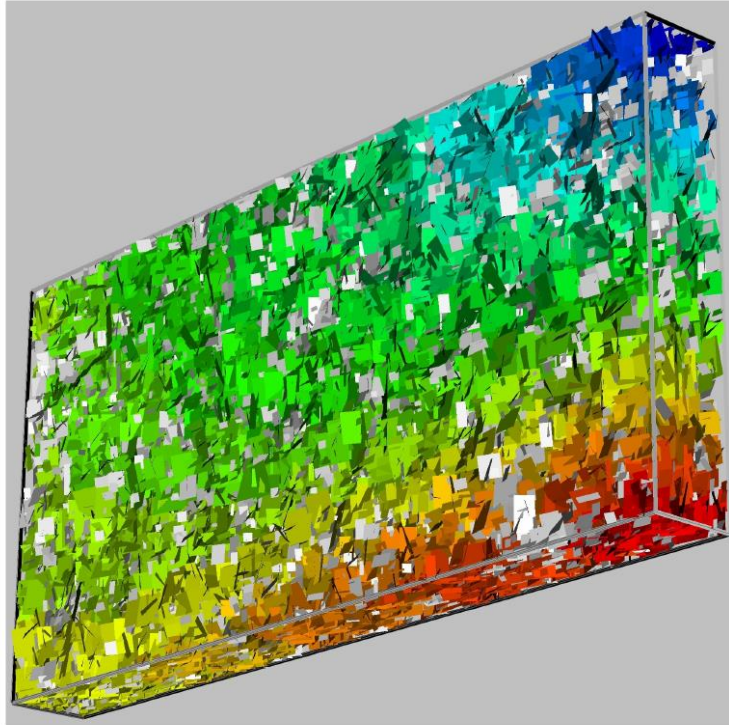


Figure 6-13: An example of the distribution of residual pressure for a calculation of coupled groundwater flow and salt transport. (Unconnected fractures are coloured grey.)

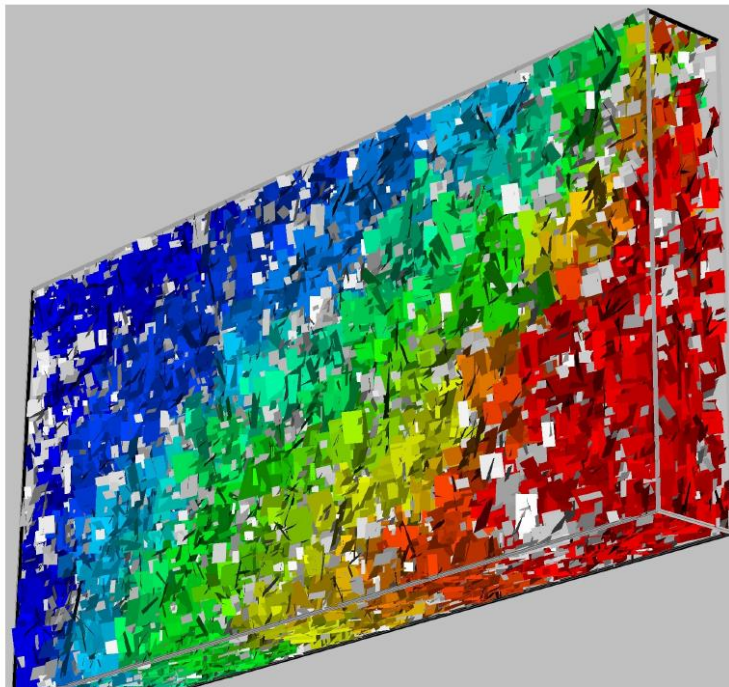


Figure 6-14: An example of the distribution of salinity for a calculation of coupled groundwater flow and salt transport. (Unconnected fractures are coloured grey.)

6.14 Multi-Component Solute Transport

6.14.1 Background

The previous sections describe the DFN functionality of ConnectFlow with regards to a single salt species (coupled with the pressure calculation via the density). This section describes the simultaneous transport of multiple solute components, fully coupled with the pressure calculation. This facility allows the chemical composition of the groundwater to be explicitly modelled as a function of time which is highly relevant to the overall performance of geological disposal concepts. It also enables the calculation of chemical reactions within both fractures and the rock matrix, which will be described in more detail in a later section.

Concentrations of salt may be described in one of three different ways within ConnectFlow:

- 1) As a mass fraction c (also known as the salinity or mass concentration) of a chemical species i which is simply given by the mass of the species M_i divided by the total mass of water M_{wat} and all the m chemical species M_j .

$$c_i = \frac{M_i}{M_{wat} + \sum_{j=1,m} M_j}$$

- 2) As a volume concentration C of a chemical species i which is simply given by the mass of the species M_i divided by the volume of the solution.

$$C_i = \frac{M_i}{V}$$

The fluid density ρ of the solution can be used to convert to a mass fraction if required.

- 3) Using a set of defined compositions of chemical species, known as reference waters. In this case a set of n reference waters is specified, each of which has a fixed composition of m different chemical species. The mass fraction of an individual chemical species i in a mixture of reference waters is given by the fraction of each reference water c_w multiplied by the mass fraction of species i within that reference water $c_{i,w}$.

$$c_i = \sum_{w=1,n} c_w c_{i,w} = \sum_{w=1,n} \left(\frac{c_w M_{i,w}}{M_{wat} + \sum_{j=1,m} M_{j,w}} \right)$$

ConnectFlow calculates the fraction of each reference water and then the concentrations of the components are inferred from the above equation. Note that the fraction of each reference water varies between zero and one and the total fraction of all reference waters sums to one.

$$\sum_{w=1,n} c_w = 1 \quad \text{Equation 6-50}$$

Reference waters are beneficial when groundwater composition can be inferred from mixtures of a small number of waters of identifiable origins, for example glacial melt water, meteoric water or sea water, and when the water sources have a larger number of dissolved salt species (i.e. when $m > n$). In that case it is more efficient to transport the n reference waters rather than the m chemical species and save computational time. If there are no clearly defined reference waters in the system or if hydrogeochemical calculations are required then reference waters are not appropriate and the concentrations of each solute must be individually calculated.

6.14.2 Mathematical Representation of Multi-Component Solute Transport in DFN

The equations of single component solute transport are extended to transport n reference waters in the following manner. First, Equation 6-43 is used to calculate the fraction c_w of $n - 1$ reference waters, this equation becomes,

$$\frac{\partial(e_t \rho c_w)}{\partial t} + \nabla \cdot (\rho \vec{q} c_w) = \nabla \cdot (e_t \rho D \cdot \nabla c_w) \quad \text{Equation 6-51}$$

Next, the concentration of the remaining reference water is then inferred from Equation 6-50. When transporting mass-fractions of individual solutes, rather than reference waters, the transport equations have the same form as Equation 6-51. However, in this instance all the n solutes must be calculated using this equation rather than calculating $n - 1$.

Finally, the manner in which the density and viscosity are calculated is significantly different between the single-component solute transport algorithm and multiple component salt transport. In the former case, the density is calculated using Equation 6-45 and the viscosity is assumed constant. In the latter case, the density and viscosity are calculated according to an empirical method described by Kestin et al (1981). This method calculates the density and viscosity according to the total mass of dissolved solids of all species as well as the pressure and the temperature (a fixed temperature distribution can be specified at the start of the calculation). The expression was originally derived using NaCl but it is considered a reasonable approximation for multiple salt species. This mirrors the approach used for ConnectFlow CPM calculations. The rock matrix diffusion algorithm has also been extended to work for an arbitrary number of chemical species.

Transients are typically calculated using a fully implicit scheme to avoid unphysical oscillations, although a Crank-Nicholson scheme is also available. Where steady state calculations are performed the derivatives with respect to t are zero.

There are some limitations to the approach, for example heat transport and unsaturated groundwater flow are not considered. Additionally, the dispersion lengths and intrinsic diffusion coefficients are assumed to be the same for all species (although they can vary depending on the host rock).

6.14.3 Implementation of Multi-Component Solute Transport in DFN

While it is possible to calculate the pressure field and all the concentrations for multi-component solute transport using standard Newton-Raphson iterations, in practice this is likely to prove computationally expensive. This is particularly true given a large number of component variables. To mitigate these performance issues, a sequential iteration algorithm has been implemented in the DFN case. The effectiveness of this approach has previously been demonstrated in ConnectFlow CPM calculations.

In sequential iteration, the algorithm iterates through a list of variables, calculating each as though it were independent of all the others. For each variable (or subset of variables), it will solve the relevant equations while holding all other variables constant (in time). Typically this means solving for the pressure assuming a static reference water composition and then solving for the concentration of each reference water assuming a static pressure field. Once all the variables have been updated, a convergence check is applied to determine the relative change of all variables. If there is a significant change then the variables are updated in the same sequence repeatedly until the criterion is met. This repetition of the sequence is known as “outer iteration”. Additionally an automatic time-stepping scheme can be used to reduce the time-step and repeat a given time-step if the criterion is not met once all the outer iterations have been completed in a transient calculation.

While a coupled solve typically has two levels of iteration (Newton-Raphson iteration and iterative linear solve), sequential iteration has up to four levels (Outer iteration, sequential iteration over the pressure and reference water variables, Newton-Raphson iteration and linear iteration). Figure 6-15 provides an example for three reference waters.

The advantage of using sequential iteration is that each linear equation solve is more tractable and requires fewer memory resources from the computer. Sequential iteration allows a solution to be found without these memory constraints. Additionally, the efficient and parallelisable GMRES-AMG linear solver can be used for single variable solves whereas the slower and sequential GMRES-ILU linear solver typically has to be used for multi-variable solves. This provides a significant extra benefit when using sequential iteration.

In the sequential iteration algorithm, certain variables may be updated without a full finite element calculation. For example, Equation 6-50 states that the fractions of reference waters must add to one. Thus if all reference waters except one have been calculated, the last is trivially inferred. Density and viscosity, where they are used as variables, may also be calculated algebraically as part of the sequence, based on the components present in the water at a given location, using the method described in Kestin et al (1981).

Where possible, an effort has been made to ensure that the DFN implementation is similar to the CPM implementation of the same functionality in ConnectFlow. This allows easy transfer of equivalent concepts between models with different kinds of rock. For example, in CPM multi-component solute transport a temperature variable is always specified, even when heat transport has not been specified. In the same way, the temperature variable is always included in DFN multi-component solute transport. A static but spatially varying temperature distribution may therefore be applied and is taken into account in density and viscosity calculations, however, heat transport calculations are not available in DFN models at this time.

```

Time-step Loop
  Newton-Raphson Loop
    Assemble flow and transport equations
    GMRES-ILU solve for pressure + reference
    waters 1 and 2
  End Newton-Raphson Loop
  Reference water 3 implied
End Time-step loop

```

```

Time-step Loop
  Outer iteration loop
    Newton-Raphson Loop
      Assemble flow equations
      GMRES-AMG solve for pressure
    End Newton-Raphson Loop
    Assemble transport equation 1
    GMRES-AMG solve for reference water 1
    Assemble transport equation 2
    GMRES-AMG solve for reference water 2
    Reference water 3 implied
  End Outer iteration Loop
End Time-step loop

```

Figure 6-15: Comparison of Standard Iteration (top) with Sequential Iteration (bottom) for a three reference water calculation. Note that the Sequential Iteration algorithm has up to four levels of iteration (for each time-step): outer iteration, iteration over variables, Newton-Raphson iteration (required if one of the variable solves is non-linear) and finally the iterations of the linear solver (GMRES-ILU or GMRES-AMG). The concentration of the third reference water is implied from other two reference waters in both cases.

6.15 Rock Matrix Diffusion in a DFN Model

6.15.1 Background

Rock matrix diffusion (RMD) is a process whereby solutes in water flowing through fractures in rock diffuse into less mobile water in the adjoining rock matrix under a concentration gradient (Neretnieks, 1980). This diffusion has the effect of retarding transport of solutes through the fractures. Because there may be a significant amount of pore surface area in the rock matrix, the rock matrix is also a significant site for chemical reactions.

Two methods are included in ConnectFlow for calculating RMD in continuous porous media (CPM). The first is the analytic method introduced by Hoch and Jackson (2004), and the second is the finite volume method introduced by Joyce et al. (2014a). Only the finite volume method has been implemented within the DFN since this can be used when chemical reactions are occurring.

6.15.2 Mathematical Representation of RMD in a DFN

The equations for the transport of saline water in a CPM affected by rock matrix diffusion are given in Equation 4-3 and Equation 4-4.

For a DFN model, the effective aperture of a fracture accessible to mobile water is characterised by the transport aperture e_t and the available volume for matrix diffusion is characterised by the size of the intervening matrix blocks between fractures, s_b . The equivalence relationships with the CPM parameters are:

$$\phi_f = \frac{e_t}{s_b} = \frac{e_t \sigma}{2} \quad \text{Equation 6-52}$$

Substituting for ϕ_f and σ into Equation 4-3, and converting Darcy flux vector, \vec{q} , to a flow-rate per unit length vector, $\vec{Q} = s_b \vec{q}$, integrated across the fracture aperture (i.e. transmissivity times head gradient vector), the transport equation for the DFN is obtained:

$$\frac{\partial(e_t \rho c)}{\partial t} + \nabla \cdot (\rho \vec{Q} c) = \nabla \cdot (e_t \rho D \cdot \nabla c) + 2\rho D_i \left. \frac{\partial c'}{\partial w} \right|_{w=0} \quad \text{Equation 6-53}$$

$$\alpha \frac{\partial(\rho c')}{\partial t} = \frac{\partial}{\partial w} \left(\rho D_i \frac{\partial c'}{\partial w} \right) \quad \text{Equation 6-54}$$

The penetration depth into the matrix is bounded to half the matrix block size ($w < s_b/2$). This is because the solute diffusion fronts typically propagate through a matrix block from both sides so that the effective penetration depth for each fracture is halved.

The equations above are appropriate for transport of a single solute but they generalise easily to the multi-solute implementation that is available in ConnectFlow.

6.15.3 Implementation of RMD in a DFN

The finite volume method employed for a DFN is identical to that for the CPM as stated in Equation 4-32, except for a factor of $\sigma/2$. Hence, for a DFN model, ConnectFlow reuses much of the algorithms that already exist for a CPM model. The most important differences in implementation arise from the fact that in a CPM model the equations are applied for each finite-element in the grid, while in a DFN model the equations are applied for each sub-fracture. Larger fractures and deformation zones can be tessellated into sub-fractures giving greater spatial resolution for the transfer between fracture and matrix as a solute mixing front moves through the network.

The following new parameters exist in the DFN in order to represent RMD:

- 4) An indication as to whether RMD is to be used or not;
- 5) The total diffusion length into the matrix w_{max} or the length of each finite volume cell, w_i ;
- 6) The number of finite volume cells, n_{fv} ;
- 7) The intrinsic diffusion coefficient, D_i ;
- 8) The matrix porosity, α .

It is important to note the distinction between the matrix block size, s_b and the maximum diffusion length into the matrix, w_{max} . The matrix block size is the distance to the next fracture. The diffusion length is the distance that is accessible for RMD, which is typically half the matrix block size since the adjacent fracture will affect the other half of the matrix block.

The parameters D_i , w_{max} and α can be defined on a fracture-by-fracture basis for deterministic fractures and by fracture set for stochastically-generated fractures. The number of finite volume cells is the same for *all* fractures in a model and their sizes are the same for every fracture in a set. This contrasts with CPM modelling where the equivalent parameters are defined by rock type.

Alternatively, the user can choose to not specify w_{max} and allow ConnectFlow to automatically calculate it using the actual distances to neighbouring fractures.

The following consistency checks are made to ensure $\sum_{i=1}^{n_{fv}} w_i = w_{max}$:

- 9) If $\sum_{i=1}^{n_{fv}} w_i < w_{max}$ then $w_{n_{fv}}$ (the last block) is increased to ensure the equality.
- 10) If $\sum_{i=1}^{n_{fv}} w_i > w_{max}$ and w_{max} is chosen by the user (rather than automatically) then w_{max} is increased to ensure the equality.
- 11) If $\sum_{i=1}^{n_{fv}} w_i > w_{max}$ and w_{max} is determined automatically then the number and/or length of the w_i are reduced to ensure the equality

In addition, it is necessary to be able to specify the initial concentration of solute in the matrix. This can either be specified as a constant or linear variation across the model or the concentration in the matrix can be set equal to that in the fracture.

6.16 Reactive Transport in DFN Models

6.16.1 Introduction

Reactive transport has been implemented for DFN models using the same interface to PHREEQC as CPM models (see section 4.7). PHREEQC is an extensively used geochemical software product and is capable of simulating a wide range of chemical reactions, including equilibration of aqueous solutions with minerals, ion exchanger materials, surface complexes, solid solutions and gases. It can also simulate kinetic non-equilibrium reactions. Future upgrades to PHREEQC and/or the interface will become available for use by both DFN and CPM calculations.

The implementation in the DFN is very similar to the existing CPM implementation: the transport calculation is performed at the start of each timestep and upon completion the reactive transport at each ConnectFlow solution node is calculated using the **iPHREEQC** module. Note that in DFN calculations the solution nodes are defined at fracture intersections, rather than on the individual finite elements within each fracture.

All reactive transport scenarios in the CPM are also available in the DFN. These can be used to calculate and output Smart Kd values for radionuclide transport calculations (radionuclide transport is not yet implemented in the DFN but it is a likely future development).

In the DFN, reactive transport (like other forms of transport) may be calculated in both steady state and transient calculations, whereas CPM reactive transport is only implemented for transient calculations.

6.16.2 Rock Matrix Diffusion

The finite volume rock matrix diffusion algorithm within the DFN is able to calculate chemical reactions within the rock matrix. This is implemented in the DFN by noting the chemical makeup of the porewater within each of the finite volume cells representing the matrix and then utilising PHREEQC to carry out reactions in each cell. The matrix reactions are carried out at the end of each timestep in exactly the same manner as the reactions in the fractures themselves. Note that the temperature is needed for the chemistry calculations and this is assumed to be the same in the rock matrix as it is in the fracture.

6.16.3 Mineral Quantities

Mineral quantities are assigned a uniform quantity across the model, which defaults to 10.0 mol/kg_w (the PHREEQC default) if not specified. If the initial quantity of a mineral phase is set to zero then it is considered to be a secondary mineral, in which case it cannot initially dissolve, but may precipitate (and possibly subsequently dissolve) as the result of a chemical reaction.

If the quantities of the minerals change as a result of chemical reactions then the variable values associated with the minerals are updated accordingly. However, the mineral quantities are maintained internally by **iPhreeqc**.

Note that minerals quantities may not be uniformly distributed throughout a geological system but may vary, for example by rock type or depth. In CPM calculations it is possible to define these quantities as variables but this has not as yet been implemented for DFN calculations.

7 Concepts within Combined Models

7.1 Nesting of Sub-Models

The capabilities of ConnectFlow for cases using a single concept (DFN or CPM) has been discussed in the previous chapters. This chapter discusses the case where both concepts are used in a single model. The model can be constructed with sub-models that use distinct concepts either CPM or DFN. That is, the model can be split into 2 different domains: one that uses the CPM concept, and one that uses the DFN concept. However, DFN and CPM approaches cannot be used simultaneously in any part of the domain. Figure 7-1 to Figure 7-3 show a few alternative configurations.

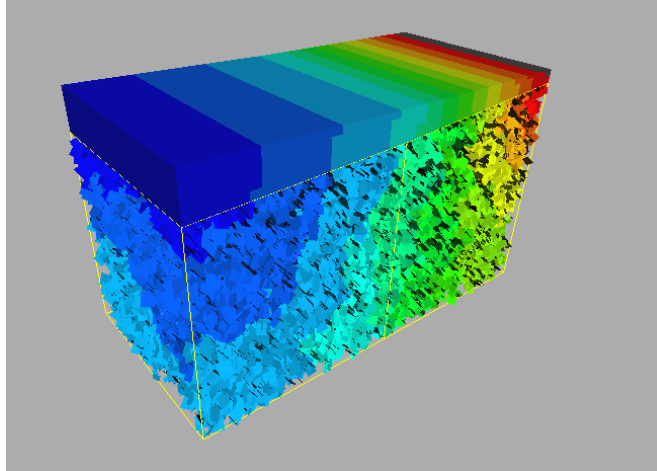


Figure 7-1: A unified CPM/DFN ConnectFlow model using a CPM to represent a sedimentary cover overlying a fractured basement. Here the grid and fractures are coloured according to head distribution.

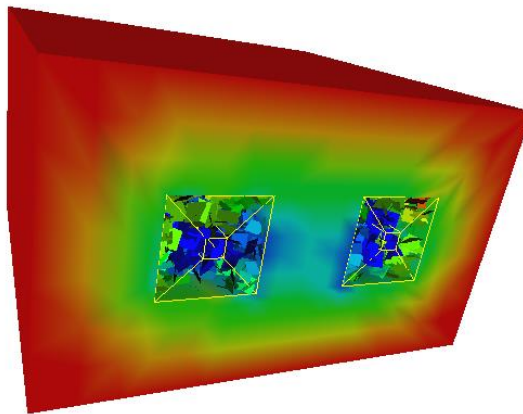


Figure 7-2: View of a model of two adjacent access tunnels being modelled using ConnectFlow. In this case, the inner region is being modelled (in detail) using a fracture network approach, the outer surrounding region (the far-field) by a porous media. The CPM region and the fractures are coloured by the pressure distribution on the surface of the model.

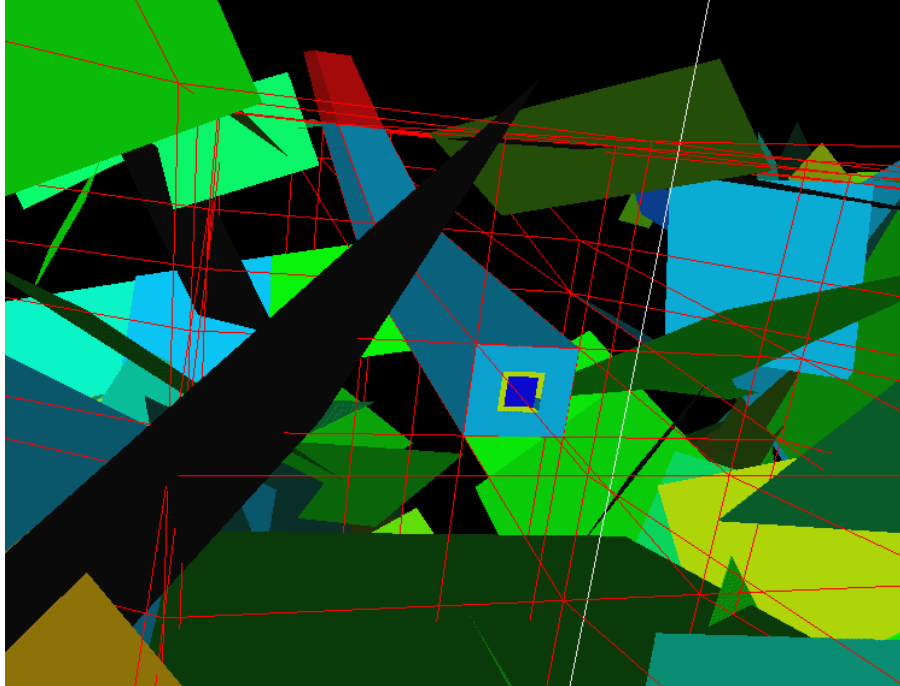


Figure 7-3: A CPM representation of a modelled tunnel (shown in the centre of the figure), embedded within a DFN model. The different colours in the CPM model relate to different properties for tunnel excavated damage zone, skin and actual tunnel. Many fractures have been removed to more clearly illustrate the tunnel.

These figures illustrate the flexibility of ConnectFlow. The benefits of this flexibility include:

- 12) being able to use the most appropriate concept for different lithological units for sedimentary settings, e.g. a fracture basement covered by a sedimentary cover;
- 13) the ability to switch easily between concepts to quantify conceptual uncertainties in using a CPM versus DFN model to calculate performance measures;
- 14) in using a single software package to implement DFN and CPM models it is easier to compare consistency between equivalent representations;
- 15) the flexibility to nest detailed models of important areas, e.g. a fractured near-field within a much larger CPM domain to capture realistic boundary conditions and guarantee rigorous coupling between the sub-models;
- 16) the ability to nest an appropriate CPM representation of engineered structures, such as repositories within a detailed DFN model.

Again, the ConnectFlow concept is that different regions can be represented in different ways and then formally nested together. This is different from the case where discrete fracture objects co-exist with a porous medium model of the rock matrix. Representations of the interaction between fractures and the rock matrix within the same domain can be represented in ConnectFlow, but it should be recognised that this is a quite different issue. Fracture/matrix interactions are dealt with in the CPM and DFN modules in different ways as described in section 2.6.4 for the CPM module. In the DFN module, the rock matrix can be represented by either special sets of fractures (matrix fractures) or by using a finite-difference approach (as described for CPM models in section 4.6.1).

In a combined DFN/CPM model, flow in the DFN and CPM models is nested formally by internal boundary conditions at the interface between the two sub-regions. These boundary conditions are implemented as equations that ensure continuity of pressure and conservation of mass at the interface between the two sub-regions. On the DFN side of the interface, these boundary conditions are defined at nodes that lie along the lines (traces) that make up the intersections between

fractures and the interface surface. On the CPM side, the boundary conditions are applied to nodes in finite-elements that abut the interface surface. Thus, extra equations are added to the discrete system matrix to link nodes in the DFN model to nodes in the finite-element CPM model. By using equations to ensure both continuity of pressure and continuity of mass, then a more rigorous approach to nesting is obtained than by simply interpolating pressures, say, between separate DFN and CPM models. The equations used in the nesting are described in section 7.3.

7.2 Representation of Fractures

The DFN module is described in detail in Chapter 5. For the purpose of this chapter, the representation of fractures can be summarized as follows. Fractures are represented as explicit planar objects with either a rectangular or triangular shape. Each fracture plane is described by the following attributes:

- 17) Geometry: defined by centre position, strike, dip, orientation (a rotation within the plane of the fracture), strike length, dip length and shape. Alternatively, a fracture can be defined by the positions of its corners.
- 18) Flow properties: defined by either hydraulic aperture or transmissivity, based on a parallel plate concept. Additional parameters include storativity and transport aperture, which are defined in terms of one of a choice of models and the associated parameters.
- 19) Additional: the fracture set is stored for each fracture. Also, fractures can be subdivided into sub-fractures to represent fracture roughness or channelling. In this case, a reference to the original unsubdivided fracture is stored.

Fractures can be generated in several ways either as deterministic fractures defined individually or as stochastic sets of fractures with their attributes defined in terms of probability distribution functions (PDFs) for each fracture attribute. Deterministic fractures can be input in terms defining the attributes of each fracture individually or by reading a formatted file.

The DFN concept is that fluid flow passes through a rock volume primarily via the interconnected network of fracture objects, there is no flow through the inter-fracture volumes. Hence, the DFN model has to include all fractures that contribute significantly to flow on the scale of interest. An example of a DFN model is shown in Figure 7-4.

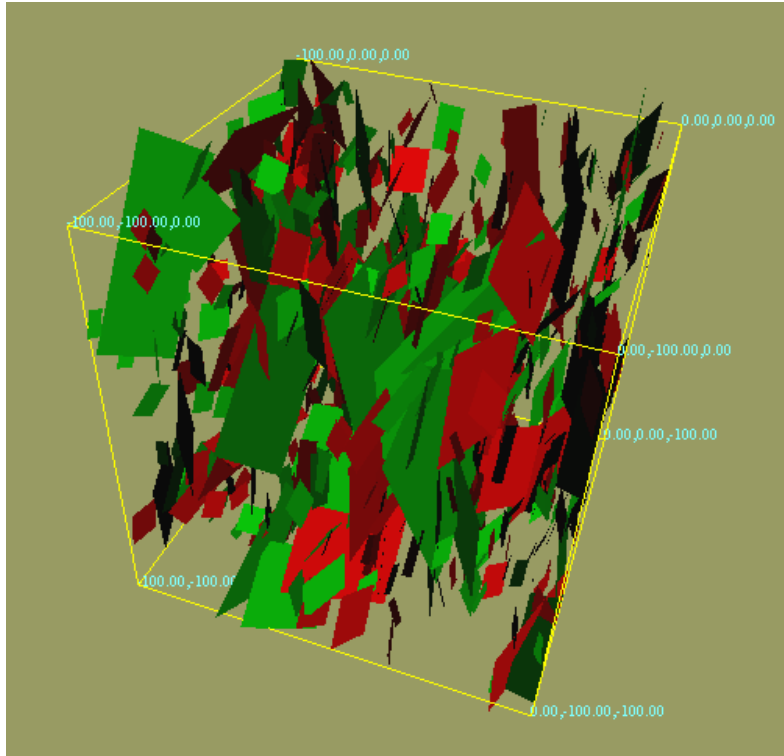


Figure 7-4: An example of a simple DFN model within a cube. Here, two stochastic sets of fractures are generated both sub-vertical but with different mean strikes. Fractures are coloured by set.

In order to construct nested models of the same fractured rock (mixing DFN and CPM sub-regions), then the data used for the DFN and CPM models should be self-consistent. For example, if a repository scale DFN model is nested within a stochastic continuum model, then flow statistics on an appropriate scale, the size of the elements in the CPM model, need to be consistent. This is achieved by using parameters to represent the stochastic continuum (mean, standard deviation, correlation length) that are obtained by upscaling the DFN model on the scale of the CPM elements. To ensure consistency of how larger scale fractures zones are represented when they cross between DFN and CPM models then the fracture zone geometries have been defined consistently. An easy way of doing this is to use the IFZ format to define such fracture zones in a file, as both modules can read this format. This is achieved by specifying that the IFZ file can be read into both parts of the model. The parts of a fracture within each sub-region are calculated automatically.

Figure 7-5 shows an illustration of how a large deterministic fracture that crosses between DFN and CPM sub-regions can be modelled in such a way as to ensure there is continuity in its representation, and hence in flow between the regions.

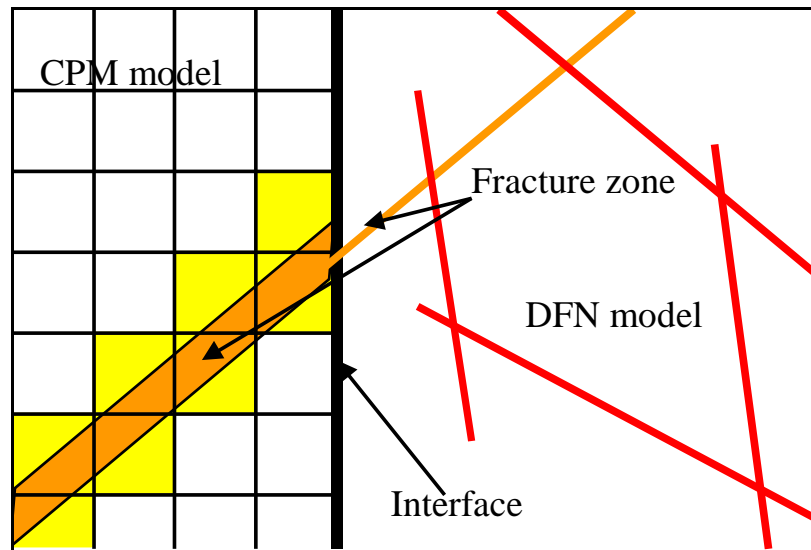


Figure 7-5: Schematic illustration of continuity of fracture zones across a CPM/DFN interface in a ConnectFlow model. The DFN region is to the right with a CPM grid to the left. A few fractures are shown in red and orange in the DFN region. The red fractures may be stochastic for example. The orange fracture is a deterministic fracture that crosses the interface. On the DFN side it is shown as a plane, while on the CPM side it is drawn with its actual thickness. The elements crossed by the fracture zones are coloured yellow. Permeability in these elements will be modified in the IFZ method to represent the effect of the fracture zone on flow.

7.3 Current Physics

7.3.1 CPM Physics

In CPM-only models a wide range of physics are implemented as described in Chapter 3, including:

- 20) Saturated groundwater flow;
- 21) Unsaturated groundwater flow;
- 22) Dual porosity flow;
- 23) Coupled groundwater flow and salt transport (variable density flow);
- 24) Coupled groundwater flow and heat transport;
- 25) Radionuclide transport with chains, decay, sorption and solubility limitations;

7.3.2 DFN Physics

A more restricted range of physics is currently available for DFN models, as described in Chapter 6:

- 26) Saturated groundwater flow;
- 27) Unsaturated groundwater flow;
- 28) Coupled groundwater flow and salt transport (variable density flow);

7.3.3 Nested DFN/CPM physics

For nested models, currently only saturated groundwater flow with linear boundary conditions is supported. The coupling between DFN and CPM regions at their common interface is implemented as additional equations that link residual pressure values at nodes in the fracture planes to pressure values in the CPM finite-element mesh. These equations ensure continuity in pressure and conservation of groundwater flux (i.e. mass flux) across the interface. Figure 7-6 shows this configuration.

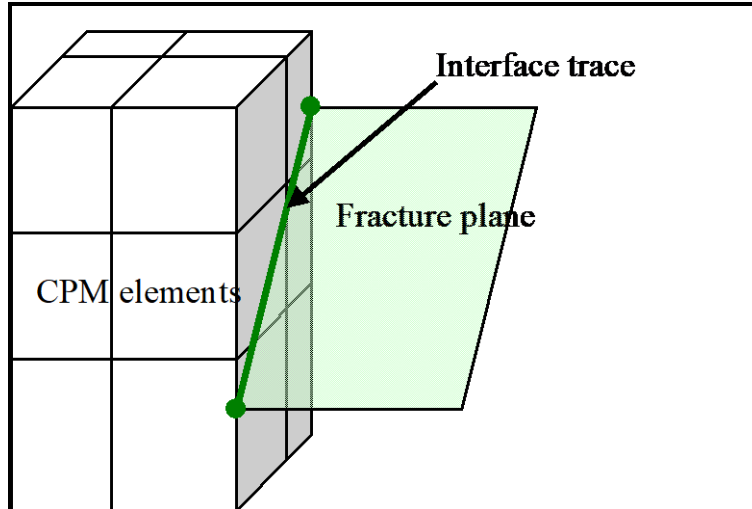


Figure 7-6: Sketch of coupling between DFN and CPM sub-models. A finite-element CPM mesh is shown on the left. The right-hand surface is intersected by a single fracture plane. Extra equations are used to link the DFN to the CPM. These equations are applied at nodes (dark green points) in the fracture plane along the intersection (dark green line).

The steps in coupling the two regions are:

- 29) Calculate the intersections of fractures with the boundary of the DFN region.
- 30) Select the surfaces of the DFN region that abut the CPM region and specify a coupling type boundary condition.
- 31) For each fracture that intersects these DFN region surfaces, identify the CPM finite-elements that abut the fracture. A single fracture may abut several elements, or several fractures may abut the same element.
- 32) Add extra equations to the discrete system matrix to link the pressure values at nodes on the fracture intersects with the pressure values in the adjoining finite-elements.
- 33) Solve the discrete system matrix.

Hence, extra internal boundary conditions have to be specified for a nested model to link DFN and CPM regions.

7.4 Boundary Conditions

7.4.1 DFN Equations

The DFN equation for the i th global flow node is given by

$$\int_{\Omega_f} \sum_j \rho_0 \frac{\tau}{\mu} \nabla \Psi_i \nabla \Psi_j \bar{P}_j - \int_{\partial \Omega_f} \Psi_i F = 0 \quad \text{Equation 7-1}$$

where Ω_f is the DFN subdomain, $\partial \Omega_f$ is the boundary of the DFN subdomain, ρ , is the groundwater density, τ is the fracture transmissivity, μ , is the fluid viscosity, Ψ_j , is the linear basis function for the global flow nodes on the fracture, \bar{P}_j is the DFN residual pressure at the j th global flow node and F is the consistent mass flux out of the fractures for those fractures that intersect the boundary. The summation in j is taken over the global flow nodes on the fracture

$$F = \sum f_i \Psi_i \quad \text{Equation 7-2}$$

A new mass-flux freedom f_i is introduced into the DFN discrete system at each global flow node on the boundary at which a Dirichlet type boundary condition has been set. Therefore, on the boundary

between the region containing the fractures and the region containing the equivalent porous medium there are two DFN freedoms per global flow node; the pressure and flux.

7.4.2 CPM Equations

The CPM equation for the l th degree of freedom is

$$\rho_0 \left(\int \sum \frac{k}{\mu} \nabla \varphi_i \nabla \varphi_j P_j^E - \int \phi_i \mathbf{v} \cdot \mathbf{n} \right) = 0 \quad \text{Equation 7-3}$$

where k is the permeability, P_j^E and φ_j are the CPM pressure and finite-element basis functions evaluated at the l th degree of freedom on the element respectively. Ω is the CPM subdomain, $\partial\Omega$ is the boundary of the CPM subdomain, \mathbf{v} is the darcy velocity, \mathbf{n} is the unit outward normal on the CPM boundary. For the CPM equations, the summation j is taken over the degrees of freedom.

7.5 Interface Conditions

7.5.1 Approach 1 (“Mass Lumping”)

The basic requirement linking the CPM and DFN subdomains are continuity of pressure and conservation of mass. One approach to achieve this is to distribute the mass across the interface over a set of discrete point sources, namely the set of DFN global flow nodes on the interface. Hence by writing,

$$F' = \sum_i f_i \delta(\mathbf{x} - \mathbf{x}_i) \quad \text{Equation 7-4}$$

Equation 7-1 becomes

$$\int_{\partial\Omega_f} \sum \nabla \Psi_i \nabla \Psi_j \bar{P}_j - f_i = 0 \quad \text{Equation 7-5}$$

Conservation of mass across the interface requires

$$\rho_0 \left(\int \sum \frac{k}{\mu} \nabla \varphi_i \nabla \varphi_j \bar{P}_j \right) - \sum_j \varphi_i(x_j) f_j = 0 \quad \text{Equation 7-6}$$

Continuity of pressure at the interface requires

$$\bar{P}_i = \sum_j \Psi_j(x_i) P_j^E \quad \text{Equation 7-7}$$

Hence the solution to Equation 7-5 and Equation 7-6 are the constraints for the discrete interface problem.

This approach amounts to interpolating the pressures from the CPM model at the DFN global flow nodes on the interface and ‘mass-lumping’ the flux between the two regions into point sources at the global flow nodes.

7.5.2 Approach 2 (“Distributed Flux”)

Alternatively, it is more precise to insert F from Equation 7-2 into Equation 7-3 to get

$$\int \sum \frac{k}{\mu} \nabla \varphi_i \nabla \varphi_j P^E_j - \int_{\partial\Omega} \varphi_i F = 0 \quad \text{Equation 7-8}$$

In this case, F is a line source of mass into the CPM element in which the i th freedom lies, distributed along the lines of intersections with the fracture planes. Thus the second term in Equation 7-8 may be written as

$$\int_{fracture} \varphi_i \Psi_j f_j dl \quad \text{Equation 7-9}$$

where the integral is along the trace of the fracture on the finite-element boundary, and the summation is over the fractures that abut the current finite-element.

The following condition is consistent with the above treatment of conservation of mass. If we take a weighted residual approach to the continuity of pressure

$$\int \Psi_i (P^E - \bar{P}) dl = 0 \quad \text{Equation 7-10}$$

where I ranges over all the global flow node on the edge of the fracture, the integral is along the trace of the fracture on the finite-element boundary, P^E is the CPM pressure and \bar{P} is the DFN pressure.

Since

$$\begin{aligned} P^E &= \sum_i \varphi_i P^E_i \\ \bar{P} &= \sum_i \Psi_i \bar{P}_i \end{aligned} \quad \text{Equation 7-11}$$

Equation 7-9 and Equation 7-10 imply

$$\int_{fracture} \sum_j \Psi_i \varphi_j P^E_j dl - \int_{fracture} \sum_j \Psi_i \Psi_j \bar{P}_j dl = 0 \quad \text{Equation 7-12}$$

Note that the cross terms in the interface problem are transposes of each other. The second approach to distributing the flux along the fracture is more robust than the first since it distributes the flux from the DFN fractures along the trace of the fracture on the CPM elements that it abuts. Thus, if a long fracture abuts many CPM elements then this approach ensures an appropriate amount of flux enters or exits each element.

7.6 Transport

Particle tracking algorithms for advective transport of a solute are implemented for both the CPM and DFN concepts. In CPM models, particles can be tracked in 3 different ways.

- 34) A deterministic method by moving along a discretised path with a local finite-element velocity field. At each discrete section of the path, the local velocity vector is calculated, and then the particle is moved with that velocity for an appropriate time-step.
- 35) A mass-conserving deterministic method by moving along a discretised path using velocities calculated using the mass-conserving Cordes-Kinselbach algorithm (as described in section 4.4). These velocities are constant across tetrahedral sub-elements.
- 36) A mass-conserving stochastic method, again using the Cordes-Kinselbach algorithm, to calculate the particle velocities (as described in section 4.5). The difference with this implementation is that particles are constrained to travel between transport nodes defined on the surface of each element. The stochastic nature of this method arises when a particle is tracked from a transport node. Each particle is given four different start points that are slightly perturbed from the original location of the transport node. Consequently the particle can sometimes have more than one destination node. For a given realisation, the destination picked is determined using weightings for each destination (determined by the number of start points that send the particle there) and a calculated pseudo-random number.

In DFN models, a stochastic ‘pipe’ network type algorithm is used. Particles are moved between pairs of fracture intersections stepping from one intersection to another. At any intersection there may be several possible destinations that the particle may potentially move to next as flow follows different channels through a fracture. A random process, weighted by the mass flux between pairs of intersections (connected by a ‘pipe’), is used to select which path is followed for this particular particle. Hence, there is explicit hydrodynamic dispersion process built into the transport algorithm used in the DFN module. The time taken to travel between any two intersections, the distance travelled and flow-wetted surface are calculated for each pipe based on flow rates and geometries. The pipe network is created using either an exact approach (section 6.12.1 or section 6.12.2) or an approximate approach (section 6.12.3).

In a nested ConnectFlow model particles can be traced through both DFN and CPM regions continuously, using the appropriate algorithm according to the region the particle is currently in.

Note particles starting at a given coordinate in the DFN region are very unlikely to be located in a fracture, so that they have to be started in a nearby fracture to ensure they are in a flow channel. This process can be controlled by the user by specifying a ‘search radius’ around the start point for a list of potential fractures to start the particle in. Particles can then be started from fractures in this list by selecting them according to a flux weighting.

8 Simulation Setup and Execution

Input to ConnectFlow is specified using a structured free-format input language, which has been designed to be readily comprehensible to the user. Input files can be created manually or via a graphical user interface described in section 8.1. The input data specifies the finite-element grid, the variables of interest, the boundary conditions, the processes to be modelled, generation of fractures and properties, and the outputs required.

The input language allows the user to specify the execution of the program in a flexible manner. The individual components of a run (model generation, specification of processes to be modelled, output required, etc.) can be specified in any logical order and may appear more than once in any run. The results of a calculation may be saved for later post-processing or for use as an initial condition in a later calculation. An existing model may be modified and the results of a calculation may be interpolated from one finite-element grid to another.

The full set of ConnectFlow commands and their syntax is recorded in the Command Reference Manual that is available as an on-line HTML document. Hypertext links are used in such a way as to show the hierarchy of commands.

The ConnectFlow executable can be used to run pure CPM (>> CPM CONCEPT), pure DFN (>> DFN CONCEPT) or combined ConnectFlow (>> COMBINED DFN AND CPM CONCEPT) input datasets, using the top-level commands as indicated. Jobs can be run in batch using a command line executable on either Linux or Windows. Alternatively, the Graphical User Interface (GUI) is available for both creating input data and submitting jobs to a specified computer.

The names NAMMU and NAPSAC are historic and reflect the initially separate developments of the codes. Now that they are combined in ConnectFlow, they are largely superseded but may still be encountered in some circumstances. The acronym NAMMU stands for 'Numerical Assessment Method for Migration Underground'. NAMMU was also the name of the Sumerian goddess of the abyssal waters, whose name was expressed by the ideogram for 'sea' [Jacobson, 1949].

8.1 ConnectFlow Graphical User Interface

The intention of the graphical user interface (GUI) is to make it easier for the new user to define a model without having learn the input language structure and syntax (Figure 8-1). The GUI is organised in an object based approach where objects represent the base building blocks of a model such as grids, fracture sets, deterministic fracture zones, lithological units etc. The GUI provides a framework for defining the properties of each object side using panels, and storing the data within a project. A particular model is then a collection of objects. The input commands to define the model are created automatically when a job is run as a pre-processing step.

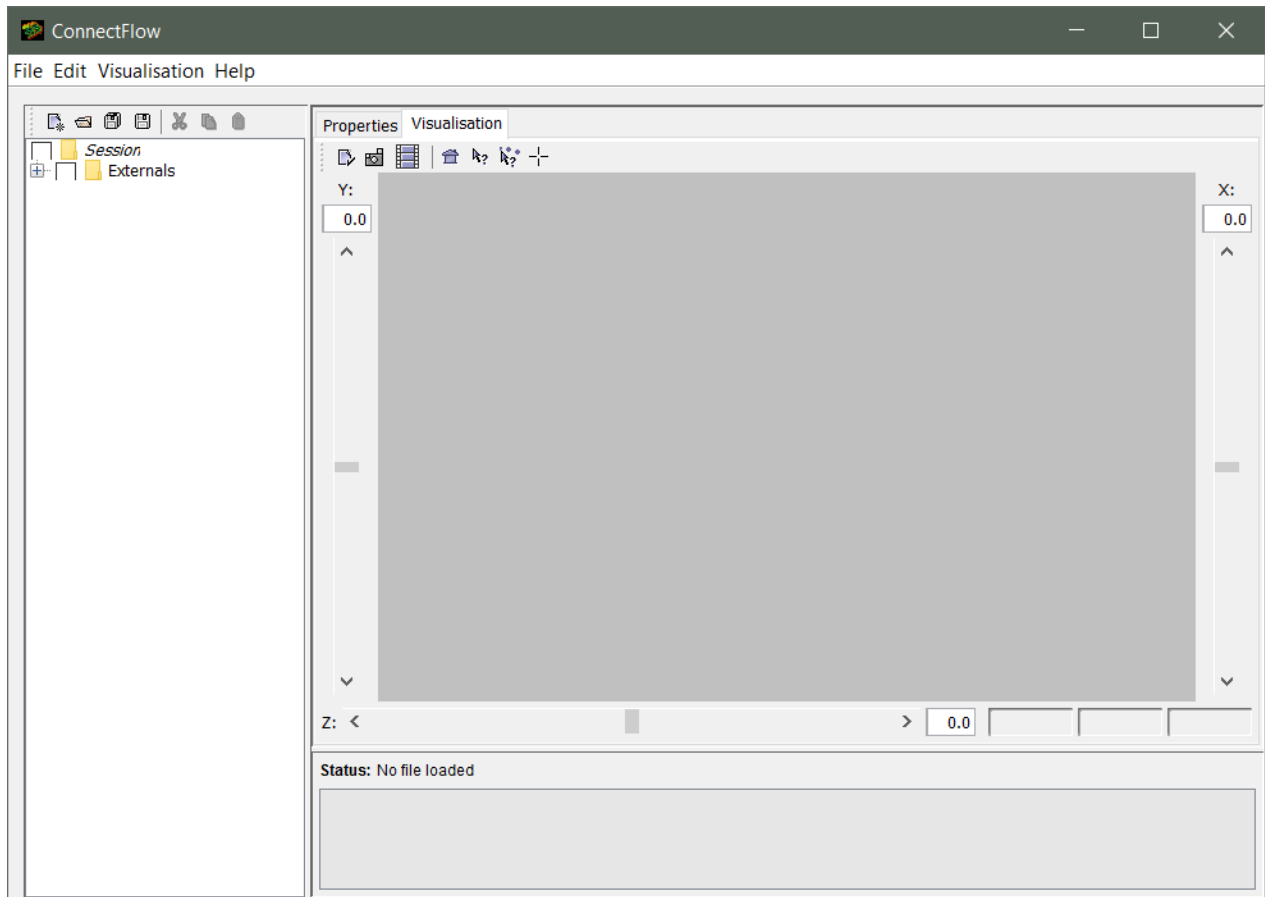


Figure 8-1: ConnectFlow GUI window

The GUI has been designed so that it is very simple to create alternative concepts within the same domain, such that it is fast to switch between CPM, DFN and combined DFN/CPM models (e.g. Figure 8-2).

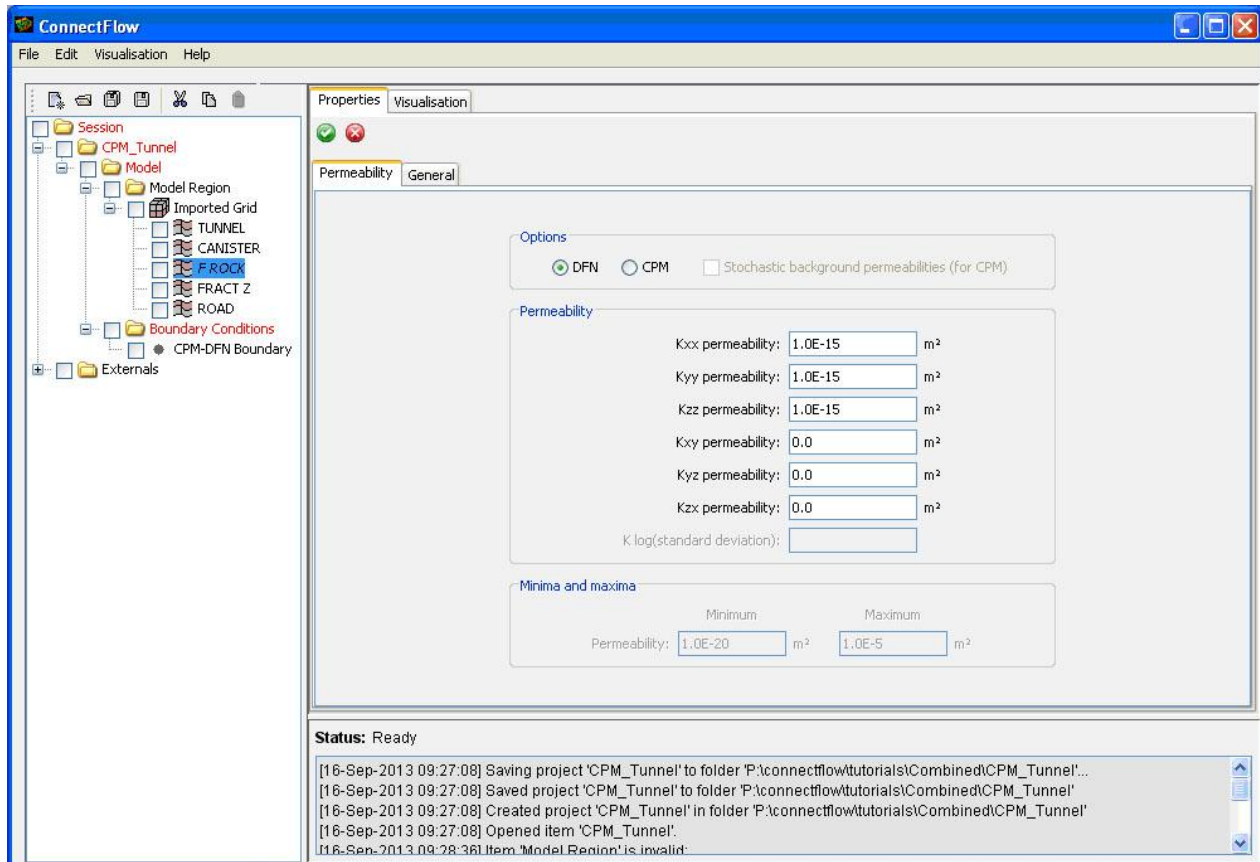


Figure 8-2: The ConnectFlow window for defining rock properties. This makes it simple to define whether a rock is to be represented by CPM or DFN concepts.

The steps in setting up a ConnectFlow model typically are as follows:

1. Create a model and select the type of simulation required.
2. Set up a model domain made up of cells or patches with each cell/patch assigned to a rock type.
3. For each rock, select which type of representation, CPM or DFN, is to be used. Define the hydrogeological parameters e.g. permeability, porosity. There may be several instances of a rock type with either different concepts or properties to quantify conceptual and parametric uncertainties.
4. Define deterministic fracture geometries and parameters.
5. Define stochastic fracture sets.
6. Solve for flow and transport for the model.
7. Visualise the output.

There are other facilities available in ConnectFlow, such as exporting fracture geometries and upscaling DFN models to obtain equivalent CPM permeabilities. The full facilities are described in the GUI online help, including a user guide and tutorials.

9 Output

The output from ConnectFlow currently takes four forms:

- 37) Text files containing information about the model, the performance of the solver and any output options requested;
- 38) ASCII files used to export results such as transport statistics, pathlines, grids, fracture geometries, upscaled equivalent permeabilities from DFN models;
- 39) Binary files that contain models, solutions, particle tracking libraries, generated physical properties.
- 40) Postscript graphics files.

The binary files and some of the ASCII files can be used for further runs or for visualisation using the 3D visualisation package. This is a fully interactive tool with the capability of displaying and manipulating images of the ConnectFlow model on the screen.

Some images generated with the visualisation package have been shown earlier in the report, in particular in section 7.1 for nested models. In the following sections, specific outputs for DFN models and CPM models are listed, together with some further visualisations.

9.1 CPM Outputs

A wide variety of output options are available for CPM models. These include:

- 41) Plots of the finite-element grid;
- 42) Plots of the grid with elements shaded according to rock type;
- 43) Plots showing planar slices through three-dimensional grids;
- 44) Plots showing the grid surface or certain internal surfaces for three-dimensional grids;
- 45) Plots of the grid boundary;
- 46) Shaded plots or contour lines of scalar functions of the variables;
- 47) Plots of vector quantities;
- 48) One-dimensional line graphs of scalar functions of the variables along a line;
- 49) One-dimensional line graphs of scalar functions of the variables as a function of time;
- 50) Plots of advective pathlines;
- 51) Calculation of capture zones;
- 52) Mass balance calculations;
- 53) A number of options for colouring plotted quantities, for example, according to the values of the variables, scalar functions of the variables and user defined functions of the variables;
- 54) Superimposing any combination of plots, and addition of user-defined text and lines to build up complex images.

The finite-element model and the modelled results can also be visualised in 3D. The following figures illustrate some of the types of pictures that can be produced for CPM models by the 3D visualisation package.

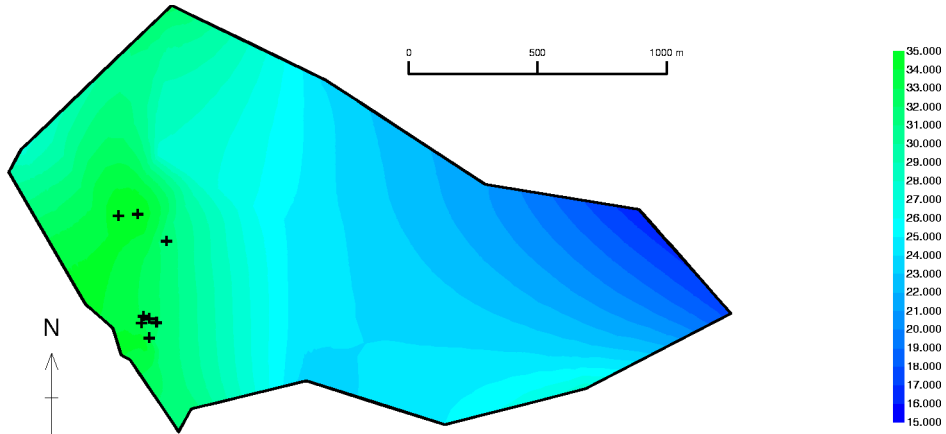


Figure 9-1: Shaded contour plot of groundwater head.

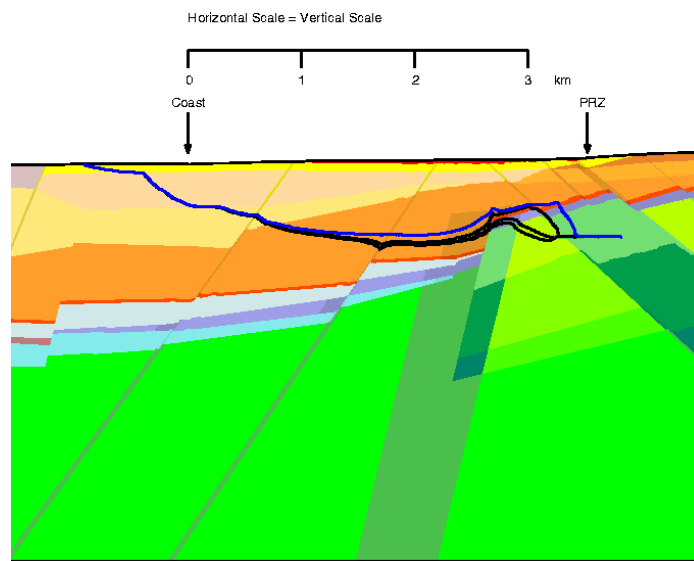


Figure 9-2: Pathlines for a model based on the grid shown in Figure 4-2.

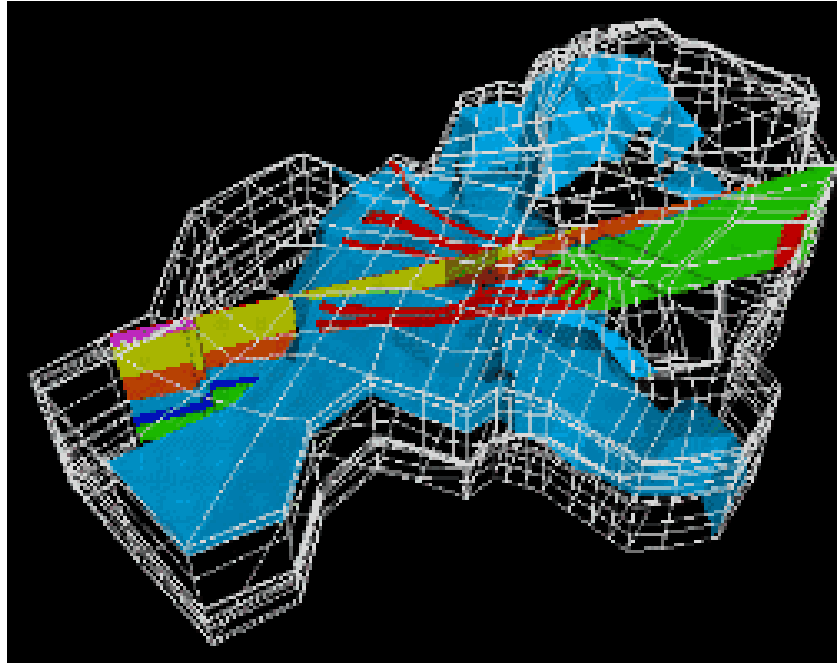


Figure 9-3: Complex image for a 3D version of the model shown in Figure 4-3, showing (i) a slice through the grid, (ii) a surface of constant salinity and (iii) a number of pathlines.

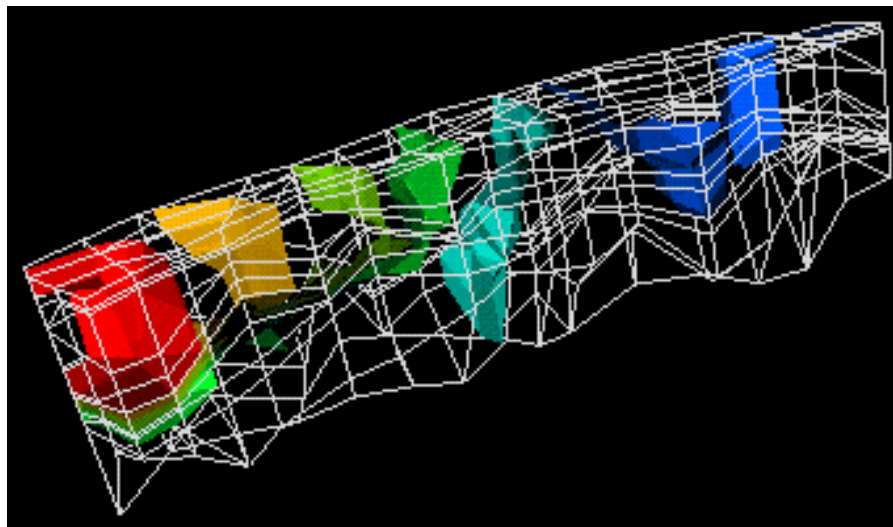


Figure 9-4: Isosurfaces of pressure for the model shown in Figure 4-3.

9.2 DFN Outputs

The problems modelled by ConnectFlow can be highly complex, so it is useful to have a variety of ways of displaying output from the model, in order to facilitate the interpretation of results.

9.2.1 Standard Output File

During the model generation and calculation phases of a DFN model run, text based summary output is written to the ASCII standard output file (.out file), as for any ConnectFlow run. This contains information such as a summary of the statistical properties of the fractures generated, groundwater fluxes through surfaces, pressures and fluxes to engineered features. Some output options generate further text based output, such as the option to sample fractures along hypothetical cores.

9.2.2 Graphical Output

Most output options produce graphical output via an internal graphics package that creates flat plot (2D) images in PostScript format.

Some options draw perspective diagrams illustrating views of the network in three dimensions. The user has complete flexibility to specify the point from which the network is observed, but may instead choose from a set of standard view options. For clarity, lines hidden from the observation point by other parts of the network are not shown in the picture.

9.2.3 Inspecting the Network

There are several options that allow detailed inspection of the fracture-network, including one that simply draws a perspective diagram of either the whole system or a specified subset of fractures. Another option (“trace mapping”) can be used to examine any (plane) cross-section through the network. As well as producing a diagram showing where fractures intersect the cross-section, it can scan along selected lines in the plane, reporting information on all the intersections encountered.

This information consists of the distance from the start of the scan line, and the angle at which the fracture was crossed, and the length of the intersection of the fracture with the cross-section plane.

There is also a facility for probing the network with line segments similar to boreholes. The “core logging” option produces both geometrical and hydraulic information for all fractures crossed by the line segment. This includes the distance from the start of the segment, the dip direction and dip angle of the fracture, the angle relative to the core, the fracture set number, the aperture and transmissivity of the fracture.

Another option is useful when simulating the local variation of the aperture over individual fractures. This produces maps of the aperture width on one or more fractures, with contours at equal intervals of the logarithm of the aperture. In addition, one can request the printing of data on the two-point correlation of apertures.

9.2.4 Examining the Pressure and Flow Solutions

There are many options available to display the flow solution. The user may request a plot of the fracture-network showing pressure contours or flux vectors, represented by arrows, on fractures. Plots of pressure on individual fractures may also be requested. Pressure profiles in which graphs of pressure against distance along a line segment through the network are plotted can be drawn for steady-state and transient flow options. Plots of pressure at a point against time are also available. When locally-varying apertures are specified, histograms of fluxes across a line within a fracture can be plotted.

The “pipe” model is a tool for analysing the solution of the flow problem by representing each of the fractures in the network by a collection of pipes. Every pair of intersections in a fracture is connected by a set of pipes, which contains a pipe joining every node on one intersection with every node on the other. It should be understood that the fluxes in the pipes only represent an approximation to the flow field in the fracture. They are computed from exact solutions of the pressure at the nodes and the global response matrices. The pipe model can be used to estimate the flux that crosses a series of parallel plane rectangular surfaces.

9.2.5 Tracer Transport

Several types of diagram are available for displaying the results of tracer transport simulations. To look at the results of a large swarm of particles sent through the network, graphs showing the proportion of particles leaving the network as a function of time or path length are available. The number of particles is scaled by the total number released to show a “breakthrough curve”. A cumulative arrival curve is plotted by integrating the number of particles arrive as a function of time.

This plot also includes a curve derived by fitting an analytical solution of the advection-dispersion equation to the times by which 25% and 75% of the particles have left the system.

A three-dimensional view of the network showing the swarm of particles at user specified times or a diagram of a boundary surface showing the arrival of particles can also be selected. Individual particle tracks can be investigated by producing a three-dimensional plot showing the tracks or by plotting graphs showing aperture against time or distance for individual particle tracks.

9.2.6 3D Visualisation

The most powerful way to understand and interpret the results of a 3D network simulation is naturally to visualise the results in 3D. A complementary 3D visualisation software package has been developed specifically for ConnectFlow. This is described in the next section.

The visualisation package displays in 3D all the features in a DFN model, including the model region, fractures, engineered features and upscaling, and their associated scalar and vector data. It is also able to carry out calculations on the model, including clustering, pathlines, and flux through a plane. In addition to displaying the DFN model features, it is also possible to overlay external data, such as maps.

The capabilities of the visualisation package for DFN models include the interactive 3D visualisation of the following:

- 55) the fracture-network with each fracture coloured according to transient or steady-state properties such as aperture or pressure;
- 56) a reduced network with removal of fractures according to location or properties;
- 57) engineered features;
- 58) upscaling;
- 59) pathlines generated from multiple user-defined sources;
- 60) slices through the model;
- 61) clustering around engineered features or points.

A snapshot of any screen can be saved as a 3D image using VRML (Virtual Reality Modelling Language) format. The saved image can be viewed and manipulated in 3D using a web browser (for example Netscape). Alternatively, the screen can be saved in a 2D format such as PNG, JPEG, or PostScript. 2D images can be combined to create animated movies.

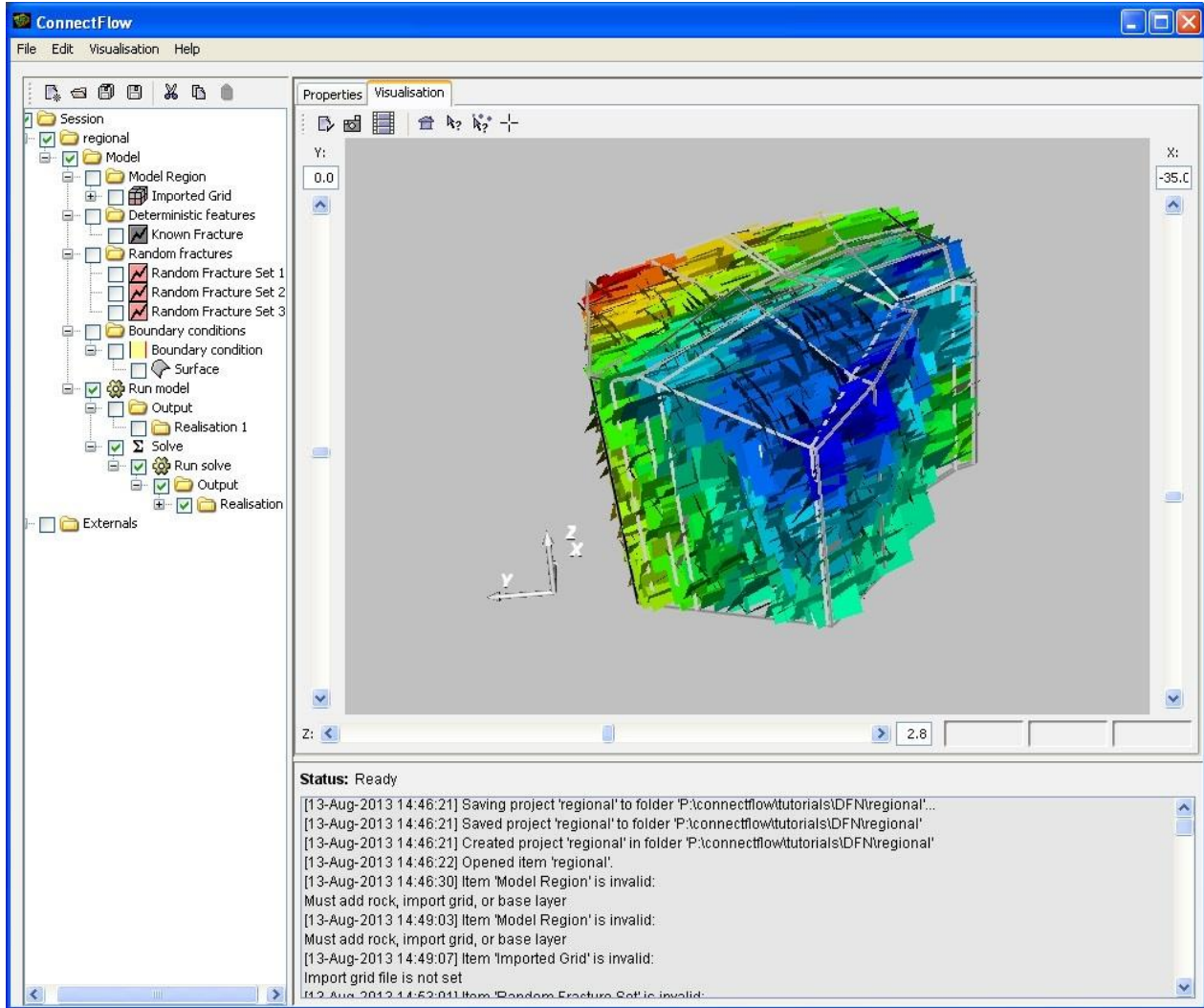


Figure 9-5: A DFN model coloured by residual pressure in ConnectFlow.

10 Nomenclature and Units

By default, ConnectFlow uses SI units, except that Celsius is used for temperature.

Symbol	Definition	Units
A_{KR}	constant in CPM default relative permeability model	$\text{Pa}^{S_{KR}}$
A_{PC}	constant in CPM default capillary pressure model	$\text{Pa}^{S_{PC}}$
B_{KR}	constant in CPM default relative permeability model	$\text{Pa}^{S_{KR}}$
B_{PC}	constant in CPM default capillary pressure model	$\text{Pa}^{S_{PC}}$
b	effective aquifer thickness (see Equation 3-10)	m
c	concentration (or mass fraction) of dissolved solute (normally salt)	–
c_0	specified inflow concentration for solute (normally salt)	–
c_l	specific heat capacity of the fluid	$\text{J kg}^{-1}\text{K}^{-1}$
c_s	specific heat capacity of the rock solids	$\text{J kg}^{-1}\text{K}^{-1}$
D	dispersion tensor for solute (normally salt)	m^2s^{-1}
D'	dispersion tensor for heat	$\text{W m}^{-1}\text{K}^{-1}$
D_i	intrinsic (or effective) diffusion coefficient	m^2s^{-1}
D_m	molecular diffusion coefficient for solute (normally salt)	m^2s^{-1}
$D_{m\alpha}$	molecular diffusion coefficient for nuclide α	m^2s^{-1}
D_α	dispersion tensor for nuclide α	m^2s^{-1}
F_A	advective radionuclide flux	$\text{mol m}^{-2}\text{s}^{-1}$
F_C	flux of solute (normally salt)	$\text{kg m}^{-2}\text{s}^{-1}$
F_D	diffusive radionuclide flux	$\text{mol m}^{-2}\text{s}^{-1}$
$F_{N\alpha}$	flux of nuclide α	$\text{mol m}^{-2}\text{s}^{-1}$
F_P	fluid flux	$\text{kg m}^{-2}\text{s}^{-1}$
F_T	heat flux	W m^{-2}
f_α	Source term for nuclide α	$\text{mol m}^{-3}\text{s}^{-1}$
g	gravitational acceleration	m s^{-2}
g	magnitude of gravitational acceleration	m s^{-2}
H	heat source	W m^{-3}
h	hydraulic head	m
I	maximum potential infiltration rate	m s^{-1}
K_d	sorption distribution coefficient (literature K_d multiplied by rock density)	–
$K_{d\alpha}$	sorption distribution coefficient for nuclide α	–
k	rock permeability tensor	m^2
k_r	Relative permeability (see section 3.4)	–
k_v	vertical permeability of semi-permeable layer	m^2

Symbol	Definition	Units
L	arbitrary transition thickness	m
N_{α}	concentration of nuclide α	mol m ⁻³
$N_{\alpha 0}$	specified inflow concentration for nuclide α	mol m ⁻³
\mathbf{n}	outward normal to a specified boundary	–
P_E	capillary entry pressure	Pa
P^R	residual fluid pressure	Pa
$P^R_{r,i}$	residual fluid pressure at node i of an element on the interface of a regional-scale mesh	Pa
$P^R_{s,i}$	residual fluid pressure at node i of an element on the interface of a site-scale mesh	Pa
P^T	total fluid pressure	Pa
P_0^T	reference total fluid pressure	Pa
Q	Source term (in 2D areal model of groundwater flow, see section 3.1.4)	kg m ⁻² s ⁻¹
\mathbf{q}	specific discharge (or Darcy velocity)	m s ⁻¹
q_z	vertical component of specific discharge	m s ⁻¹
R_{α}	retardation factor for nuclide α	–
S	saturation	–
S_{KR}	constant in CPM default relative permeability model	–
S_{PC}	constant in CPM default capillary pressure model	–
S_{res}	residual saturation	–
S_{α}	function of saturation used in Van Genuchten relative permeability model (see Equation 3-21)	–
T	temperature	°C
T_0	reference temperature	°C
t	Time	s
\mathbf{v}	average porewater velocity	m s ⁻¹
v	magnitude of porewater velocity	m s ⁻¹
v_i	i -component of porewater velocity	m s ⁻¹
z	elevation	m
z_0	reference elevation	m
z_b	elevation of bottom of aquifer	m
z_s	elevation of ground surface	m
z_t	elevation of top of aquifer	m

Symbol	Definition	Units
α	compressibility of freshwater	Pa ⁻¹
α_L	longitudinal dispersion length for solute (normally salt)	m
α'_L	longitudinal dispersion length for heat	m
$\alpha_{L\alpha}$	longitudinal dispersion length for nuclide α	m
α_T	transverse dispersion length for solute (normally salt)	m
α'_T	transverse dispersion length for heat	m
$\alpha_{T\alpha}$	transverse dispersion length for nuclide α	m
α_c	compressibility of saturated fluid (normally brine)	Pa ⁻¹
β	coefficient of volumetric expansion of freshwater	K ⁻¹
β_c	coefficient of volumetric expansion of saturated fluid (normally brine)	K ⁻¹
Γ_a	average thermal conductivity of the rock and fluid	W m ⁻¹ K ⁻¹
Γ_l	thermal conductivity of the fluid	W m ⁻¹ K ⁻¹
Γ_s	thermal conductivity of the rock	W m ⁻¹ K ⁻¹
γ	constant in relative permeability models	–
δ_l	viscosibility	K ⁻¹
δ_{ij}	Kronecker delta	–
ε	Penalty weight (0.01)	–
φ	porosity	–
φ_0	reference porosity	–
λ_α	decay constant for nuclide α	s ⁻¹
μ	fluid viscosity	Pa s
μ_0	reference fluid viscosity	Pa s
ρ_0	reference (freshwater) fluid density	kg m ⁻³
ρ_{c0}	Density of solute-saturated fluid (normally saturated brine)	kg m ⁻³
ρ_l	fluid density	kg m ⁻³
ρ_s	Density of the rock solids	kg m ⁻³
$(\rho c)_a$	average heat capacity of the rock and liquid	J m ⁻³ K ⁻¹
τ	tortuosity	–
θ	Degree of implicitness of Crack-Nicholson solution method	–
$\psi_{r,ij}$	finite element basis function evaluated for node j of an element on the interface of a regional-scale mesh at the position of node i of an adjoining element in a site-scale mesh	–

11 References

- Agg et al., 1994.** P J Agg, R W Cummings, J H Rees, W R Rodwell and R Wikramaratna, *Nirex Gas Generation and Migration Research: Report on Current Status in 1994*, Nirex Science Report S/96/002, 1996.
- Anderson et al., 1996.** E. Anderson, Z. Bai, C. Bischof, J. Demmel, J Dongarra, J. DuCroz, A. Greenbaum, S. Hammerling, A McKenney, S Ostrouchov and D. Sorenson. *LAPACK Users' Guide, Second Edition* SIAM, Philadelphia, PA 1995.
- Batchelor, 1967.** G K Batchelor, *An Introduction to Fluid Dynamics*, Cambridge University Press, 1967.
- Baker et al., 1997.** A J Baker and N L Jefferies, *Nirex Geosphere Research: Report on Current Status in 1994*, Nirex Science Report S/97/011, 1997.
- Bear, 1972.** J Bear, *Dynamics of Fluids in Porous Media*, American Elsevier, 1972.
- Bear, 1979.** J Bear, *Hydraulics of Groundwater*, McGraw Hill, 1979.
- Boghammar et al., 1997.** A Boghammar, B Grundfelt and L J Hartley, *Investigation of the Large Scale Regional Hydrogeological Situation at Ceberg*, SKB Report TR-97-21, 1997.
- Bogorinski, 1984.** P. Bogorinski, C.P. Jackson and J.D. Porter, *INTRAVAL Test Case 13: Simulation of an Experimental Study of Brine Transport in Porous Media*. GRS-A-1984, 1984.
- Bolt et al., 1995.** J.E. Bolt, P. Bourke, N. L. Jefferies, R. Kingdon, D. Pascoe, and V. Watkins. *The Application of Fracture Network Modelling to the Prediction of Groundwater Flow Through Highly Fractured Rock*. Science Report NSS/R281, Nirex, 1995.
- Carrera et al., 1998.** J Carrera, X Sánchez-Vila, I Benet, A Medina, G Galarza, J Guimerà, *On matrix diffusion: formulations, solution methods and qualitative effects*, Hydrogeology Journal 6, 178–190, 1998.
- Charlton et al., 2011.** S R Charlton, D L Parkhurst, *Modules based on the geochemical model PHREEQC for use in scripting and programming languages*, Computers & Geosciences, 37(10), 1653–1663, 2011.
- Cliffe et al., 1993.** K A Cliffe and C P Jackson, *Stochastic Modelling of Groundwater Flow at the WIPP Site*, Proceedings of the Fourth International High level Radioactive Waste Management Conference, Las Vegas, 1993.
- Cordes et al., 1992.** Christian Cordes and Wolfgang Kinzelbach, *Continuous Groundwater Velocity Fields and Path Lines in Linear, Bilinear, and Trilinear Finite Elements*, Water Resources Research, Vol. 28, No. 11, Pages 2903-2911, November 1992.
- Dagan, 1988.** G Dagan, *Time-Dependent Macrodispersion for Solute Transport in Anisotropic Heterogeneous Aquifers*, Wat. Resour. Res. **24**, 1491, 1988.
- Dagan, 1989.** G Dagan, *Flow and Transport in Porous Formations*, Springer Verlag, 1989.
- Dershowitz, 1984.** W. S. Dershowitz. *Rock Joint Systems*. PhD Thesis, MIT, 1984.
- Freeze et al., 1979.** R A Freeze and J A Cherry, *Groundwater*, Prentice Hall, 1979.
- Geier et al., 1992.** J. Geier, C. Axelsson, L. Hassler, and A. Benabderahmane. *Discrete Fracture Modelling of the Finnsjön Rock Mass*. Technical Report 92-07, SKB, 1992.

- Gelhar et al., 1983.** L W Gelhar, C L Axness, *Three-Dimensional Stochastic Analysis of Macrodispersion in Aquifers*, Wat. Resour. Res. **19**, 161, 1983.
- Herbert et al., 1990.** A W Herbert and B A Splawski, *Prediction of Inflow into the D-holes at the Stripa Mine*, Stripa Report 90-14, 1990.
- Herbert et al., 1991a.** A W Herbert, J Gale, G Lanyon and R MacLeod, *Modelling for the Stripa Site Characterisation and Validation Drift Inflow: Prediction of Flow through Fractured Rock*, Stripa Project Report 91-35, 1991.
- Herbert et al., 1991b.** A.W. Herbert and G.W.Lanyon, *Modelling Tracer Transport in Fractured Rock at Stripa*. Stripa Project Technical Report 91-01, SKB, Stockholm, 1991
- Hoch et al., 2004.** AR Hoch, C P Jackson, *Rock-matrix diffusion in transport of salinity. Implementation in CONNECTFLOW*, SKB R-04-78, Svensk Kärnbränslehantering AB, 2004.
- Hood, 1976.** P Hood. *Frontal Solution Program for Unsymmetric Matrices*, Int. J. Num. Meth. Eng. **10**, 379-399, 1976.
- HSL, 1995.** HSL, *Harwell Subroutine Library Specifications (Release 12)*. Volume 1, AEA Technology Report, Harwell Laboratory, Oxfordshire, 1995.
- Irons, 1975.** B M Irons, *A Frontal Solution Program for Finite-Element Analysis*, Int. J. Num. Meth. Eng. **2**, 5-32, 1975.
- Jackson et al., 1997.** C P Jackson and S P Watson, *Nirex 97: An Assessment of the Post-Closure Performance of a Deep Waste Repository at Sellafield. Volume 2: Hydrogeological Conceptual Model Development - Effective Parameters and Calibration*, Nirex Science Report S/97/012, 1997.
- Jacobson, 1949.** T Jacobson, *Before Philosophy*, Penguin Books, 1949.
- Jost, 1960.** W Jost, *Diffusion in Solids, Liquids, Gases*, Academic Press, 1960.
- Joyce et al., 2014.** S Joyce, D Applegate, P Appleyard, A Gordon, T Heath, F Hunter, J Hoek, C P Jackson, D Swan, H Woollard, *Groundwater flow and reactive transport modelling in ConnectFlow*. SKB R-14-19, Svensk Kärnbränslehantering AB, 2014.
- Kestin J, Khalifa E, Correia R, 1981.** *Tables of the dynamic and kinematic viscosity of aqueous NaCl solutions in the temperature range 20–150 °C and the pressure range 0.1–35 MPa*. Journal of Physical and Chemical Reference Data **10**, 71.
- Lee et al., 2000.** S H Lee, C L Jensen and M F Lough, *Efficient Finite-Difference Model for Flow in a Reservoir with Multiple Length-Scale Fractures*, PE Journal **5**(3), September 2000.
- De Marsily, 1985.** G de Marsily, *Quantitative Hydrogeology*, Academic Press, 1985.
- Morris et al., 1994.** S T Morris and K A Cliffe, *Verification of HYDRASTAR: Analysis of Hydraulic Conductivity Fields and Dispersion*, SKB Report TR-94-21, 1994.
- Morris et al., 1996.** S.T. Morris and G. Webster, *Quality Sub-Programme: Computer Packages Based on TGSL*. AEA Technology Report, WEG/QAP/TGSL, 1996.
- Morris et al., 1997a.** S T Morris, J D Porter and C P Jackson, *A Comparison of Methods for Generating Correlated Random Hydrogeological Fields*, Nirex Report NSS/R304, 1997.
- Morris et al., 1997b.** S T Morris, J D Porter and C P Jackson, *An Investigation of the Accuracy of the Spectral Turning Bands Random Field Generator*, Nirex Report NSS/R320, 1997.

- Neretnieks, 1980.** I Neretnieks, *Diffusion in the Rock Matrix: An Important Factor in Radionuclide Retardation?*, J. Geophys. Res. **85**, 4379-4397, 1980.
- Norman, 1992.** S Norman, *HYDRASTAR – a Code for Stochastic Simulation of Groundwater Flow*, SKB Technical Report TR 92-12, 1992.
- Olsson et al., 1994.** O Olsson, G Bäckblom, G Gustafson, I Rhén, R Stanfors and P Wikberg, *The Structure of Conceptual Models with Application to the Åspö HRL Project*. SKB Technical Report TR 94-08, 1994.
- Olsson et al., 1995.** O. Olsson, and J. Gale. *Site Assessment and Characterisation for High-Level Nuclear Waste Disposal: Results from the Stripa Project Sweden*. Q. J. Eng. Geol. **28**, S17, 1995.
- Parkhurst et al., 1999.** D L Parkhurst, C A J Appelo, *User's guide to PHREEQC (Version 2) — A computer program for speciation, batch-reaction, one-dimensional transport, and inverse geochemical calculations*, U.S. Geological Survey Water-Resources Investigations Report 99-4259, USGS, 1999.
- Press et al., 1986.** W.H. Press, B.P. Flannery, S.A. Teukolsky and W.T. Vetterling, *Numerical Recipes. The Art of Scientific Computing*. Cambridge University Press, 1986.
- Robinson, 1984.** P Robinson, *Connectivity, Flow and Transport in Network Models of Fractured Media*, UKAEA Report TP.1072 and D.Phil. Thesis for University of Oxford, 1984.
- Scafer et al., 1995.** R. A. Scafer, J. Gale and A. Herbert. *3-D Discrete Fracture Flow Simulation Using Monterey Formation Fracture Data*. SPE 29135, p. 415, 1995.
- Scheidegger, 1974.** A E Scheidegger, *The Physics of Flow through Porous Media*, University of Toronto Press, 1974.
- Schwartz et al., 1991.** F.W. Schwartz and G. Lee, *Cross-Verification testing of Fracture Flow and Mass Transport Codes*. Stripa Project Technical Report 91-29, SKB, Stockholm, 1991.
- Simpson et al., 2004.** M J Simpson and T B Clement, *Improving the Worthiness of the Henry Problem as a Benchmark for Density-dependent Groundwater Flow Models*, Water Resour. Res., 40, W01504, 2004.
- SKI, 1996.** SKI, *SKI Site-94 Deep Repository Performance Assessment*, Swedish Nuclear Power Inspectorate Report SKI 96:36, 1996.
- Sloan, 1986.** S.W. Sloan, *An Algorithm for Profile and Wavefront Reduction of Sparse Matrices*. Inter. J. Numerical Methods in Engineering, 23, 239, 1986.
- Smith et al., 1984.** L. Smith and F. Schwartz, *An Analysis of the Influence of Fracture Geometry on Mass Transport in Fractured Rock*. Water Resour. Res., **20(9)**, 1241, 1984.
- Snow, 1968.** D.T. Snow. *Rock Fracture Spacings, Openings, and Porosities*. J. Soil Mech. Found. Div, Proc. Amer. Civil Engrs., 94, 73, 1968.
- Stratford et al., 1990.** R G Stratford, A W Herbert and C P Jackson, *A Parameter Study of the Influence of Aperture Variations on Fracture Flow and the Consequences in a Fracture Network*, Proc. Int. Symp. on Rock Joints, Norway, 1990.
- Svensson, 1999.** U Svensson, *Representation of Fracture Networks as Grid Cell Conductivities*, SKB Report TR-99-05, 1999.
- Thomas, 1949.** L H Thomas, *Elliptic problems in linear differential equations over a network*, Watson Scientific Computing Laboratory, Columbia University, New York, 1949.

Warren et al., 1963. Warren and Root, *The Behaviour of Naturally Fractured Reservoirs*, SPE Journal, 245-255, 1963.

Ward, 1975. R C Ward, *Principles of Hydrology*, McGraw Hill, 1975.

Wilcock, 1996. P.M. Wilcock, *Generic Study of Coupled T-H-M Processes in the near-field (BMT3) in Coupled Thermo-Hydro-Mechanical Processes of Fractured Media*, *Developments in Geotechnical Engineering* 79, S. Stephanson and L. Jing (Eds.), Elsevier, 1996.